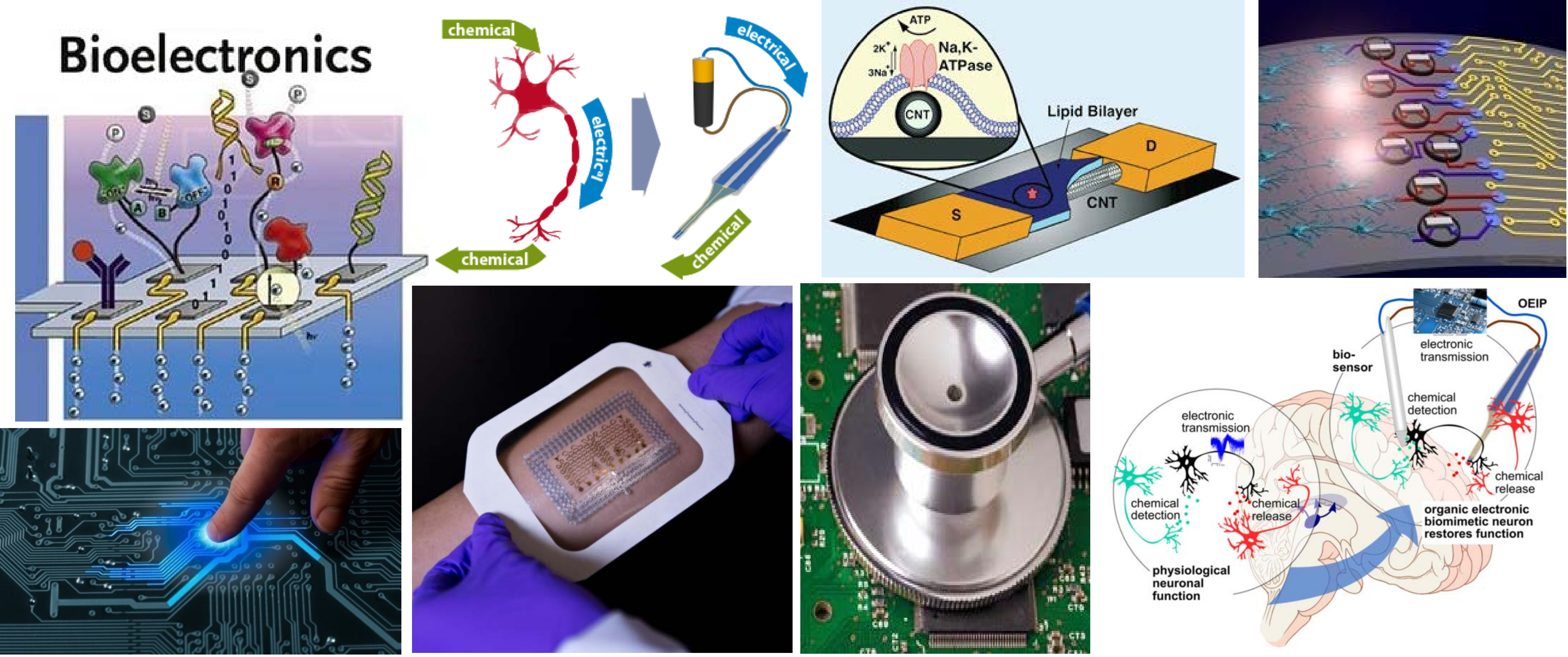

Bioelectronics:
Interfacing Electronics with Biology

Peilin Chen (Research Fellow)
Research Center for Applied Sciences (RCAS) , Academia Sinica, Taiwan

2016/04/28

What is Bioelectronics?

- **Biology + Electronics**
- The application of electronic devices to living organisms for **clinical testing**, **diagnosis** and **therapy.**
- The interactions of increased **computing power**, **advances in prosthetic devices**, **artificial implants**, and **systems** that blend electronic and biological components.

Sources: http://dictionary.reference.com/browse/bioelectronics
http://www.svegritet.se/ethics-bioethics/bioelectronics-and-implanted-devices/

Do CYBORGs exist?

- The earlier and more strict definition of **Cyborg** was almost always considered as increasing or enhancing normal capabilities, whereas now the term can also be applied to those organisms which use technology to repair or overcome their physical and mental constraints.
- Examples are artificial limbs and hands.

Source: http://en.wikipedia.org/wiki/Cyborg; http://www.motherboard.tv/2010/8/10/the-cyborg-kevin-warwick-is-the-world-s-first-human-robot-hybrid

Correlation of Biomedical Engineering, Electrical Engineering and Information Technology

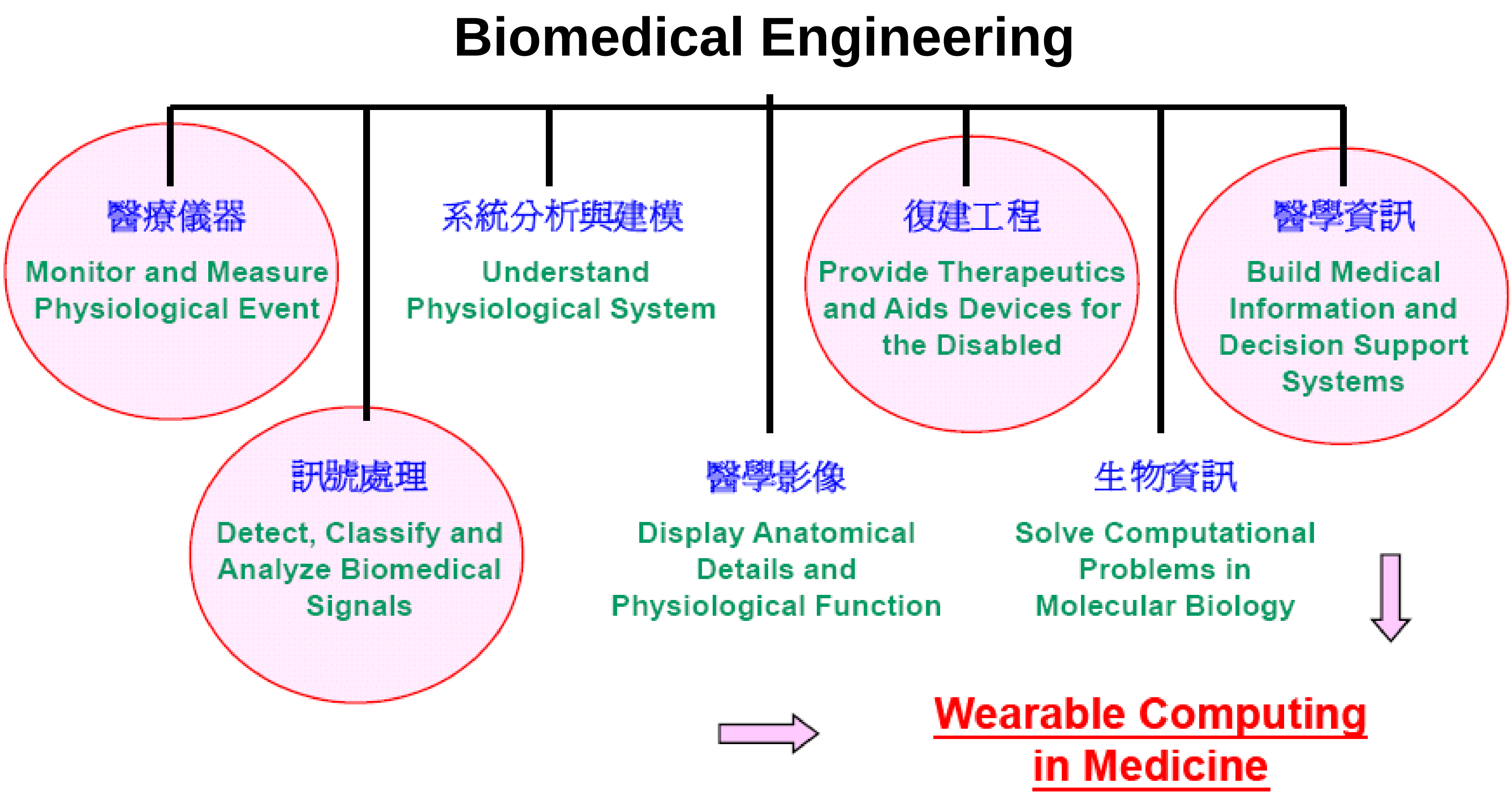

Blood Glucose Meters

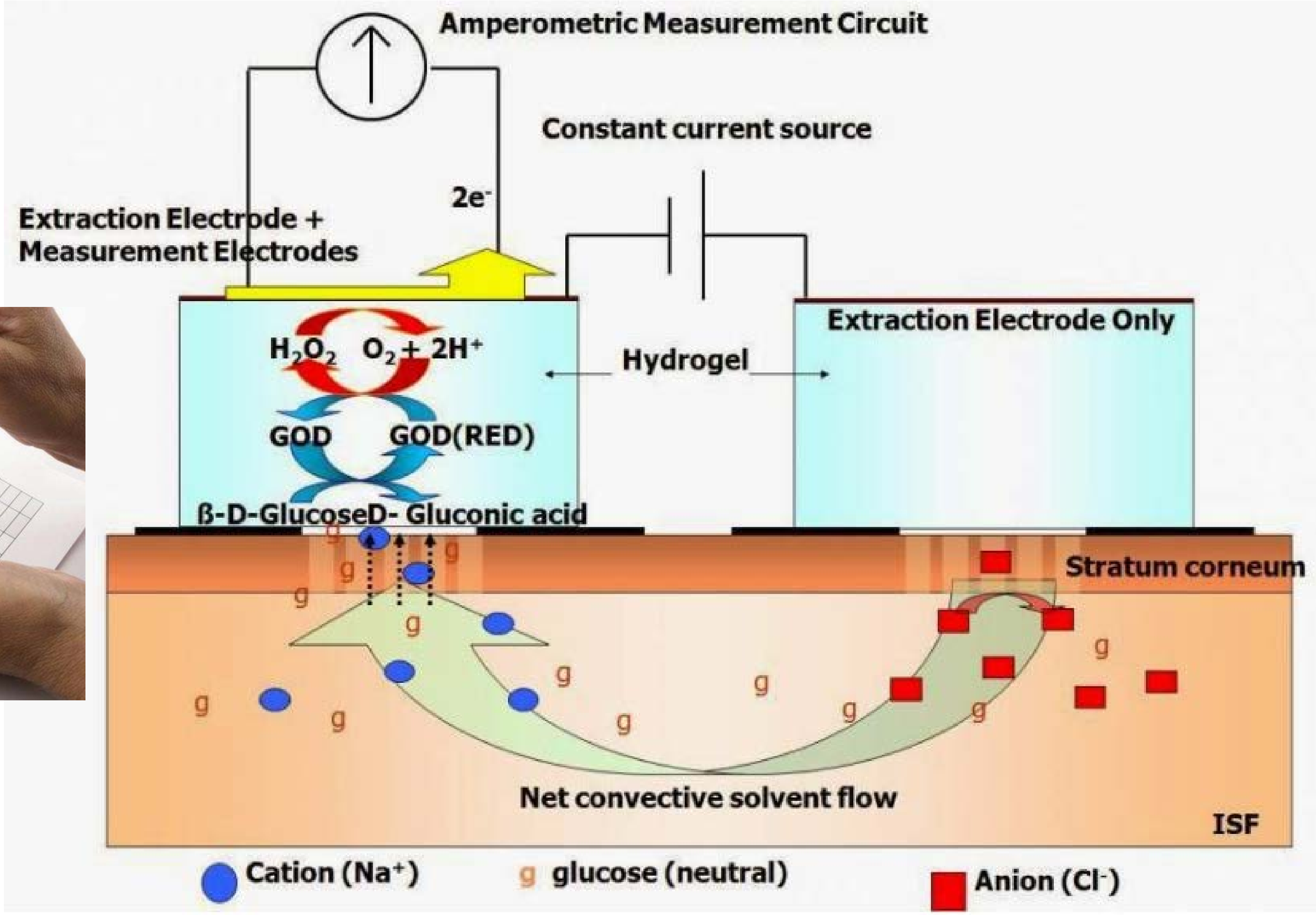

Glucose undergoes a chemical reaction in the presence of enzymes and electrons are produced during the chemical reaction. These electrons (i.e., the charge passing through the electrode) are measured and this is proportional to the concentration of glucose in the solution.

Electrocardiography (ECG) Measurement Technology

First Electrocardiograph (ECG)
by William Einthoven in 1903

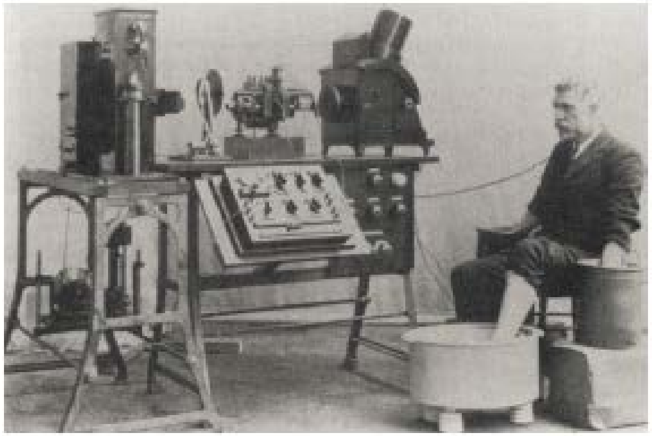

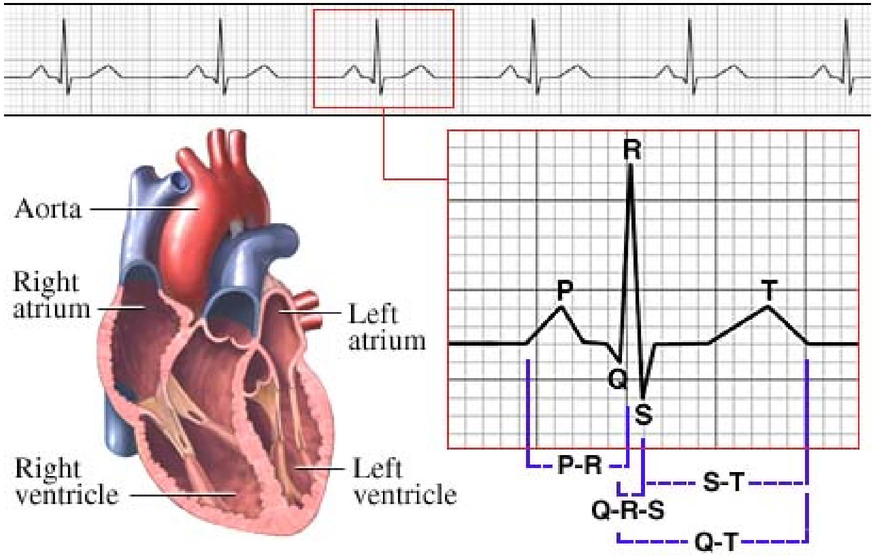

Patient Monitors

Portable ECG system

ECG Holter

Embedded ECG

ECG chip

Bioinstrumentation

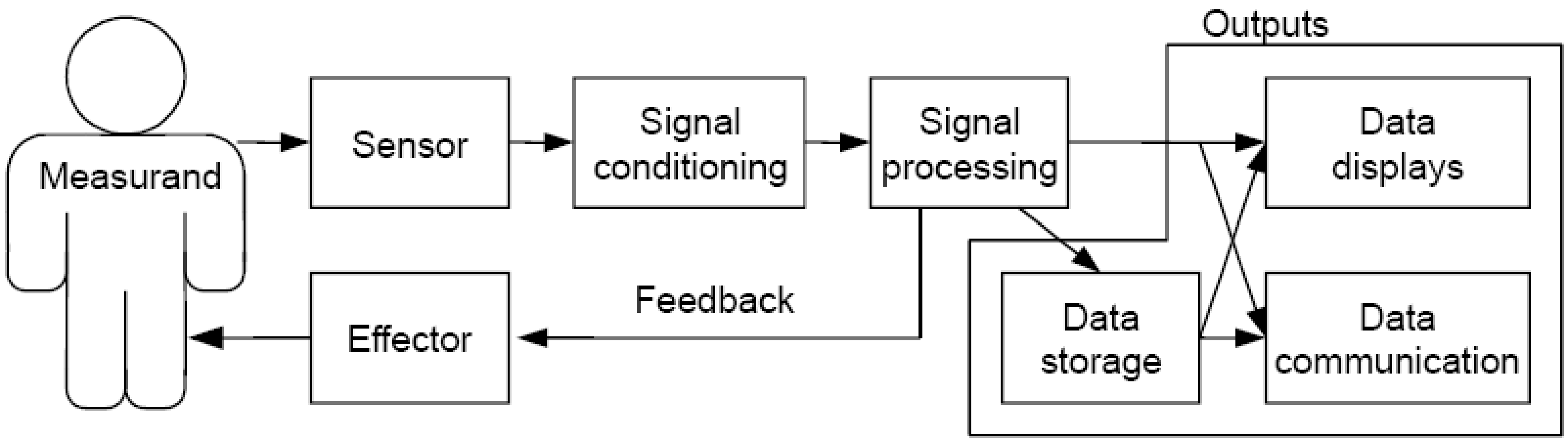

John G. Webster, Bioinstrumentation, John Wiley & Sons, 2003.

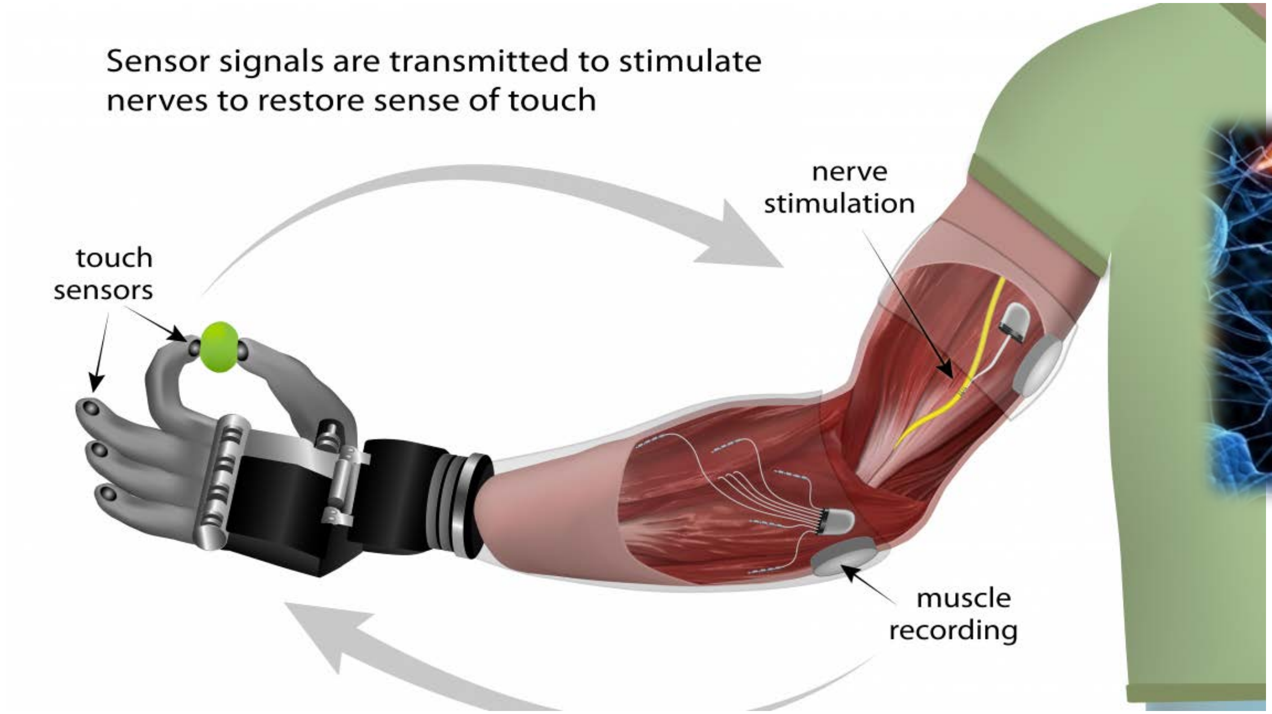

Bioelectronics and Implanted Devices

- Eyes
- Ears
- Heart
- Lung
- Liver
- Kidney
- Hands
- Foots

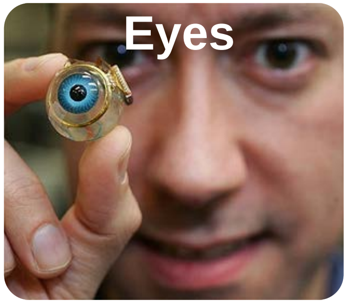

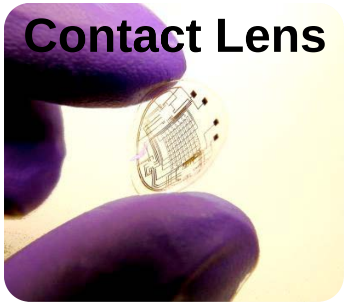

Hand

Foot

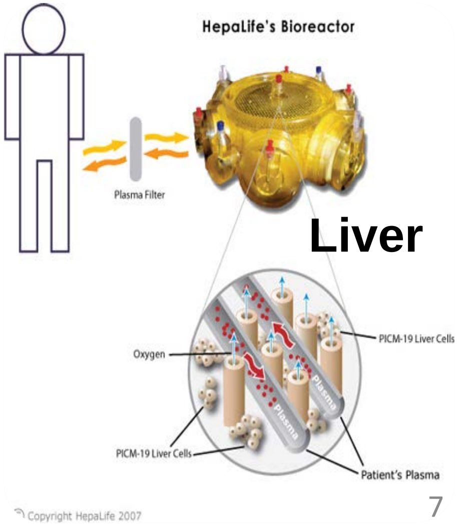

Bioelectronics for Smart Skin or Smart Textiles

Implantable device for measuring the heart's electrical output with a vast improvement over conventional devices [Science Transl. Med. 2, 24ra22 (2010)].

Electronic eyeball camera that uses a hemispherically curved array of silicon photodetectors and picture collected with a similar camera that uses a paraboloid design [Rogers et al., Science 327, 1603 (2010)].

Stretchable array of light emitting diodes (LEDs) [Kim et al., Nature Mater. 10, 316 (2011)].

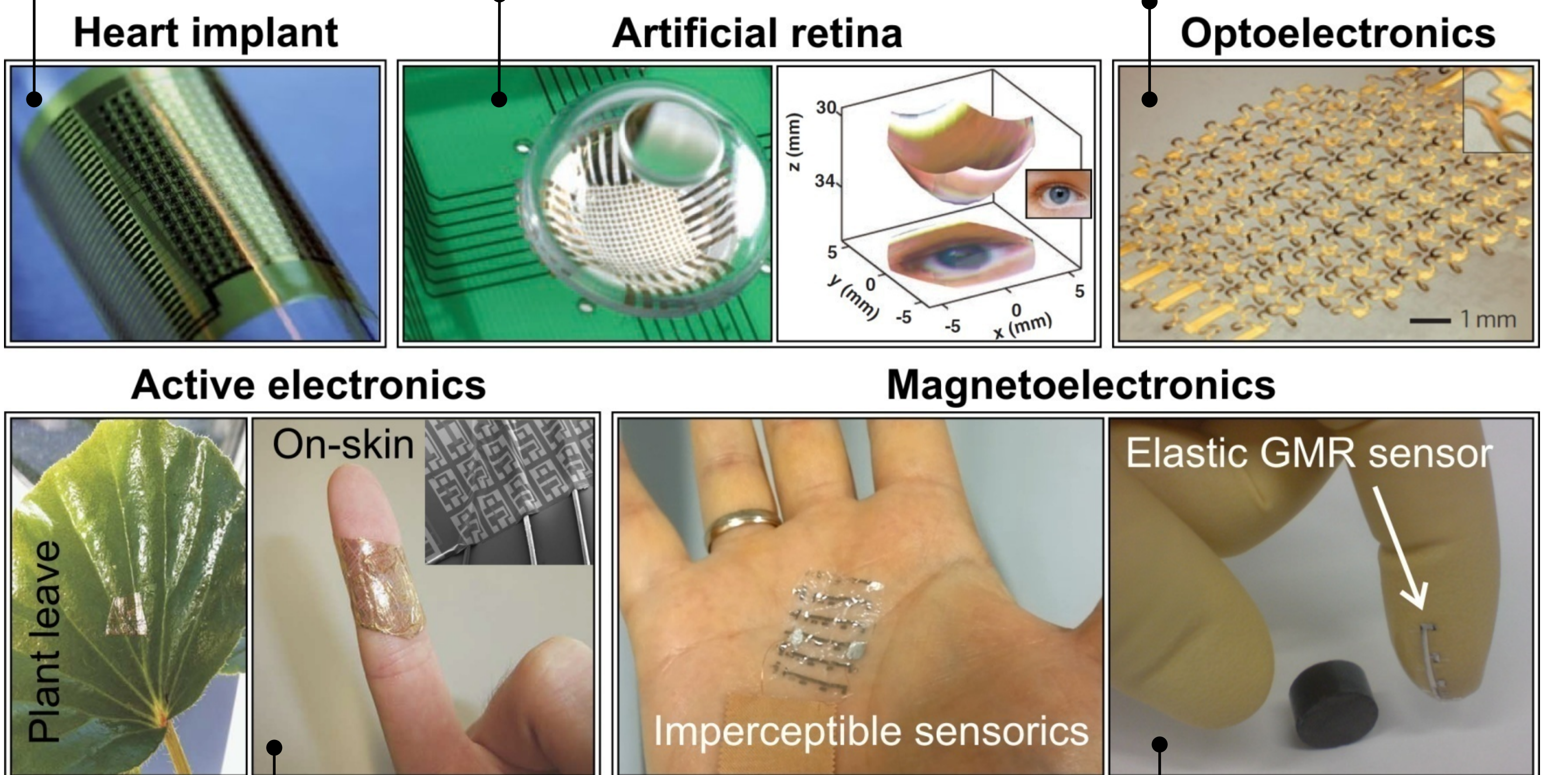

Flexible InGaZnO-Based active electronics [Salvatore et al., Nature Comm. 5, 2982 (2014)].

Flexible and stretchable inorganic magnetosensorics [Melzer et al., Nano Letters 11, 2522 (2011)].

Bioelectronics and Medicine's Future

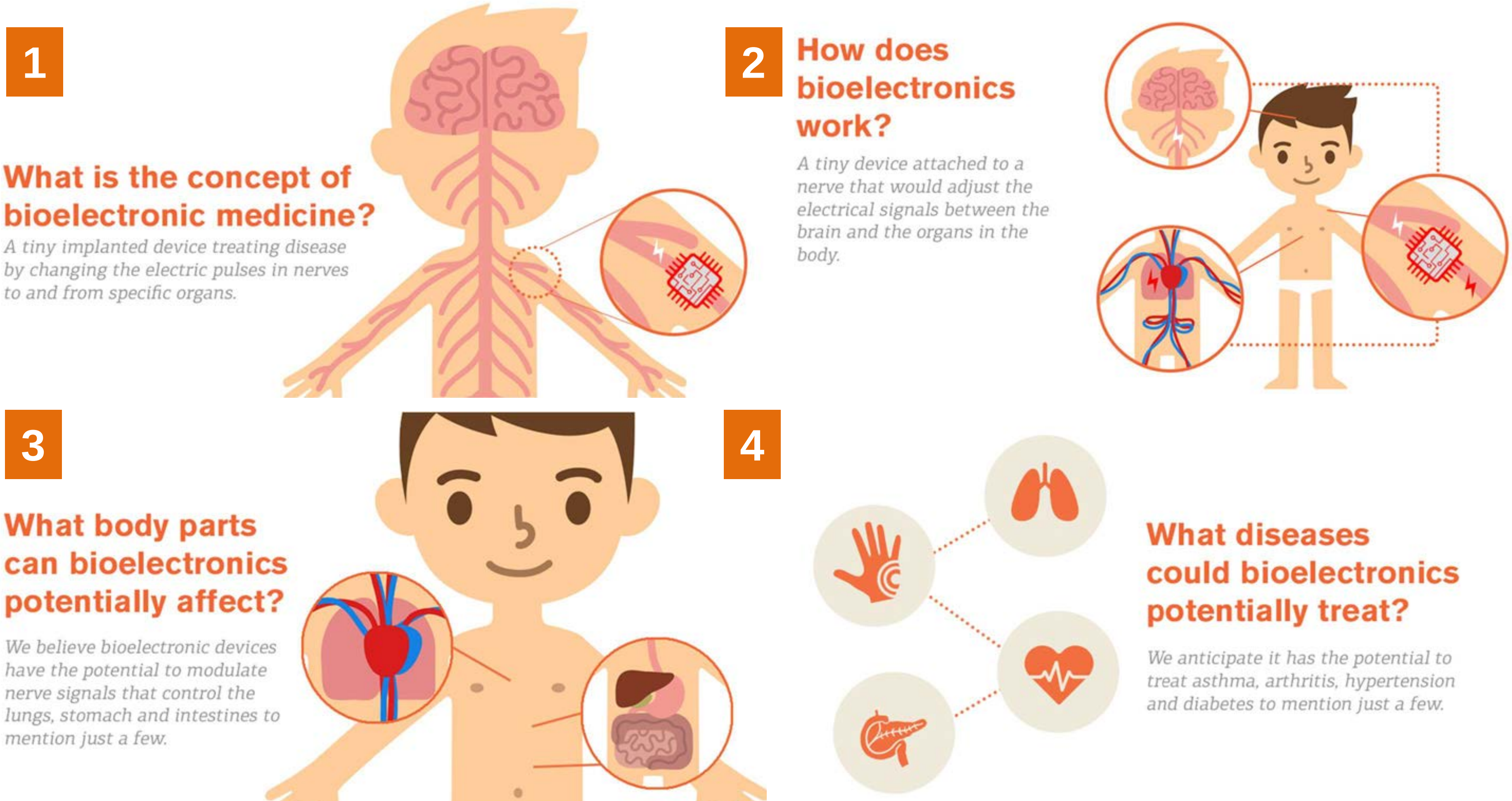

Bioelectronics will be commonly used by 2025

https://www.youtube.com/watch?v=AX4Yr02-oIo

Personalized Bioelectronic Medicines : Targets and Diseases

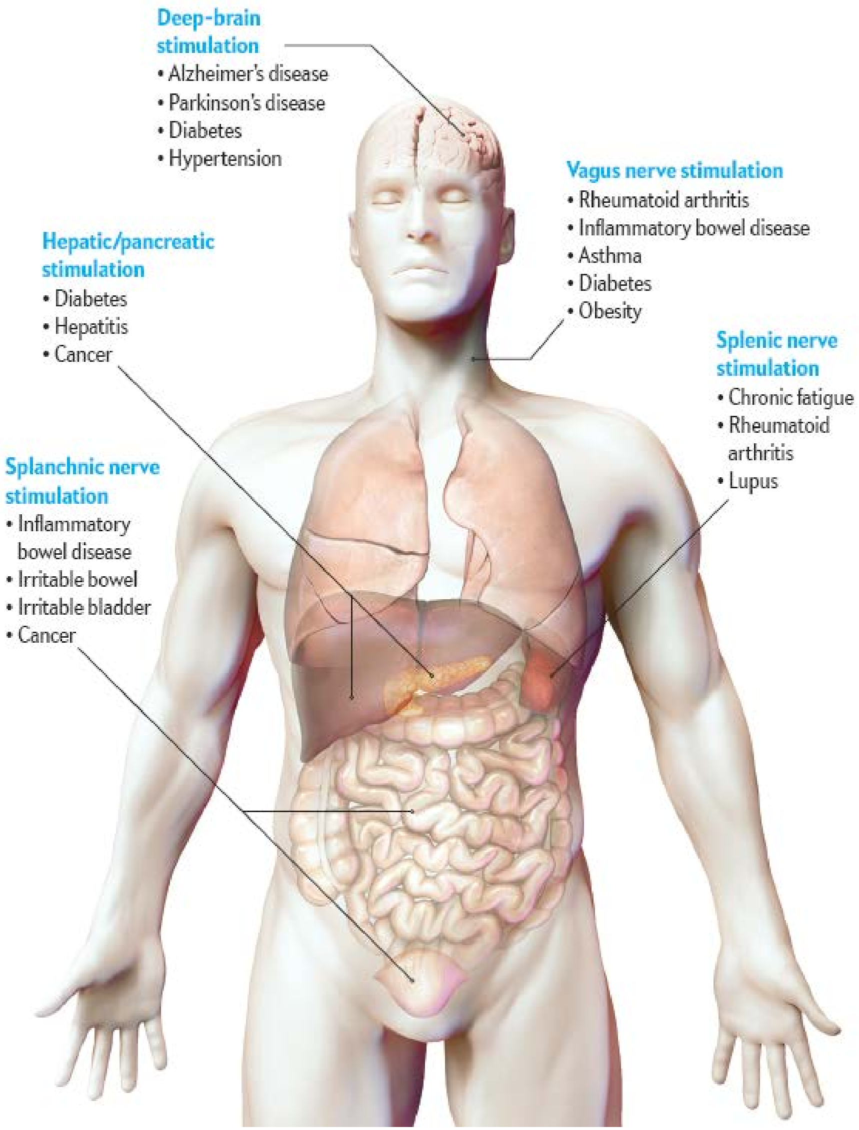

Bioelectronic medicine holds promise for using electrical stimulation technologies to treat a variety of diseases—and may become an alternative to some pharmaceuticals. Vagus nerve stimulation—the topic of this article—is only one of these techniques. Deep-brain stimulation is already helping patients with Parkinson's disease. Other therapies, such as splenic nerve stimulation, are being investigated but have not reached clinical trials.

Outline

- **Personalized Bioelectronic Medicines**
- **Why Organics? What is the Organic Electronic?**
- **Organic Bioelectronic Interfaces (OBEIs) and Pi materials**
- **Micro/Nanofabrication Technologies for Organic electronics**
- **Neuroscience**
  - Introduction to neural interfacing
  - Recording single neurons without penetrating the brain
  - Recording brain activity with high signal-to-noise ratio
  - Stopping seizures (in vitro) with localized drug delivery
  - Ion transport in conducting polymers
- **Stem Cell Therapies**
- **Cancer Treatment and Diagnostic□**

Personalized Bioelectronic Medicines

1) Neuroscience

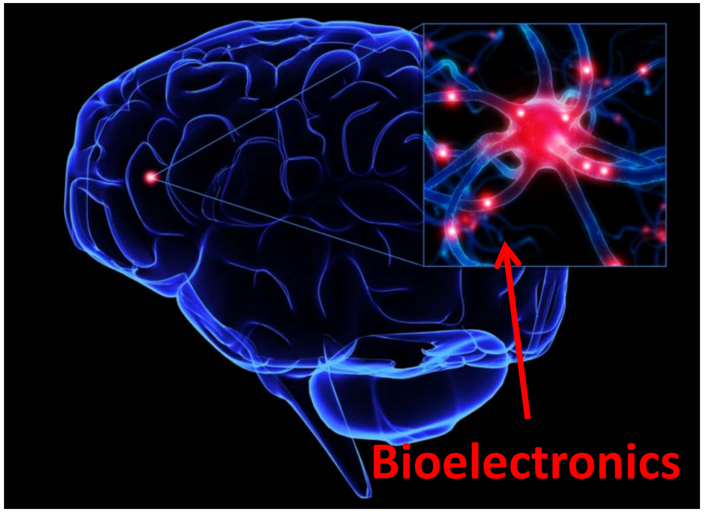

2) Stem Cell therapies

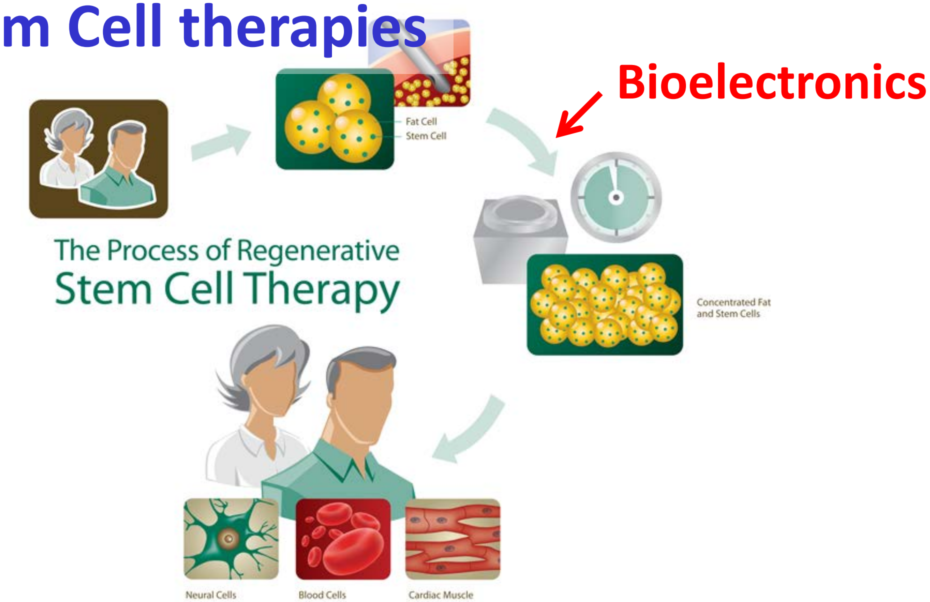

3) Cancer Treatment and Diagnostic

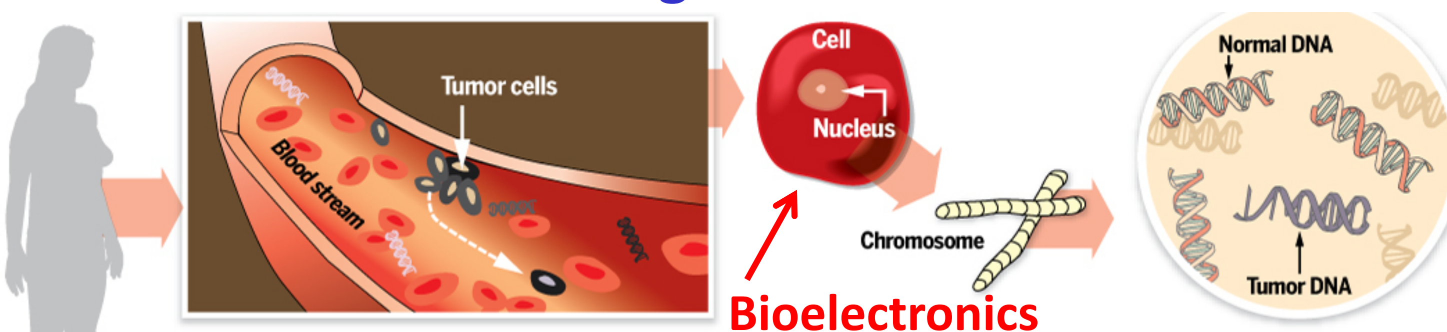

Detecting tumor cells

Tumor cells die routinely just like other cells, and when they do, they shed DNA into a person's bloodstream. This means the bloodstream will contain DNA from all over the tumor, not just one section.

Blood is drawn

Once a patient's blood sample is taken, technicians isolate the DNA by removing red blood cells, platelets and plasma. Technicians get the DNA from the nuclei of white blood cells.

DNA tumor

The DNA is then read searching for markers of cancer. These are areas of the genetic script in which cancer cells differ markedly from normal cells.

Bioelectronics: Coupling biology and electronics

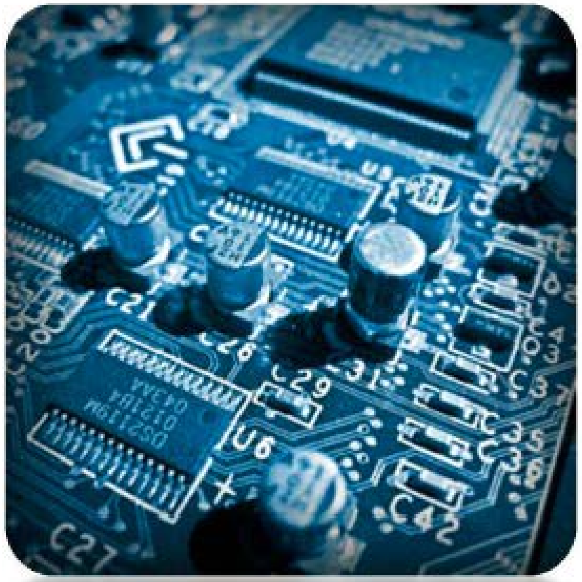

Mostly soft

Complex signaling

Dynamic

Sensing

Diagnosis

Actuation

Therapy

Hard

Electrons/holes

Static

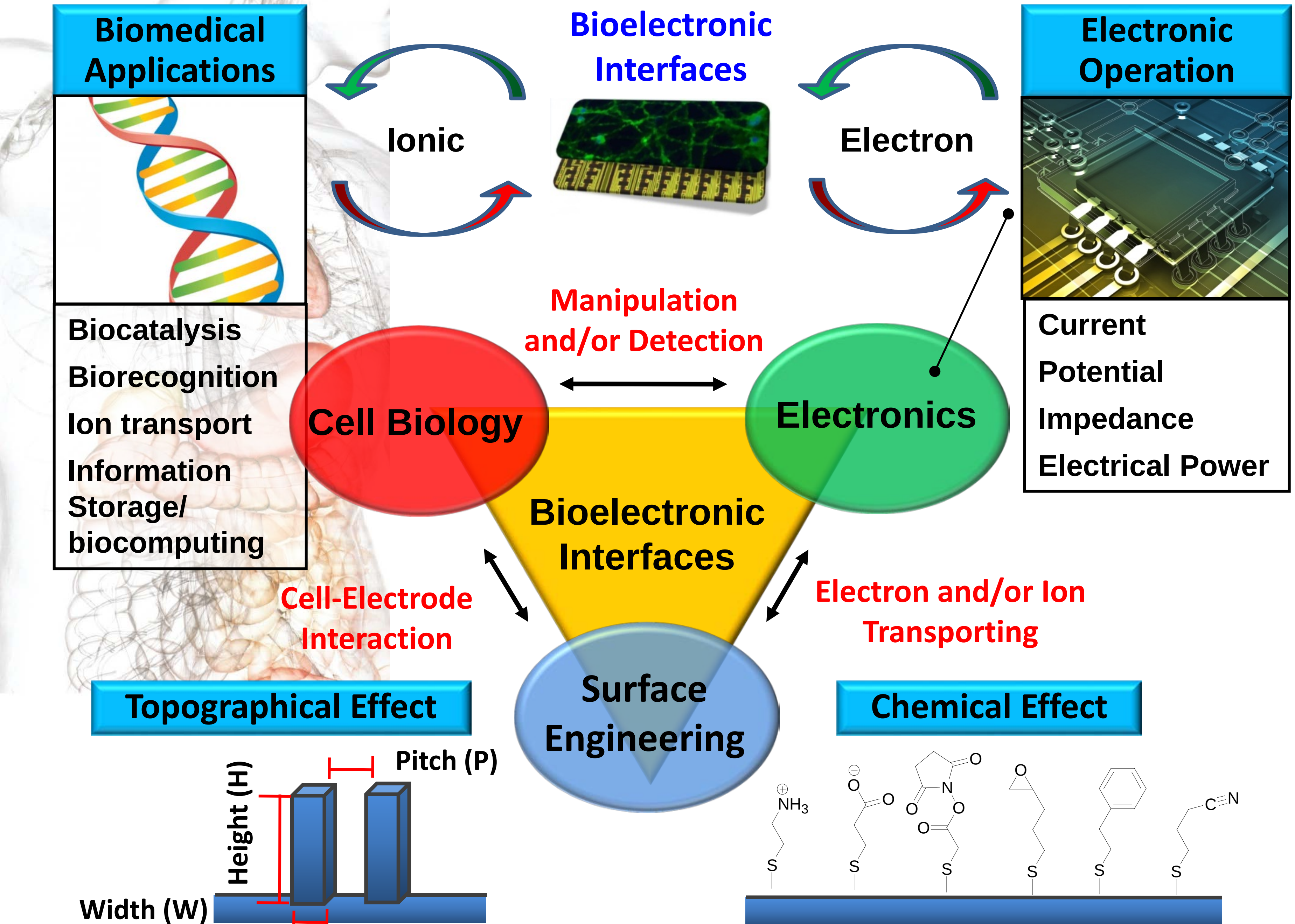
Biomedical Applications
Bioelectronic Interfaces
Electronic Operation
Ionic
Electron
Biocatalysis
Biorecognition
Ion transport
Information Storage/ biocomputing
Manipulation and/or Detection
Cell Biology
Electronics
Current
Potential
Impedance
Electrical Power
Bioelectronic Interfaces
Cell-Electrode Interaction
Electron and/or Ion Transporting
Surface Engineering
Topographical Effect
Chemical Effect
Pitch (P)
Height (H)
Width (W)

Why Organic? Bioelectronic Interfaces (BEIs)

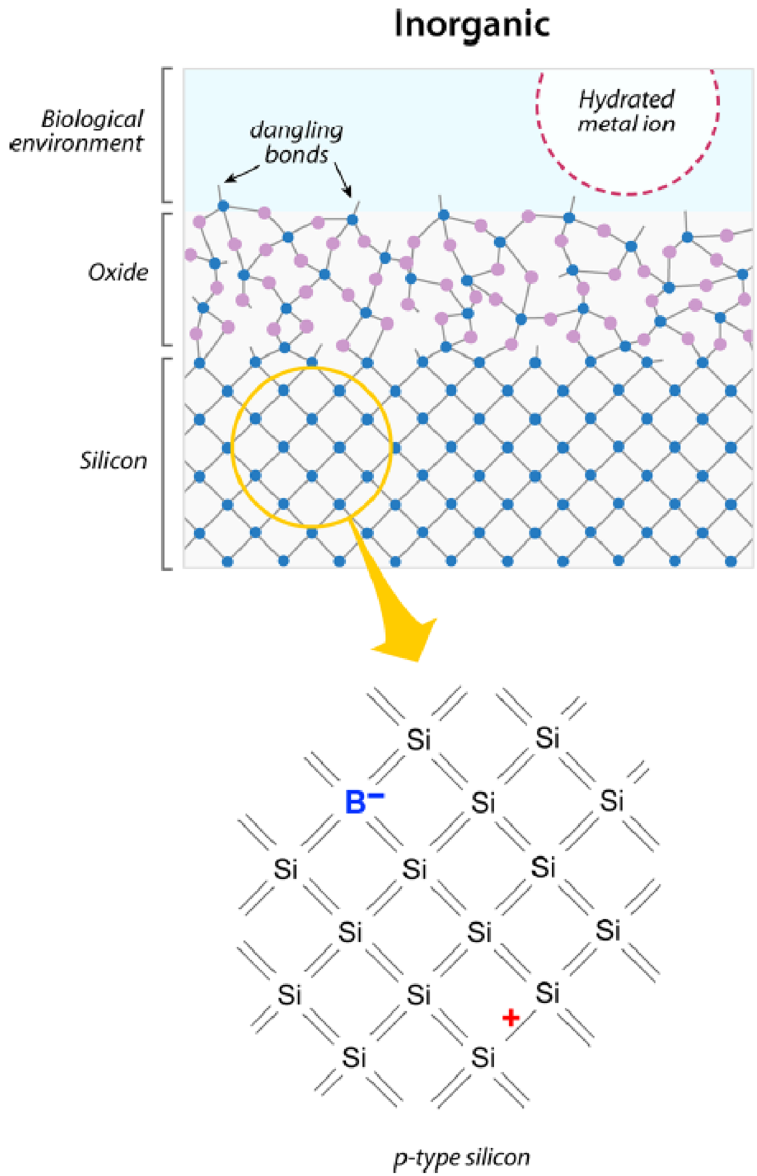

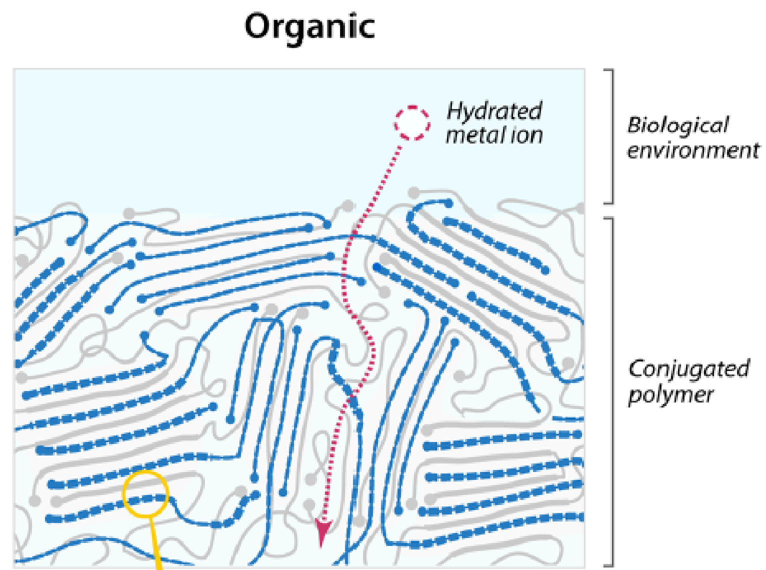

Conducting polymers show mixed conductivity

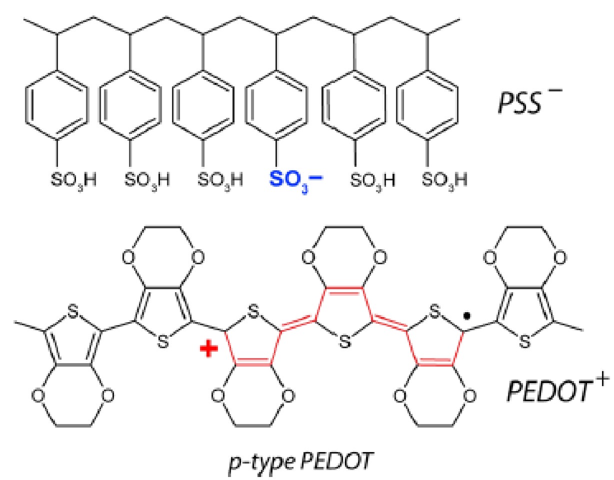

Ref. *Chem. Mater.* 2014, 26, 679−685

Organic Electronics meets Biology

Organic electronics provide the future application demand – the "silicon" based devices are unable to provide!!

Mixed conductivity leads to novel/state-of-the-art devices

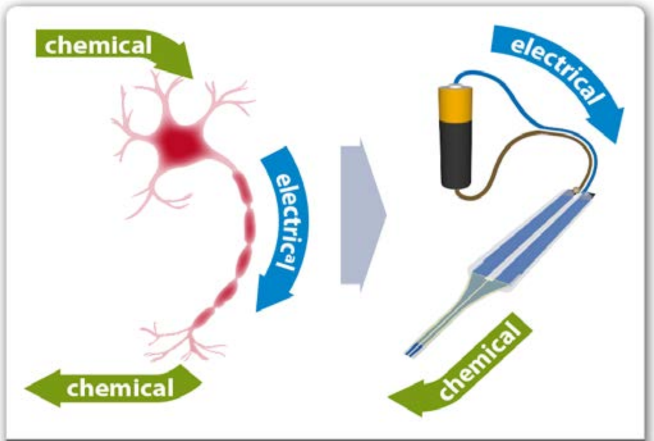

Progress toward artificial neurons.
Reported in *Nature Materials*.

Organic Electronic Ion Pump

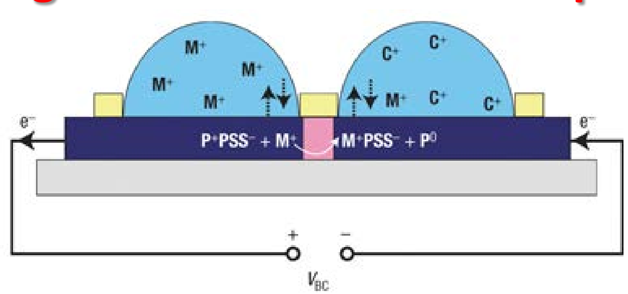

Nature Materials 2007, 6, 673-679

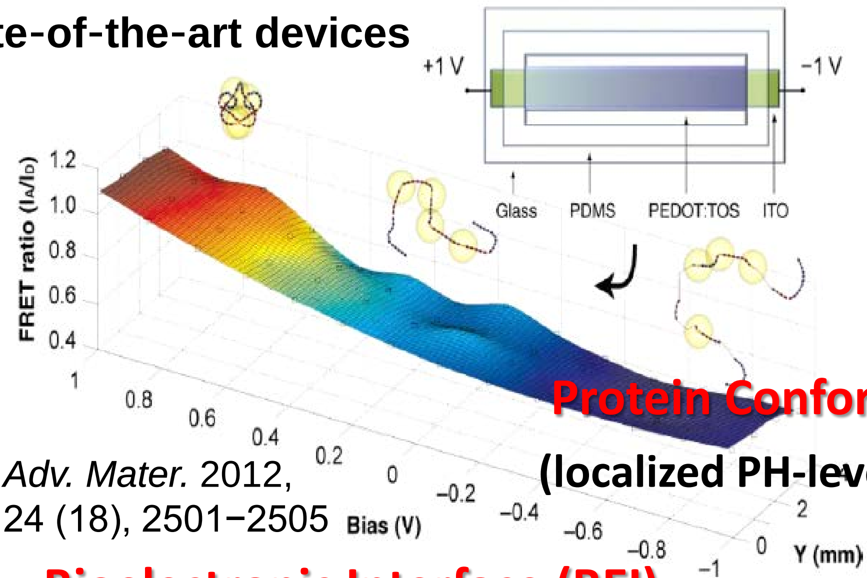

Protein Conformation

(localized PH-level change)

Adv. Mater. 2012, 24 (18), 2501−2505

Bioelectronic Interface (BEI)

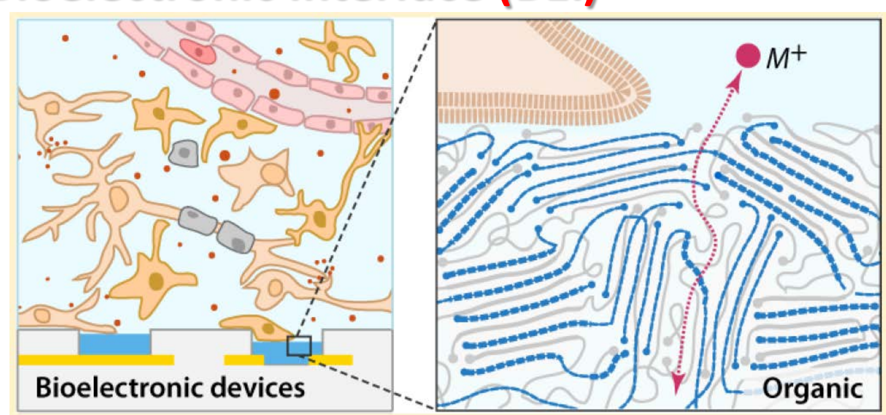

Chem. Mater. 2014, 26, 679−685

Organic Bioelectronics

Bioelectronic Medicines: **Based on the knowledge obtained from biology, electronics and surface engineering, it will help bring a new class of precision medicines to patients.**

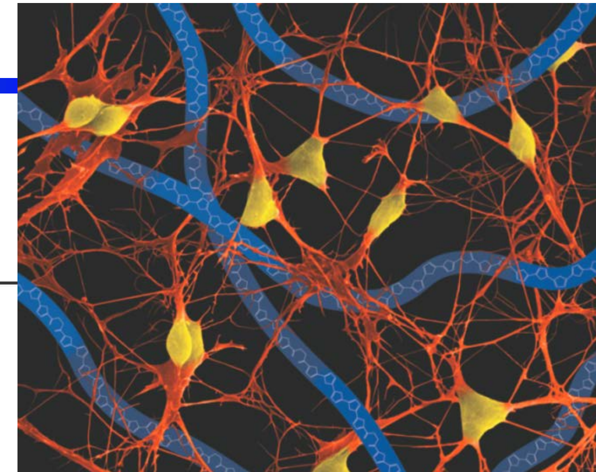

Nature Materials,13 (2014), 775.

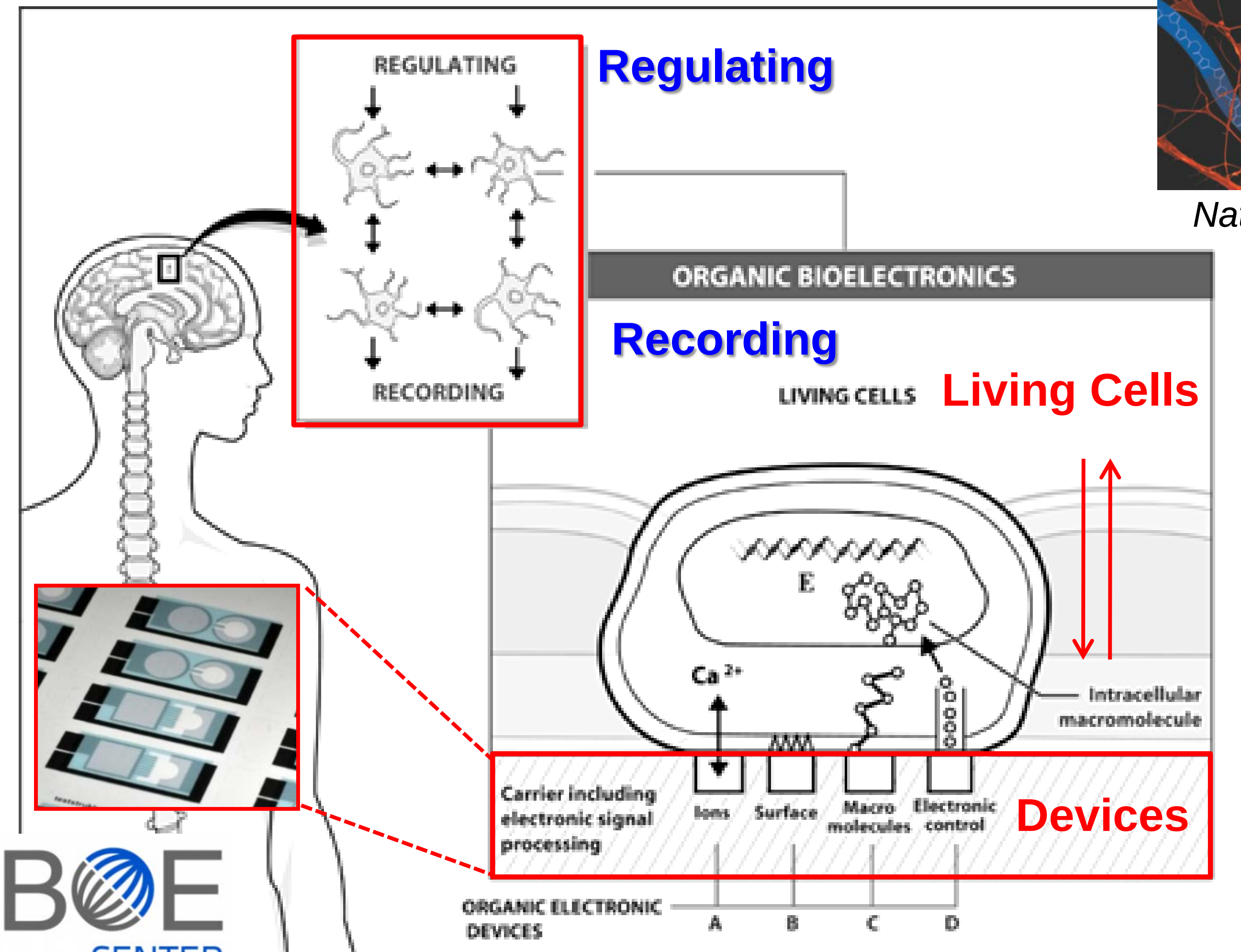

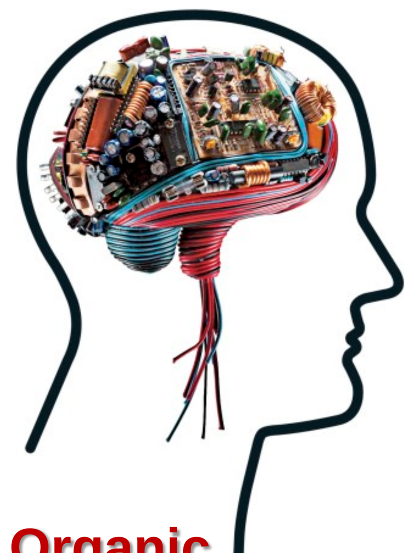

Organic Bioelectronic Medicines

OBOE CENTER

Organic Electronics and Pi Materials

Organic Light Emitting Diode (OLED)

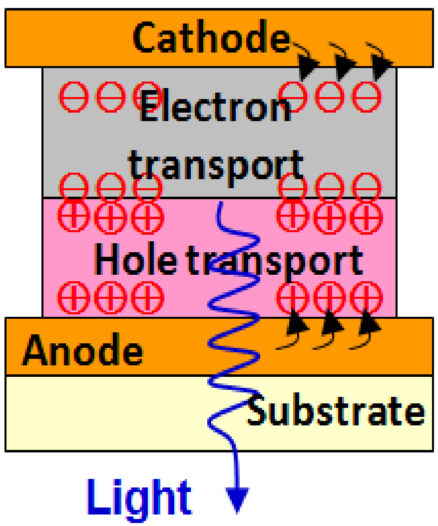

(a)Electron/Hole injection

Organic Photovoltaic (OPV)

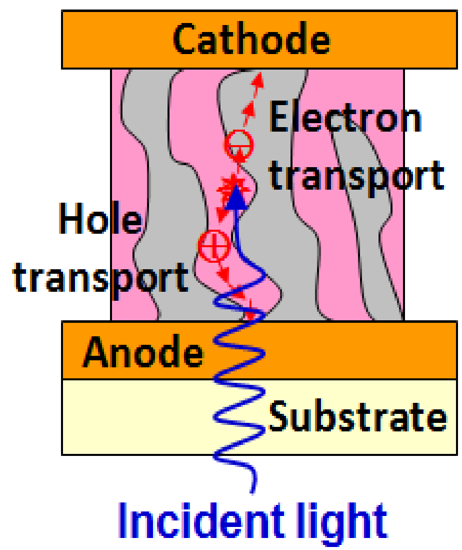

(b) Photoexcitation

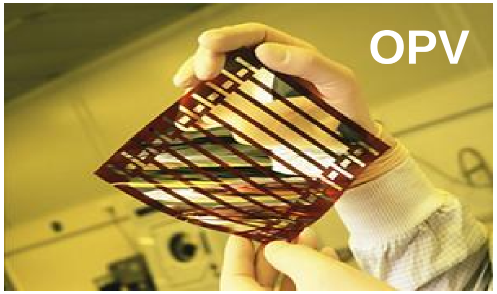

Organic Thin film Transistor (OTFT)

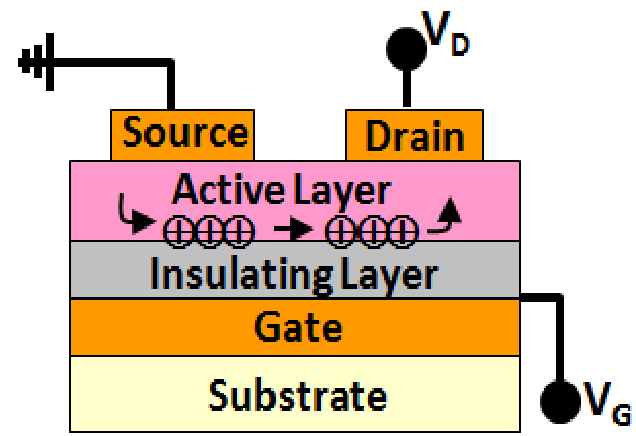

(c) Electroactive operation for dynamic doping

Fundamental knowledge of Pi Materials

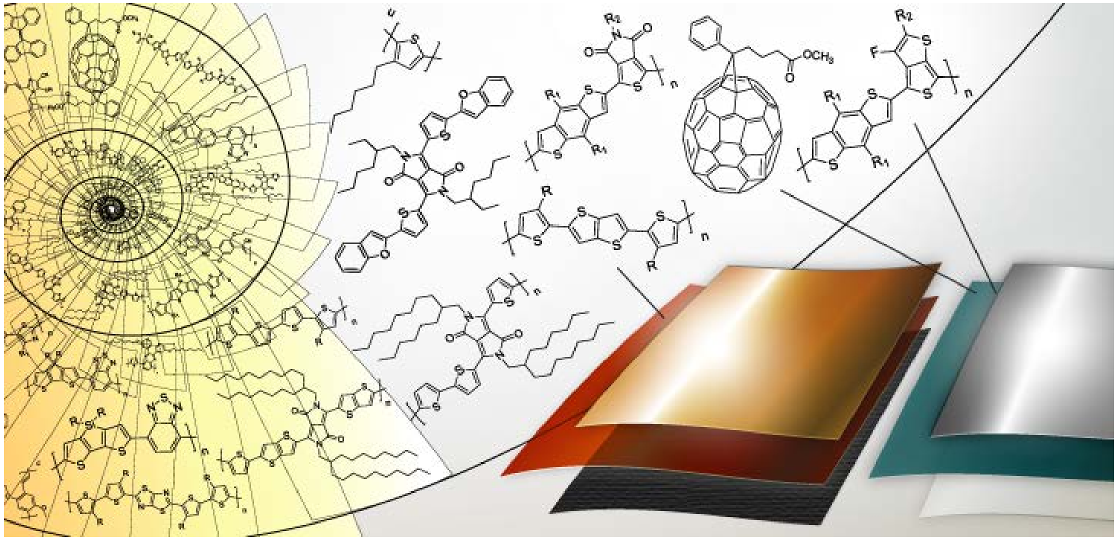

Pi-conjugated materials

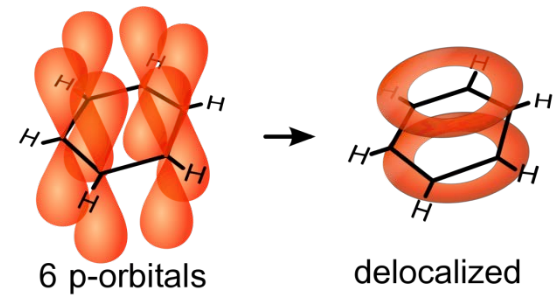

Hybridization: sp^2 and p_z

Pi-conjugated materials are carbon-based macromolecules which have extended chains of **alternating single and double bonds**. As a result, the marcomolecule has **pi-electrons that reside above and below the molecular plane of the chains**.

Conducting Polymers

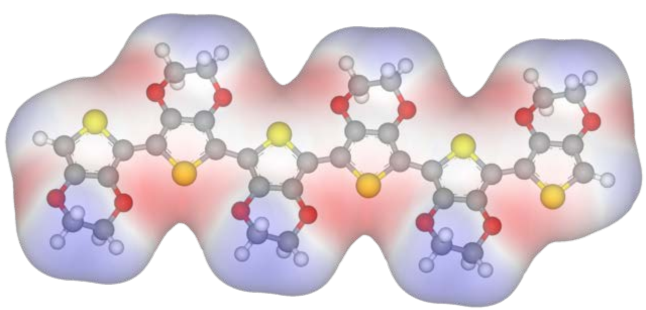

Carbon Materials

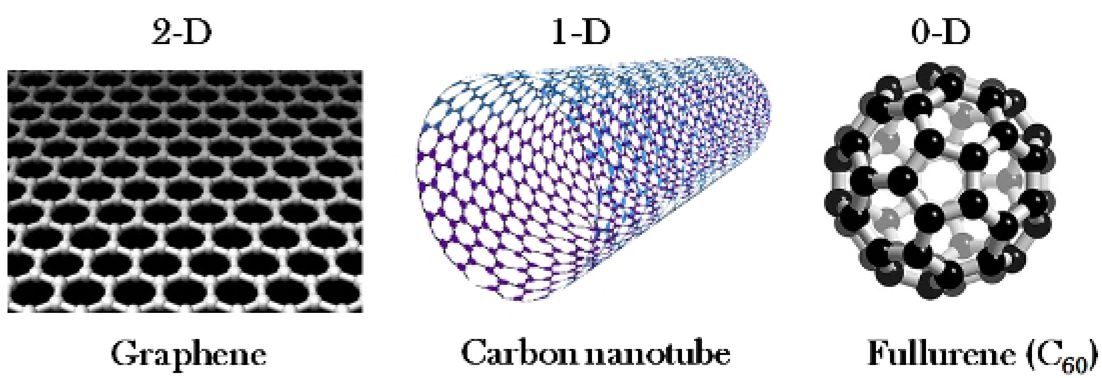

Organic BEI Materials

External Stimulation

1. Conducting polymeric materials

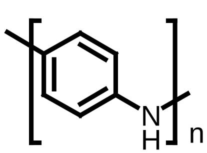

(PANI)

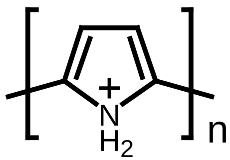

(PPy)

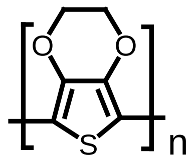

(PEDOT)

Electrical conductivity

~ 40 S/cm | **~ 40 S/cm** | **~4000 S/cm**

External Stimulation

2. Carbon materials

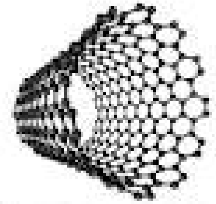

(CNT)

(C_{60})

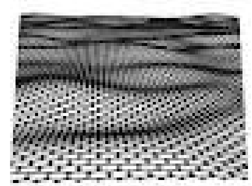

(Graphene)

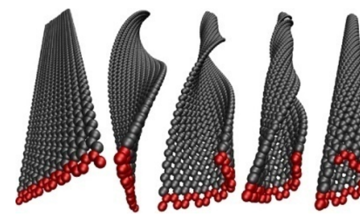

(CNR)

Localize Stimulation

3. Piezoelectric polymeric materials

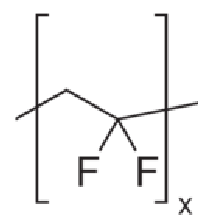

(PVDF)

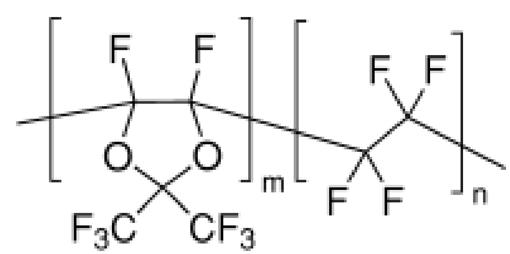

(Teflon AF)

piezoelectric coefficient

20~350 pC/N | ~600 pC/N

Biology

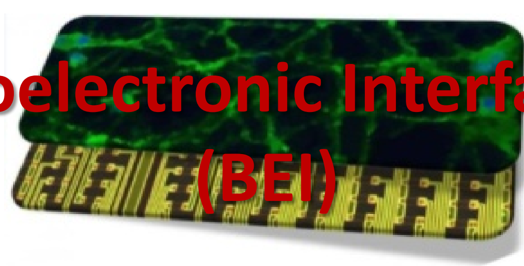

Bioelectronic Interface (BEI)

Electronics

Organic BEI Materials

PEDOT

(1) Prepare by polymer solution

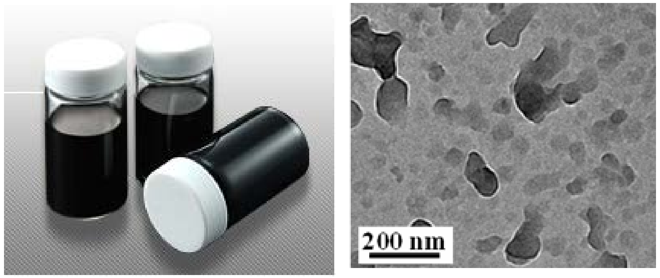

(PEDOT:PSS)

(2) Chemical polymerization

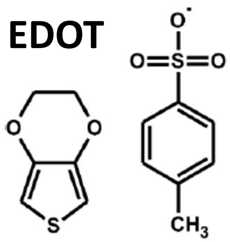

Oxidizer:
iron(III) tosylate (TOS)

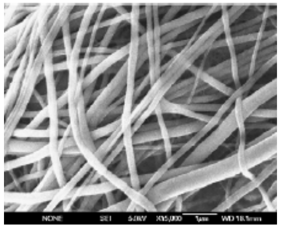

(3) Electropolymization

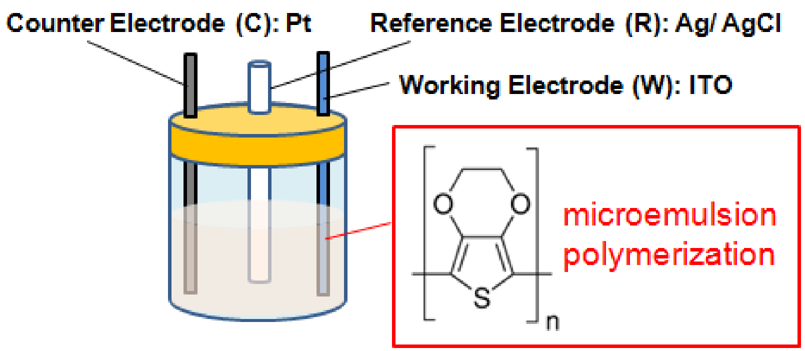

Graphene

(1) Chemical vapor deposition (CVD)

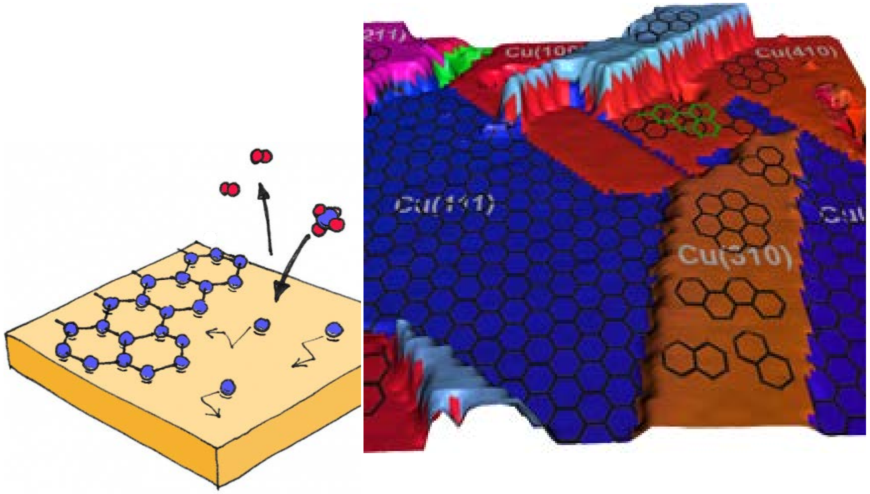

(2) Spin-coating of GO or rGO solution

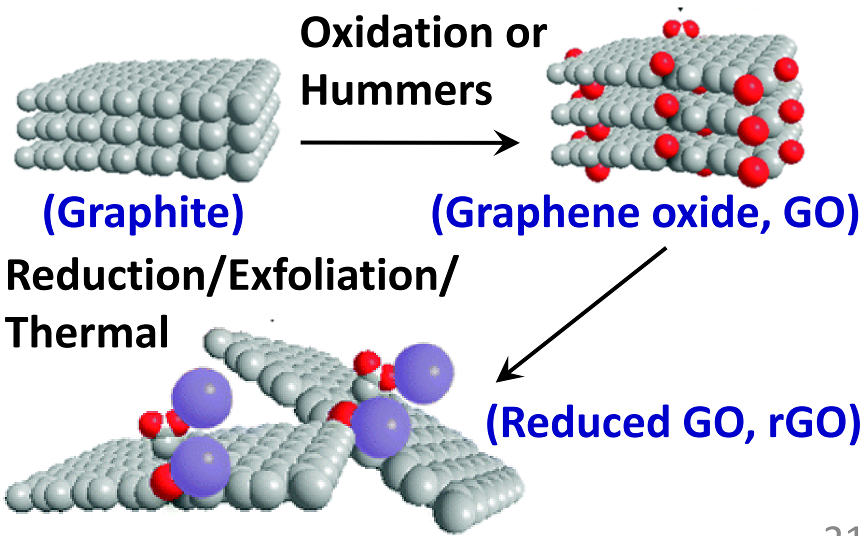

Critical Properties of Organic BEIs

- **Biocompatible and biodegradable** (surface engineering; stiffness)
- **Easily doped or conjugated with functional materials** (high functionality)
- **High integration to OM systems** (high transparency)
- **Solution process** (low cost; mass production; compatibility with fabrication)
- **Responsive actions** (temp.; PH; pressure; light; electrical etc.)
- **Cell-electrode interface** (charge-electron transporting; low Impedance)
- **Signal transduction** (biomolecules; ionic transporting; action potential)

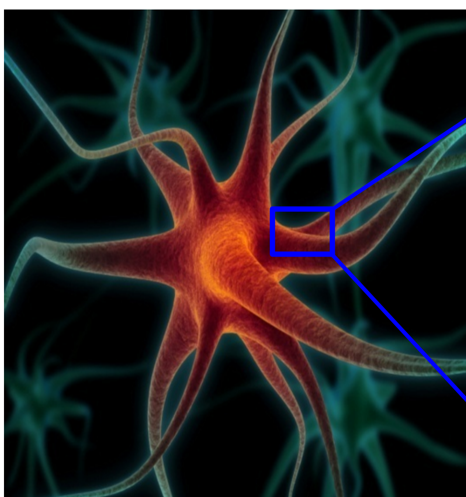

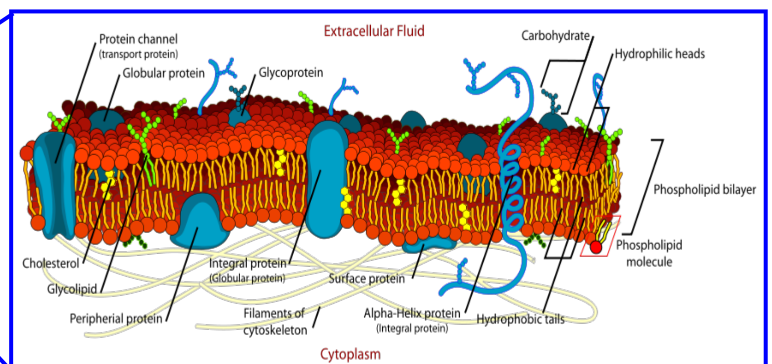

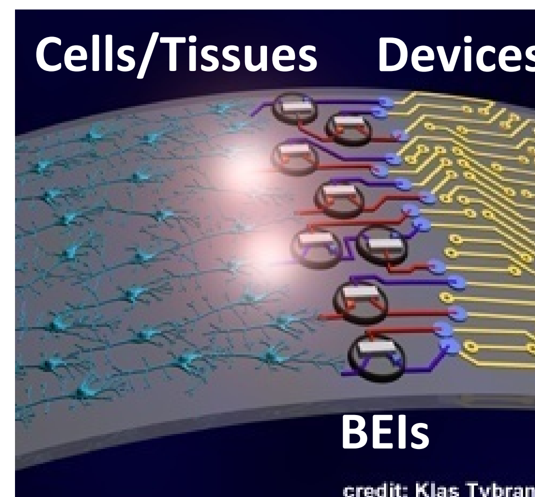

Conducting polymers match properties of tissue

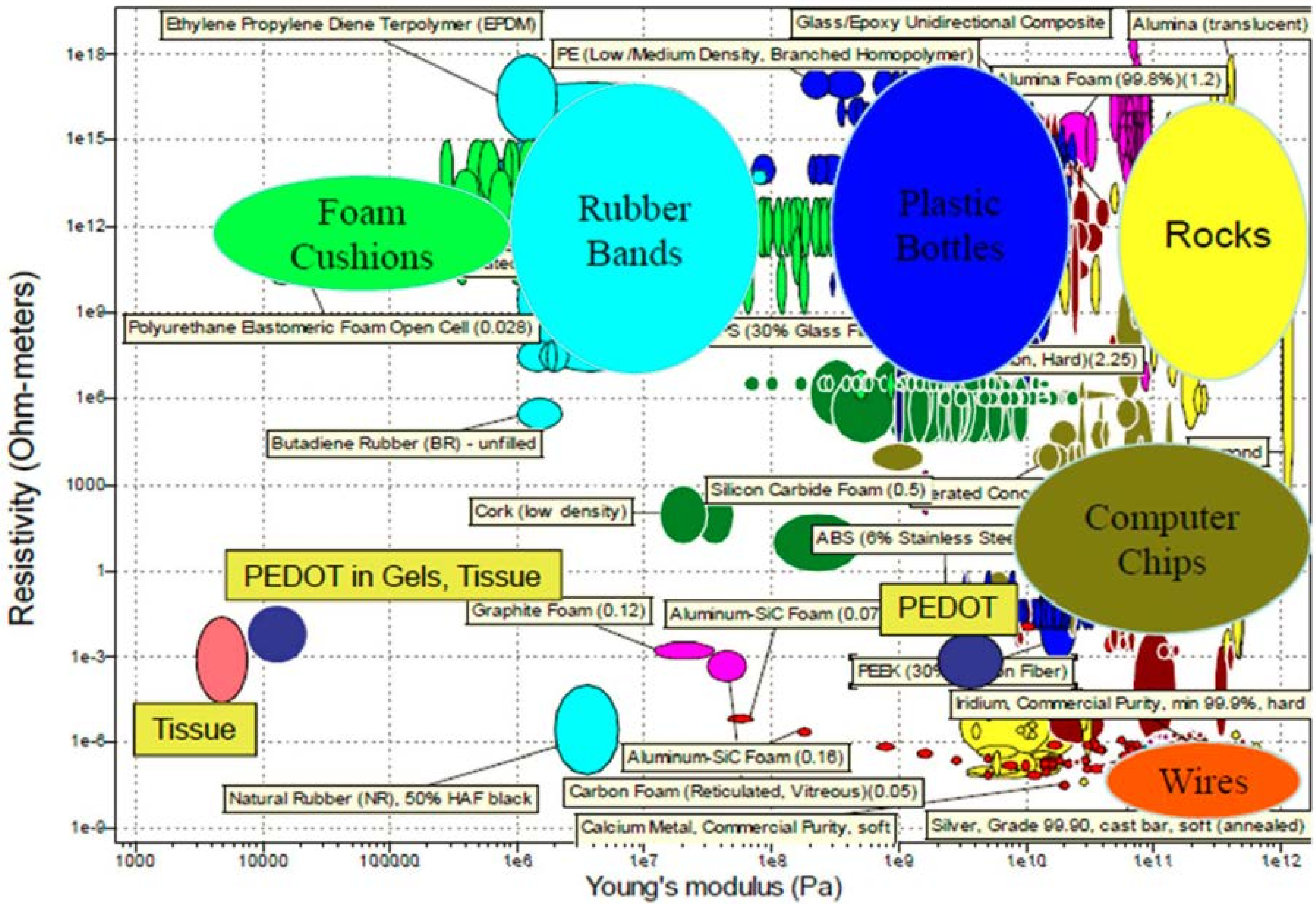

Slide courtesy of Dave Martin (U. Delaware)

Fundamental knowledge of Polymeric Materials

- **Polymers** are macro molecules formed of many identical units (called repeated units) bound to each other like pearls in a necklace.
- Flexibility & Lightweight.
- Cheap cost of production.
- Good electrical insulation.

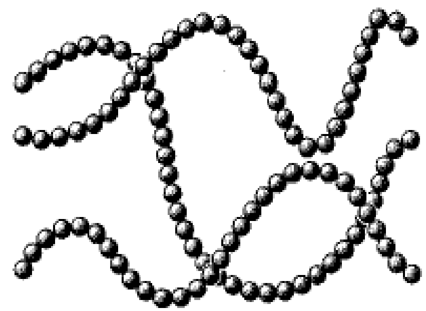

Applications:
Plastics
Rubbers
Fibers
Coatings

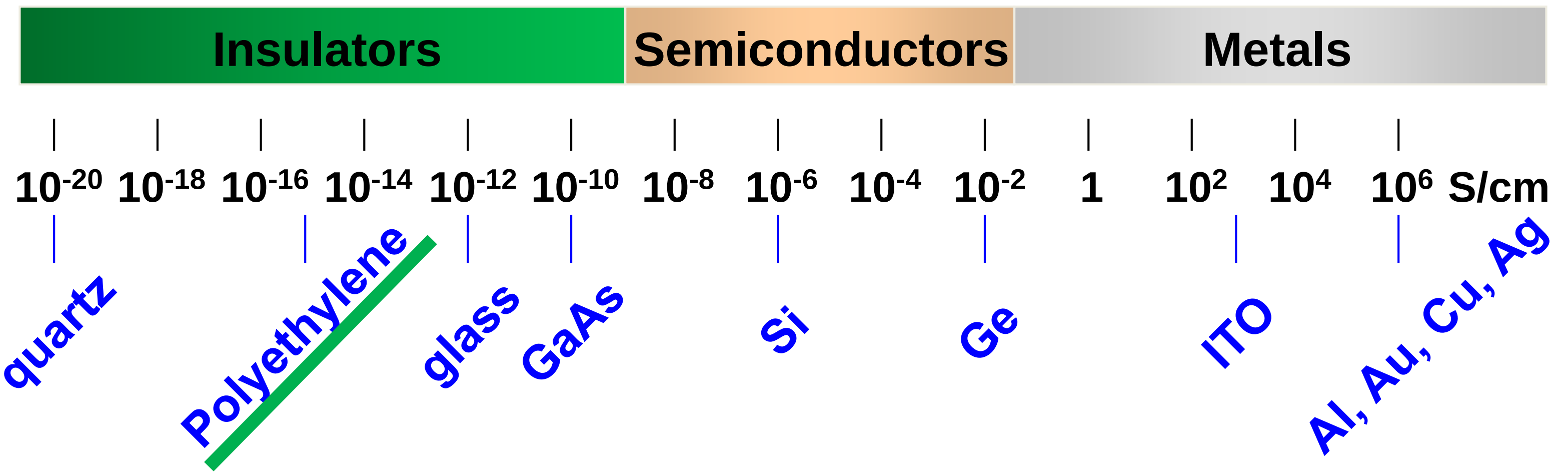

Plastics can be electrically conductive?!

The first conjugated conductive polymer established

1977, H. Shirakawa, A. G. MacDiarmid & A. J. Heeger

Doping of Polyacetylene

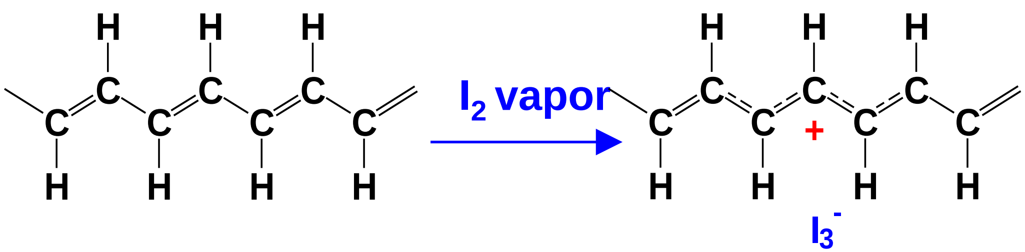

Polyacetylene (PA)
$\sigma \sim 10^{-5}$ S/cm

$\sigma \sim 38$ S/cm

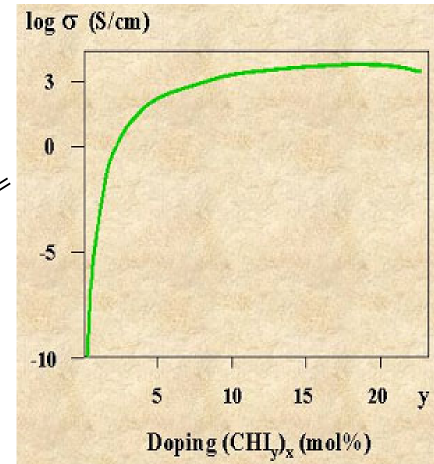

Discovery of **doping phenomena** and resulting **10 order of magnitude increase** in the conductivity of polyacetylene

Oxidation with iodine *causes the electrons to be jerked out of the polymer, leaving* ***"holes" in the form of positive charges*** *that can move along the chain.*

1977 $\sigma =$ 38 S/cm
2000 $\sigma =$ 30 000 S/cm
2000 $\sigma_{max} = 10^5$ S/cm
$\sigma_{Cu,Ag} = 10^6$ S/cm

Discovery of conducting polymers and the ability to dope these polymers over the full range from **insulator** to **metal**

J. Chem. Soc. Com. 1977, 578.
Phys. Rev. Lett. 1977, 39, 1098.

Chemical, Optical and Electrical Properties of Organic Semiconducting Materials

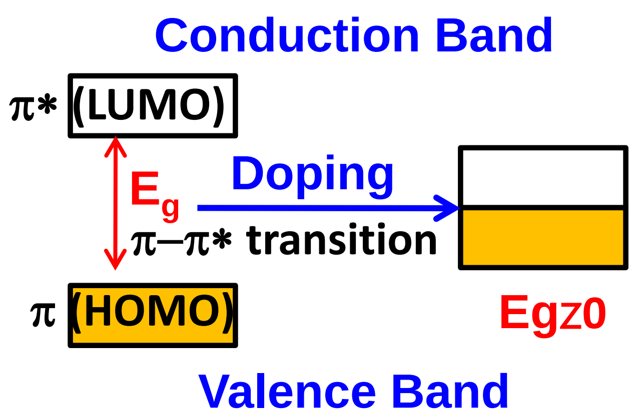

聚3,4-乙撐二氧噻吩(PEDOT)

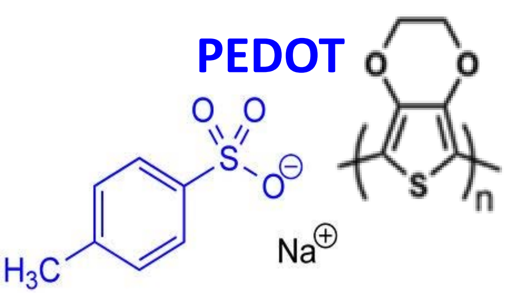

Polymer	Structure	Doping Materials	Conductivity (S/cm)
Polyacetylene PA	$(CH)_n$	I_2, Br_2, Li, Na, AsF_2	10,000[a]
Polypyrrole PPy	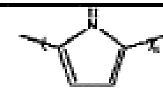	BF_4^-, ClO_2^-, tosylate[b]	500-7500
Polythiophene PTh	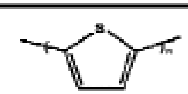	BF_4^-, ClO_2^-, tosylate[b], $FeCl_3$	1000
Poly(3-alkylthiophene) PTh	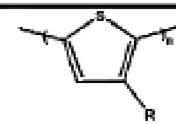	BF_4^-, ClO_2^-, $FeCl_2^-$	1000-10,000[a]
Polyphenylene sulfide PPS	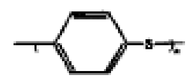	AsF_2	500
Polyphenylene-vinylene PPV	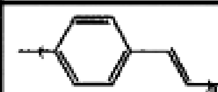	AsF_2	10,000[a]
Polythienylene-vinylene		AsF_2	2700[a]
Polyphenylene PPP	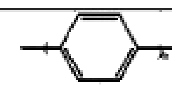	AsF_2, Li, K	1000
Polyisothianaphthene	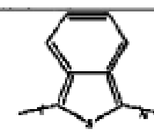	BF_4^-, ClO_4^-	50
Polyfuran	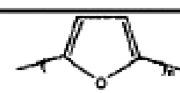	BF_4^-, ClO_4^-	100
Polyaniline PANI	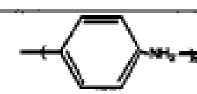	HCl	200[a]

Pi-conjugated Materials and their Applications

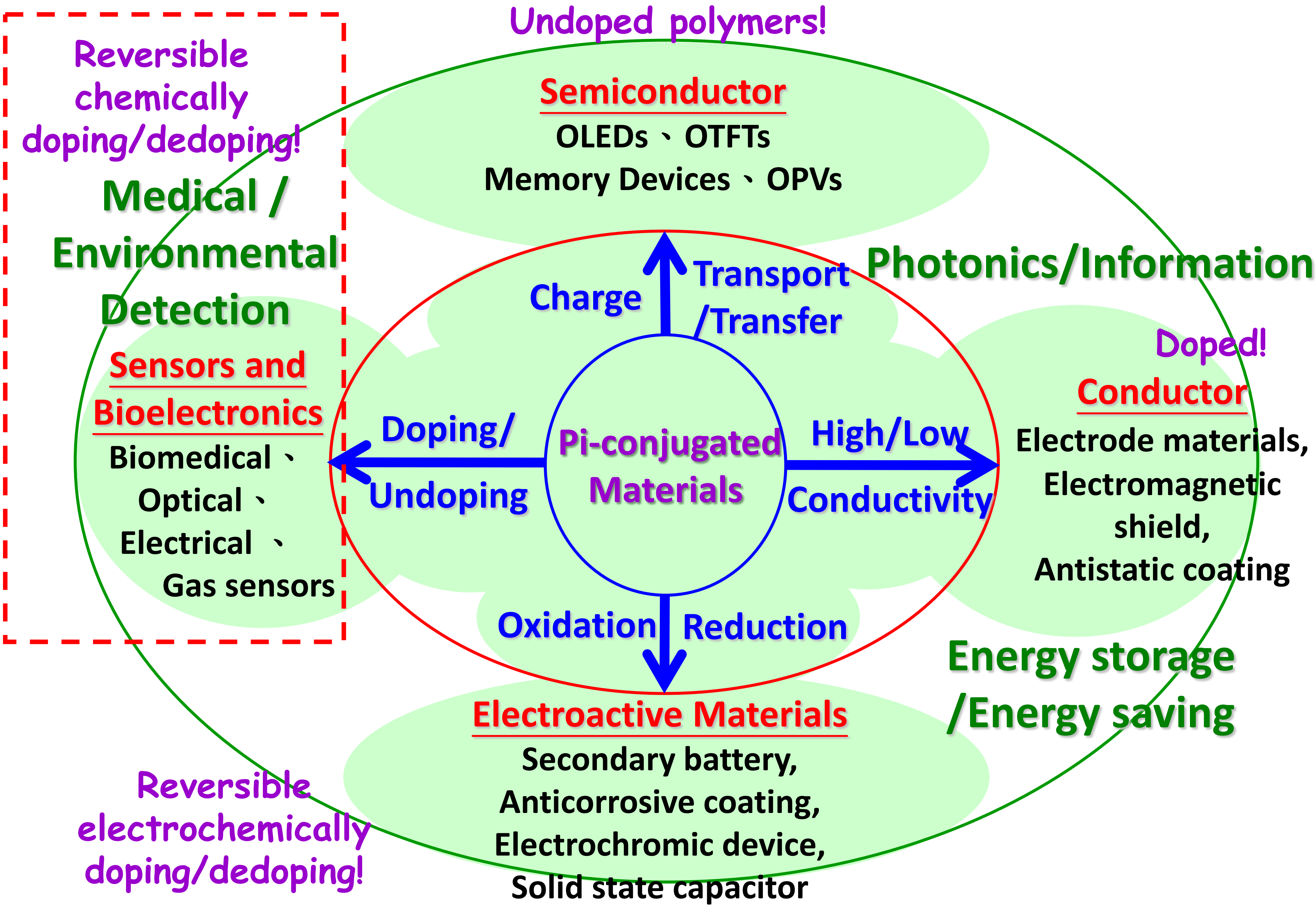

Micro/Nanofabrication Technologies

- **Chemical Vapor Deposition (CVD)**

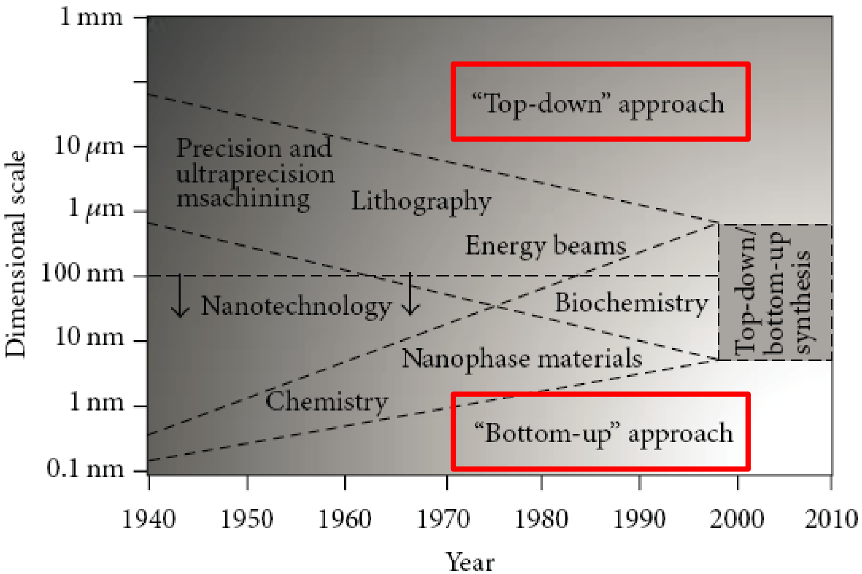

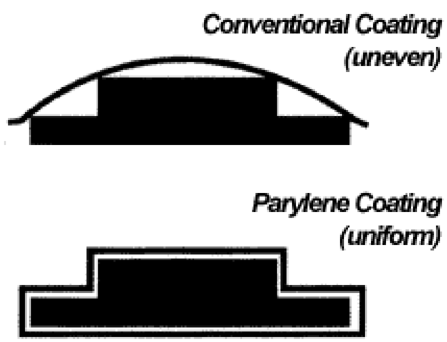

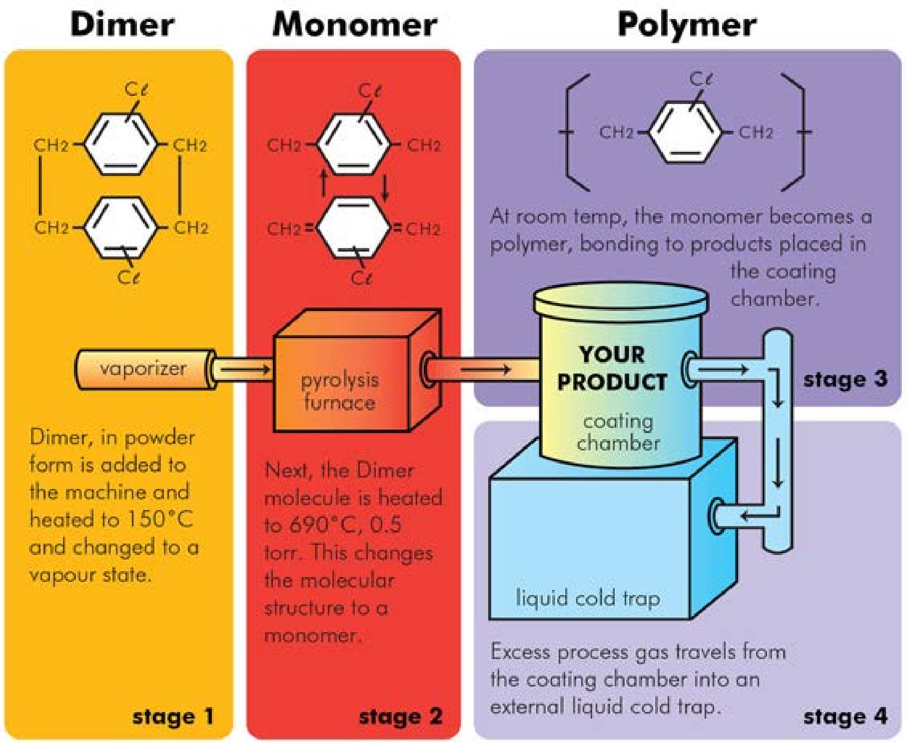

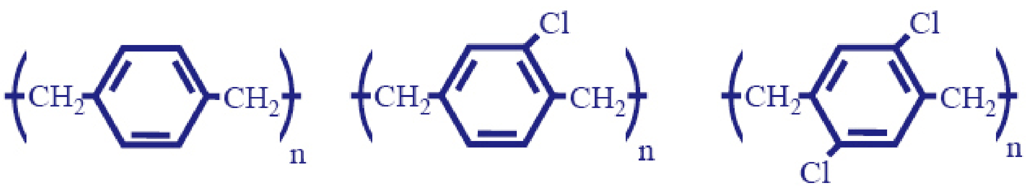

Parylene N Parylene C Parylene D

http://www.metalimprovement.co.uk/register.php

Vapor-Based Multicomponent Coatings for Antifouling and Biofunctional Synergic Modifications

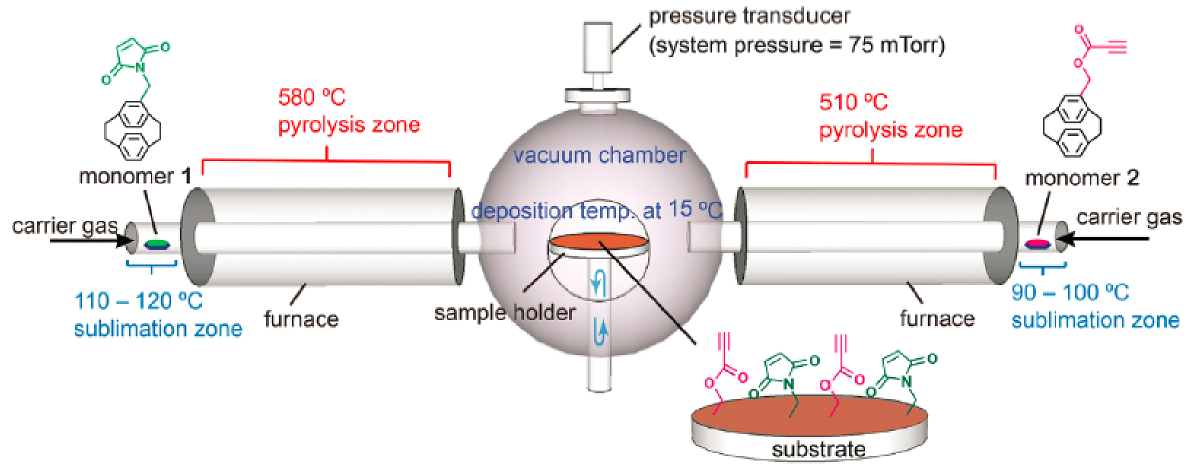

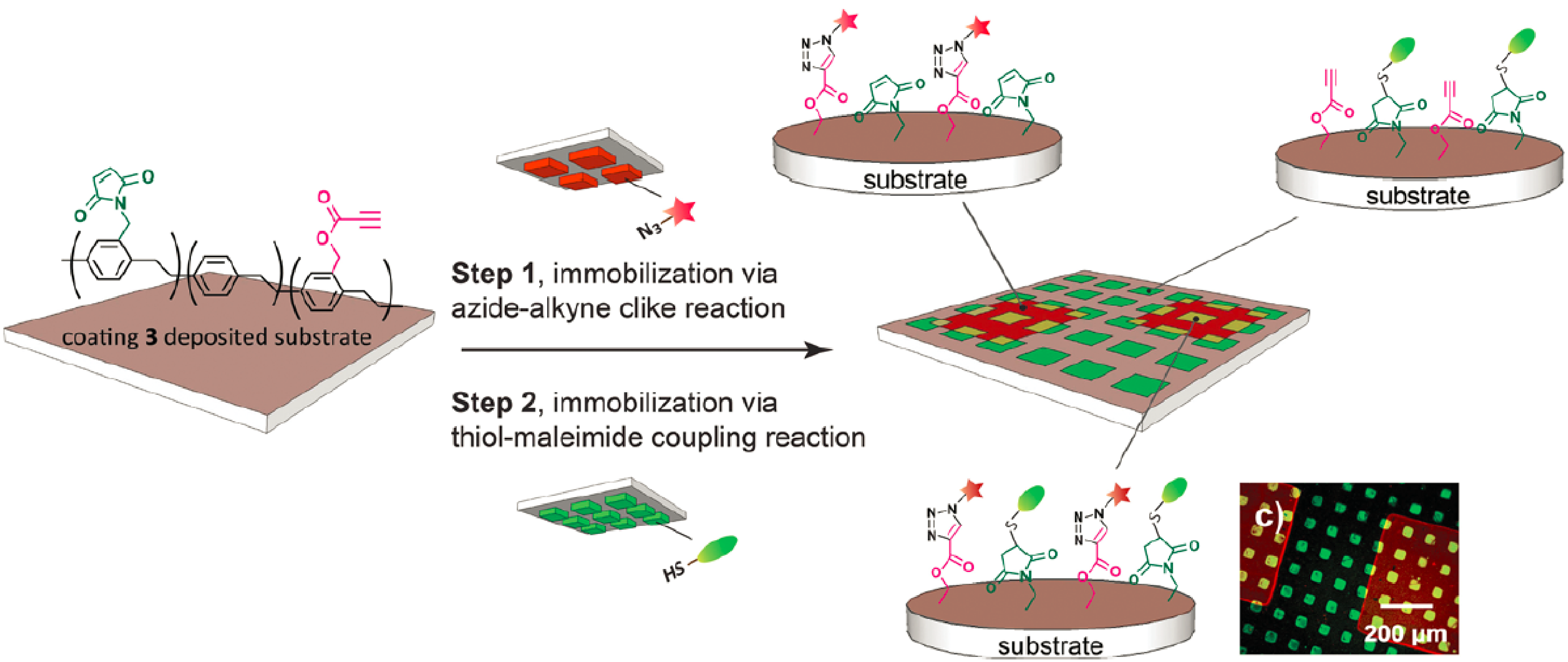

Adv. Funct. Mater. 2014, 24, 2281

• Soft Lithography

They are essentially based on **printing**, **molding**, **embossing, and transferring** with an elastomeric stamp.

4) Micro-molding in Capillaries (MIMIC)

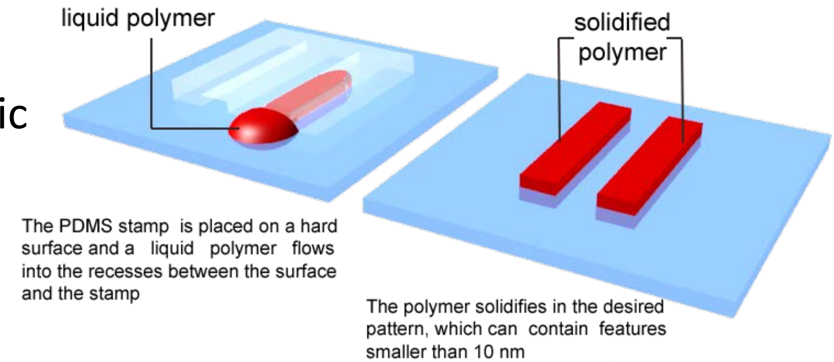

5) Nanotransfer Printing

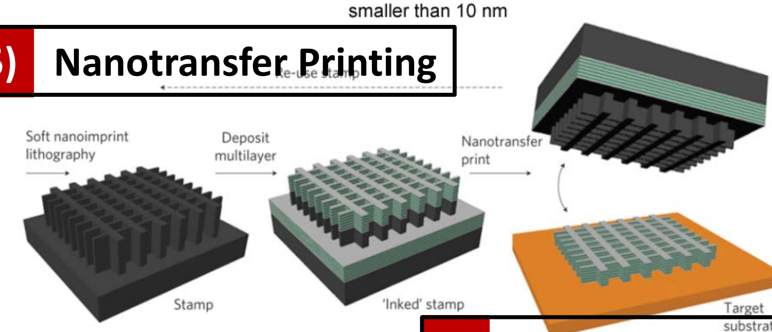

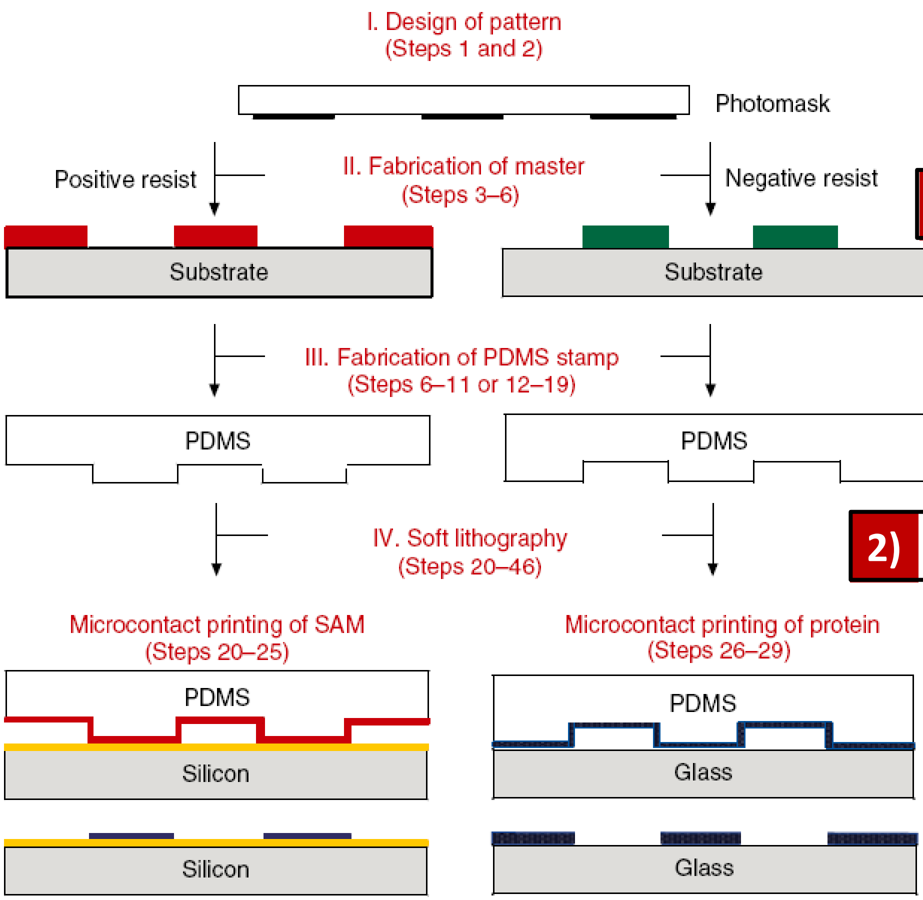

2) Replica Molding (REM)

3) Solvent-assisted Micromolding (SAMIM)

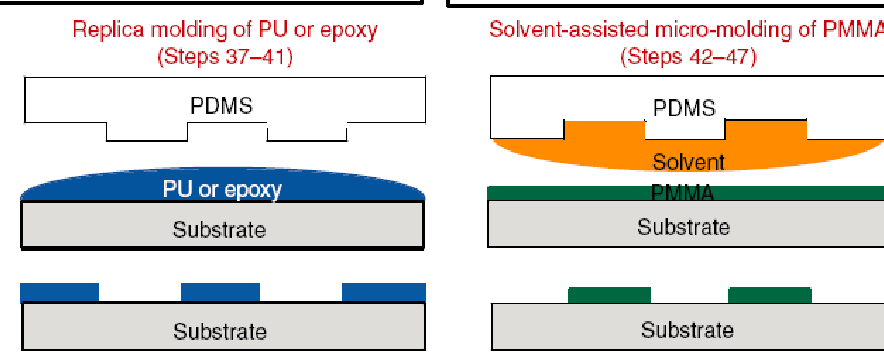

Figure 1 | Schematic illustration of the four major steps involved in soft lithography and three major soft lithographic techniques.

1) Microcontact Printing (μCP)

Nature Protoc. 5, 491–502 (2010). Nature Nanotechnology 6, 402–407 (2011)

(1) Artificial Designs for Cell Manipulation : (e. g., Neuron Cells) (1-5)

(Extracellular Environments)

1. Contact attraction

Poly-L-lysine, ECM, etc.
(+Electrical stimulation)

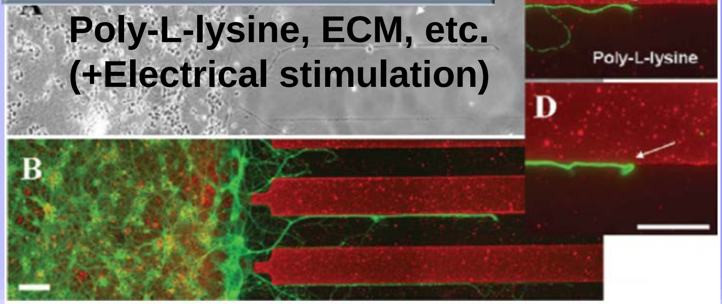

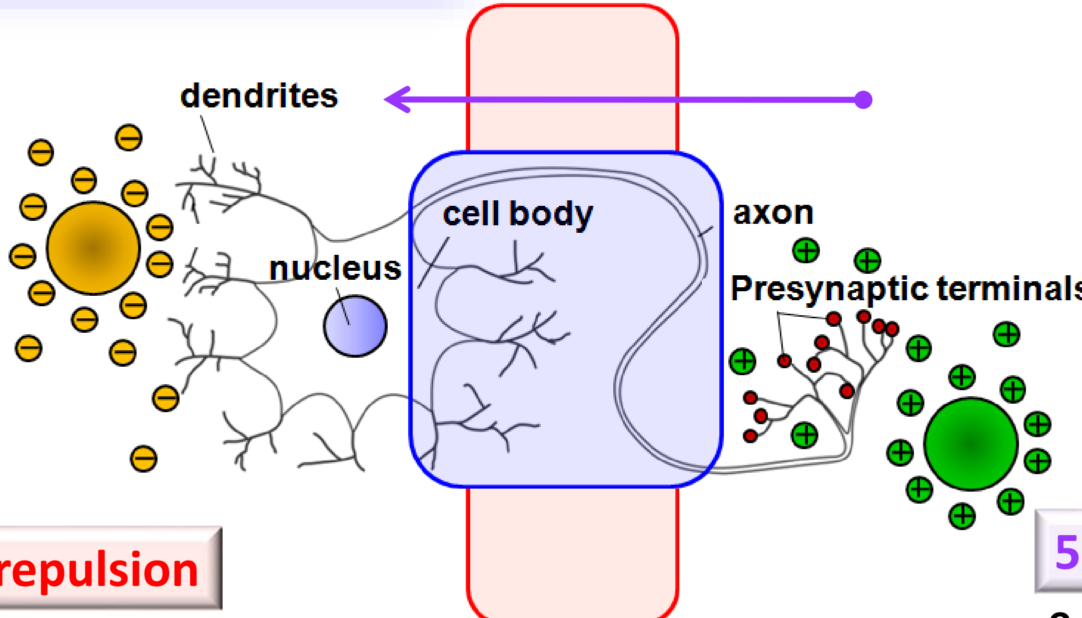

3. Chemoattraction

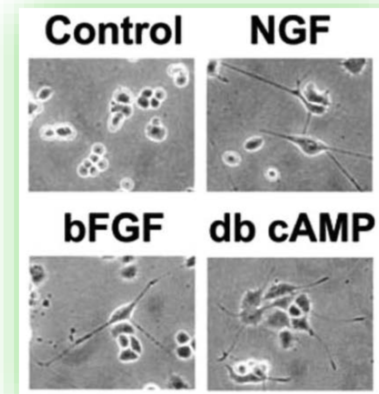

4. Chemorepulsion

2. Contact repulsion

(+Electrical stimulation)

(Pluronic, PEO-PPO-PEO)

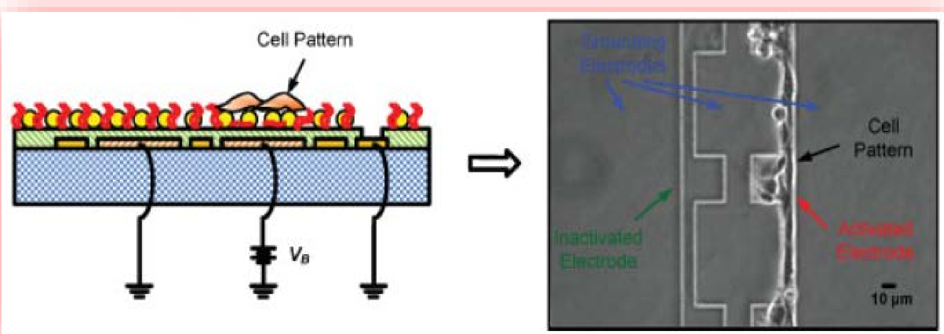

5. Electrical Field

e.g., Dielectrophoresis (DEP)

Electrical response:
- Signaling
- Stimulation

Photo response:
- Stimulation

Neuron cell.
Osteoblast.
Myoblast.
Fibroblast.

Cell–Substrate Anchorage Driving Key Cellular Processes

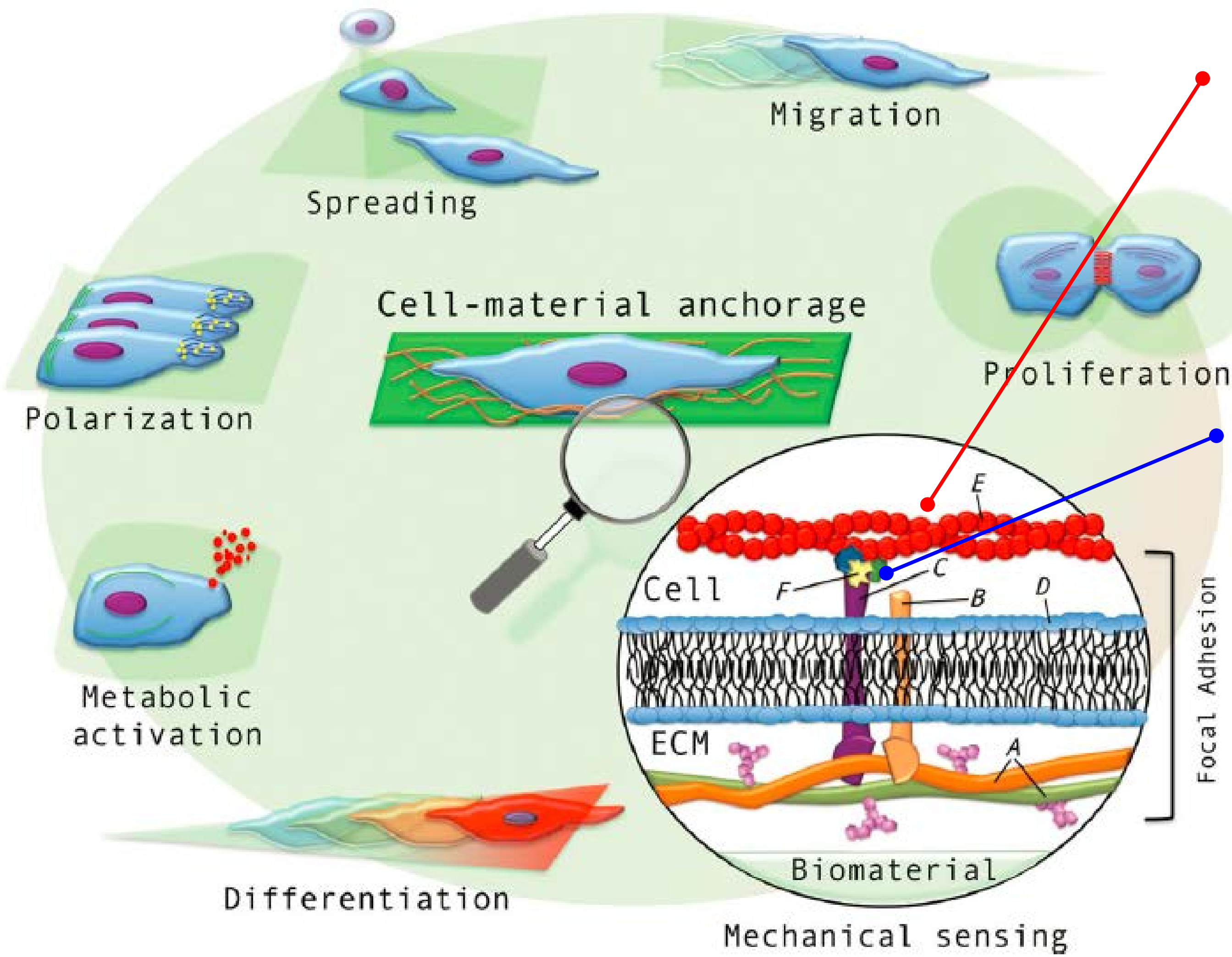

E. Action plays a key role for cell migration.

F. Cell adhesion is mediated by focal adhesions (FA)

Adv Mater, 2013, 25, 4049–4057.

Cell Adhesion

Cell-Substrate Interaction:

Weak Adhesion (attachment)

Intermediate Adhesion (Cell shape and spreading)

Strong Adhesion (Focal adhesion and stress fibers)

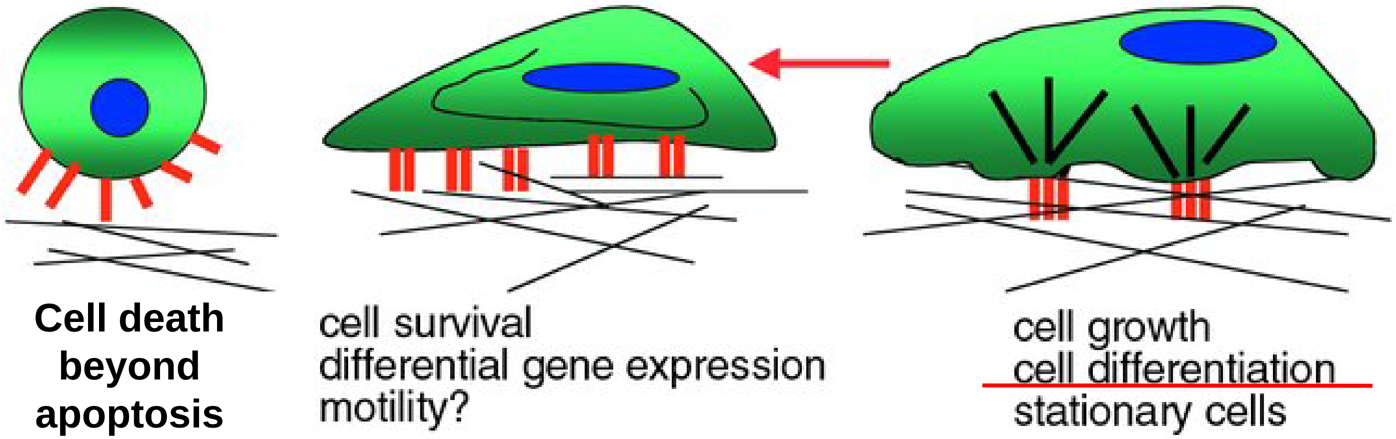

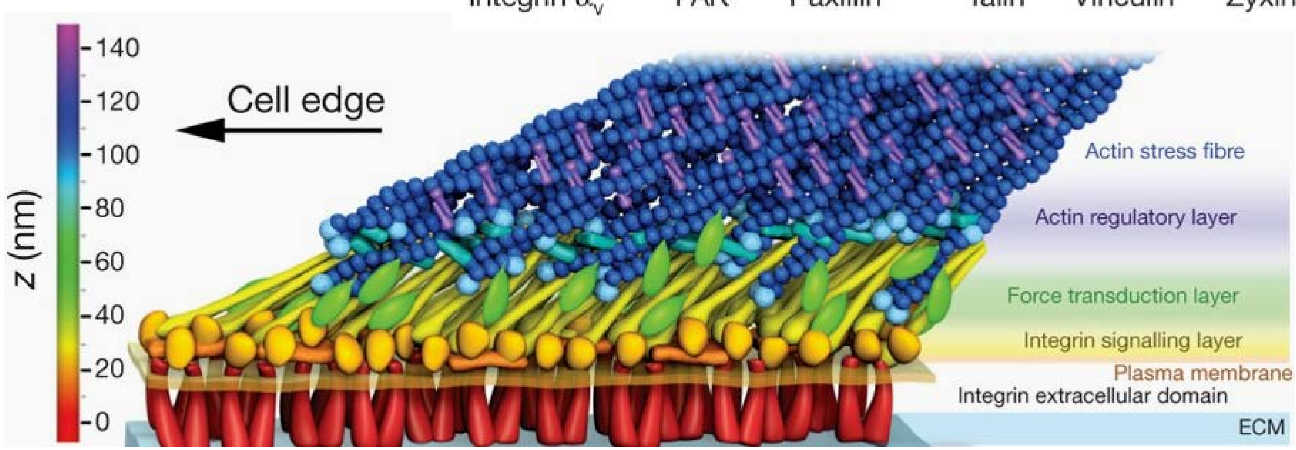

Focal adhesion proteins

Nature, 468, (2010) 580-584.

Actin Cytoskeleton in a Migrating Cell

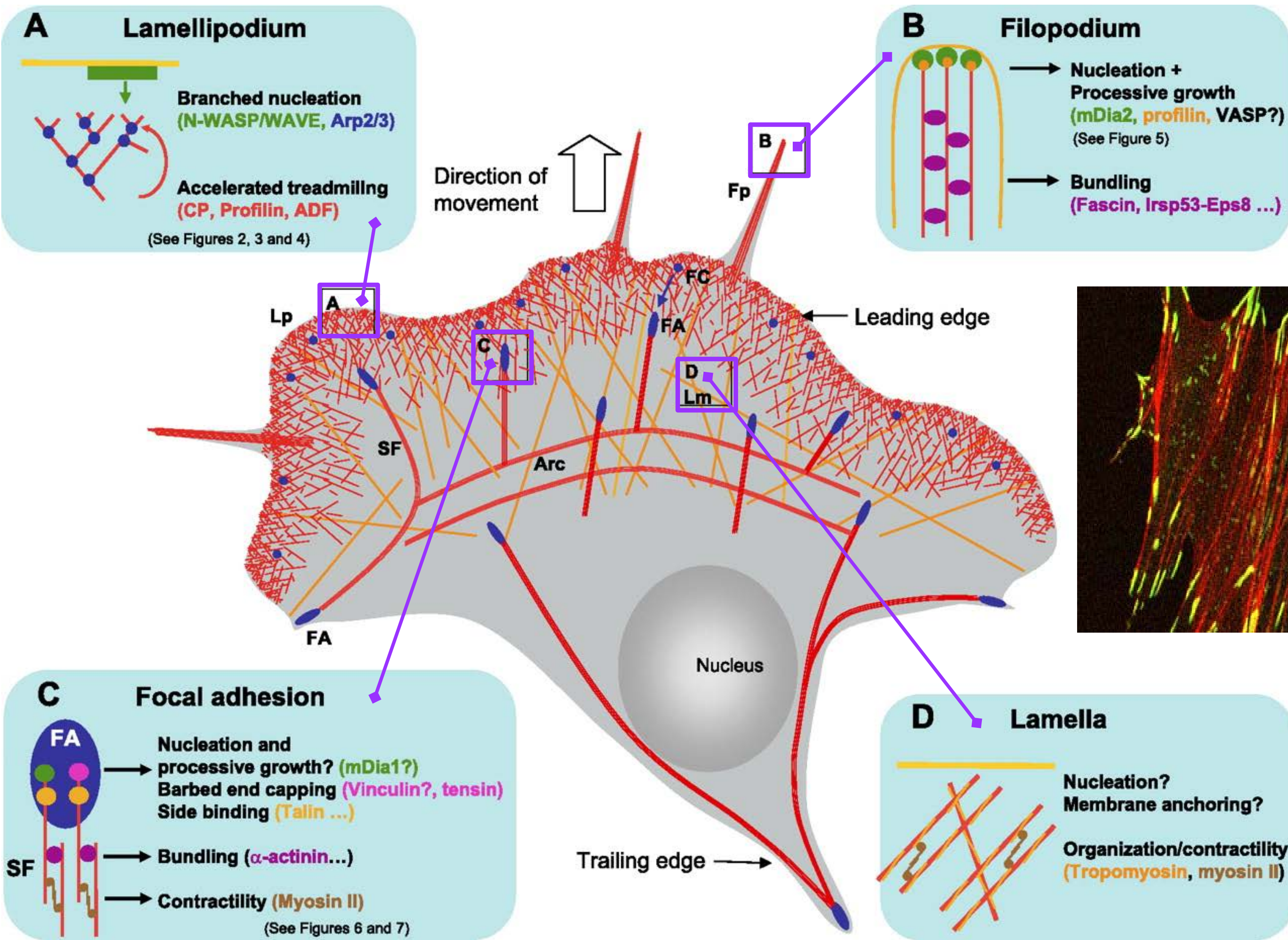

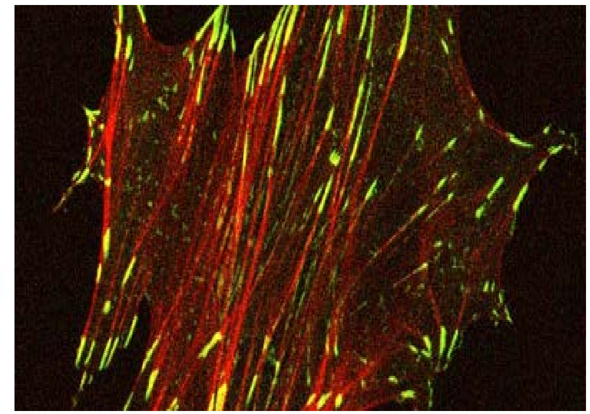

Physiological Reviews

Lp: lamellipodium; **Fp**:filopodium; **Lm**:lamella; **SF**:stress fiber; **FA**:focal adhesion; **FC**:focal complex

Physiol Rev, 88 (2008) 489-513.

Once the **lamellipodium** has formed, **adhesion complexes** assemble and attach it to the surface allowing the **cell to generate traction**. Adhesion complexes are dynamic structures and are constantly being assembled and disassembled in actively migrating cells. These adhesion sites are composed of complexes of **more than 50 different proteins**. When the cell comes to **a stop the focal adhesion complexes (FC)** can **mature into more stable focal adhesions (FA)**.

Structure of an adhesion complex in migrating cells

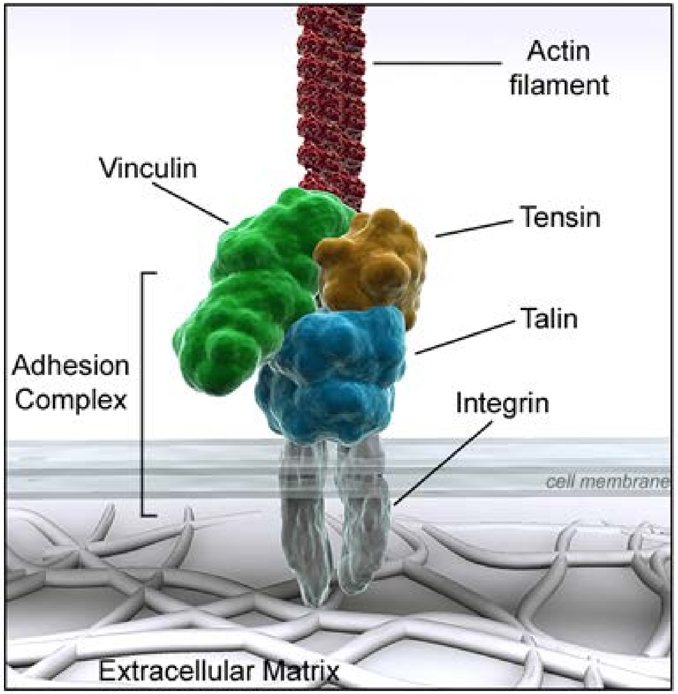

The dynamic assembly and disassembly of focal adhesions plays a central role in cell migration.

Composition of a focal adhesion

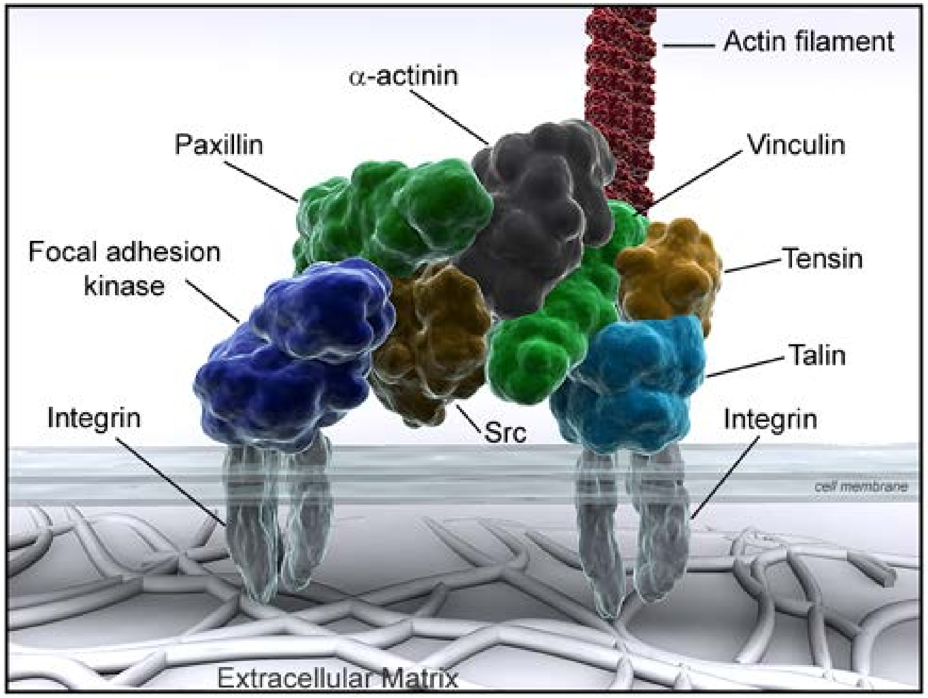

Mechanical force and regulatory signals are transmitted

Surface Potential

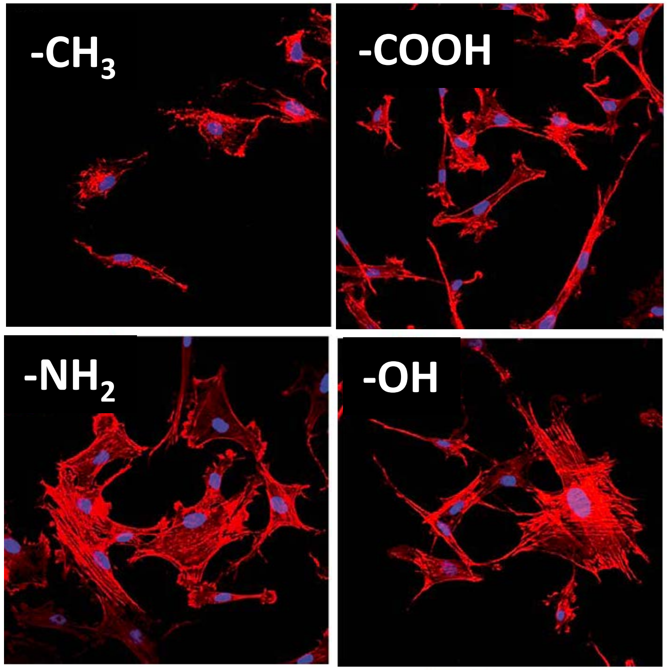

Soft Matter, 2011, 7, 3808

Hydrophobic Barrier

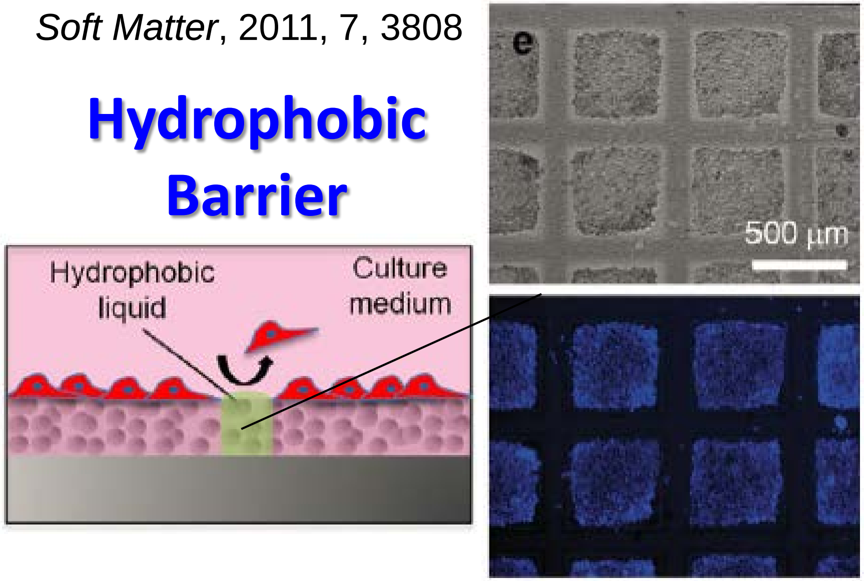

Adv. Healthcare Mater. 2013, 2, 1425.

Surface Morphology & Wettability

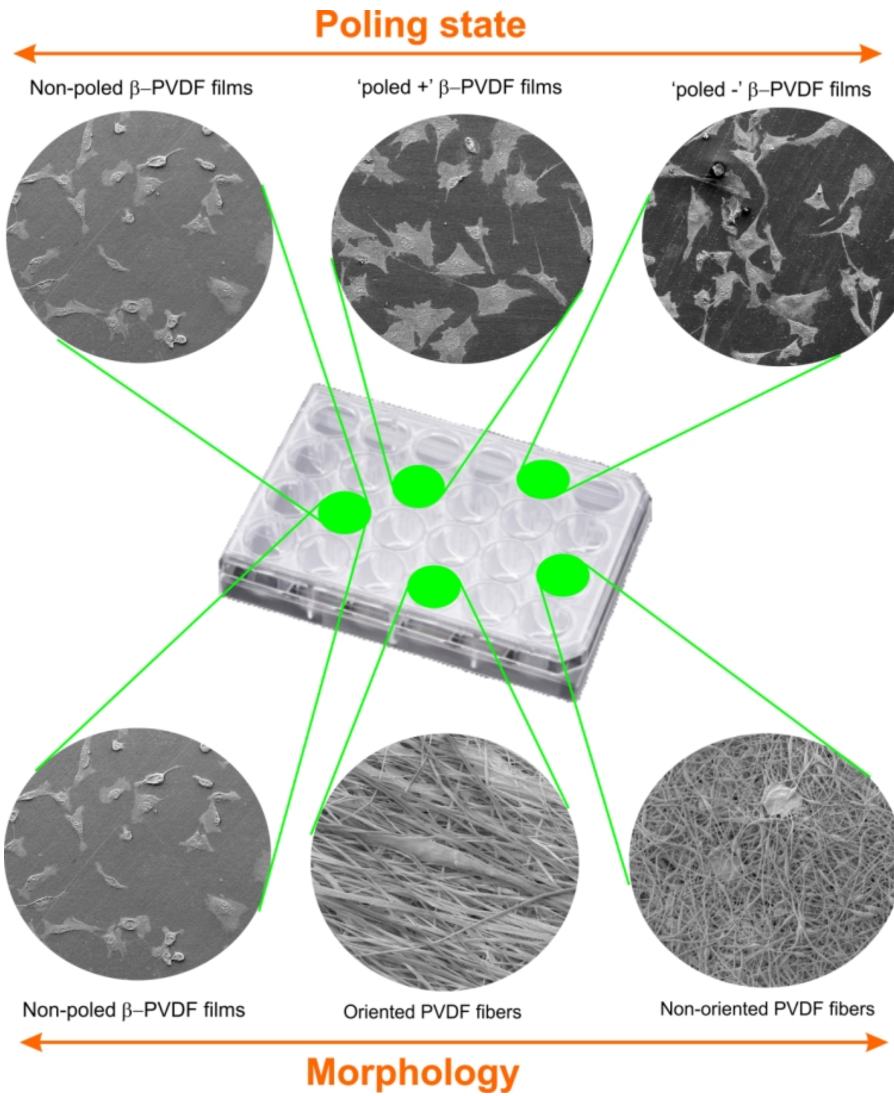

RSC Adv., 2013, 3, 17938.

Organic Bioelectronic Interfaces

(1) Materials

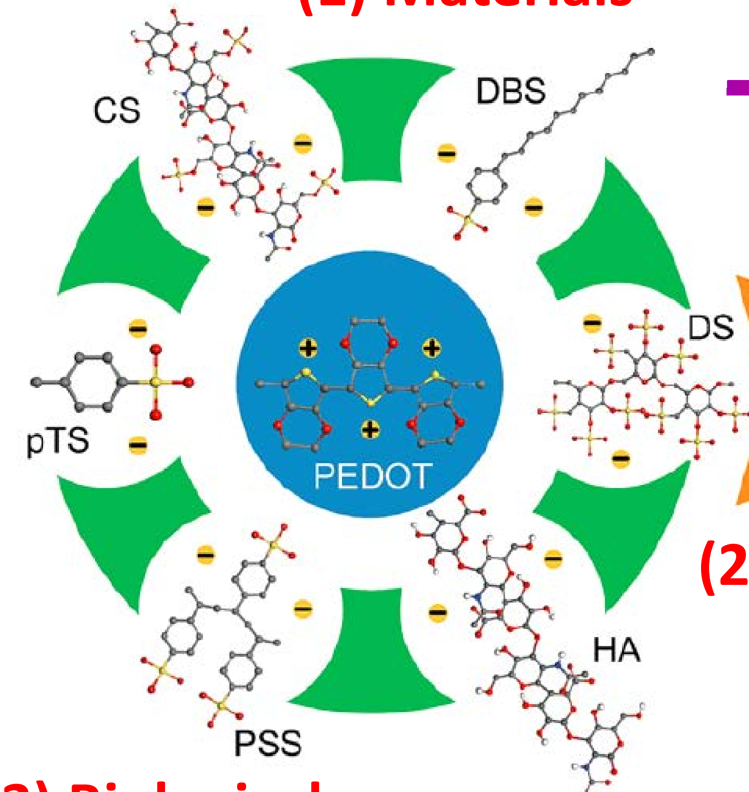

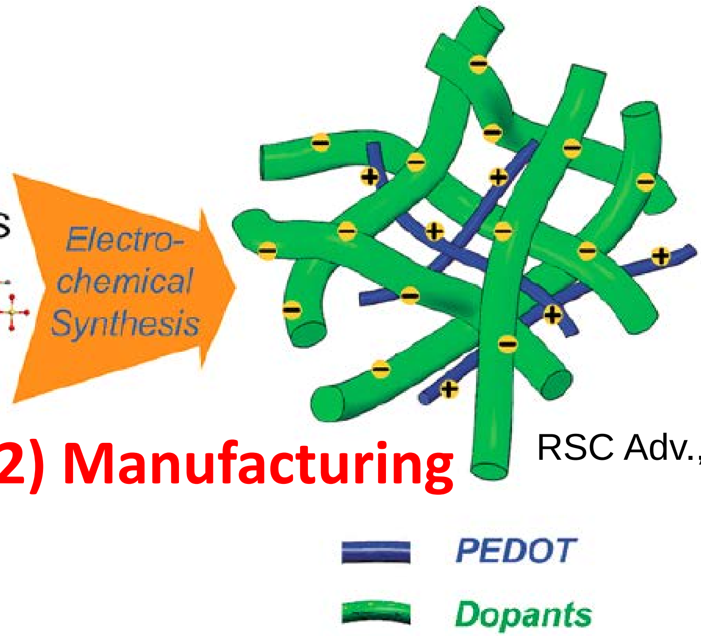

(2) Manufacturing

RSC Adv., 2014, 4, 47461–47471.

(3) Biological Applications

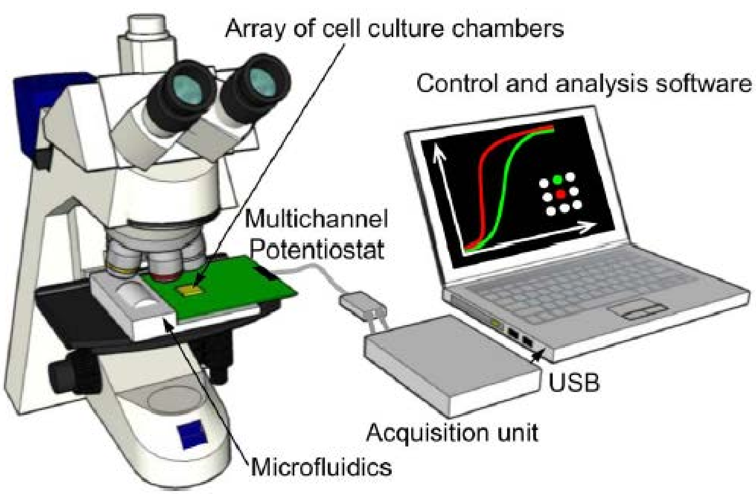

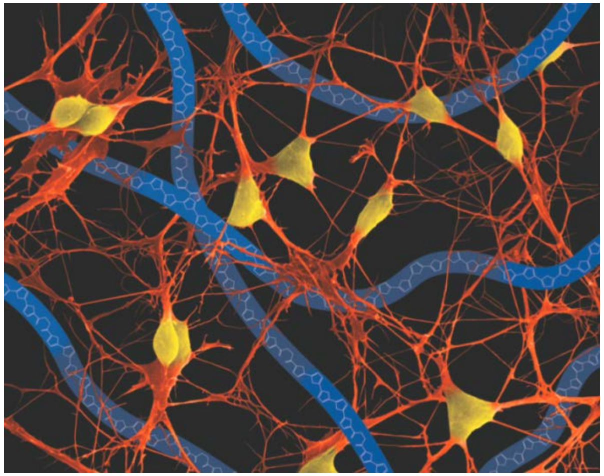

Nature Materials, 2014,13, 775.

Spatial Resolution of Biological Imaging Techniques

Abbe's Diffraction Limit (0.2μm)

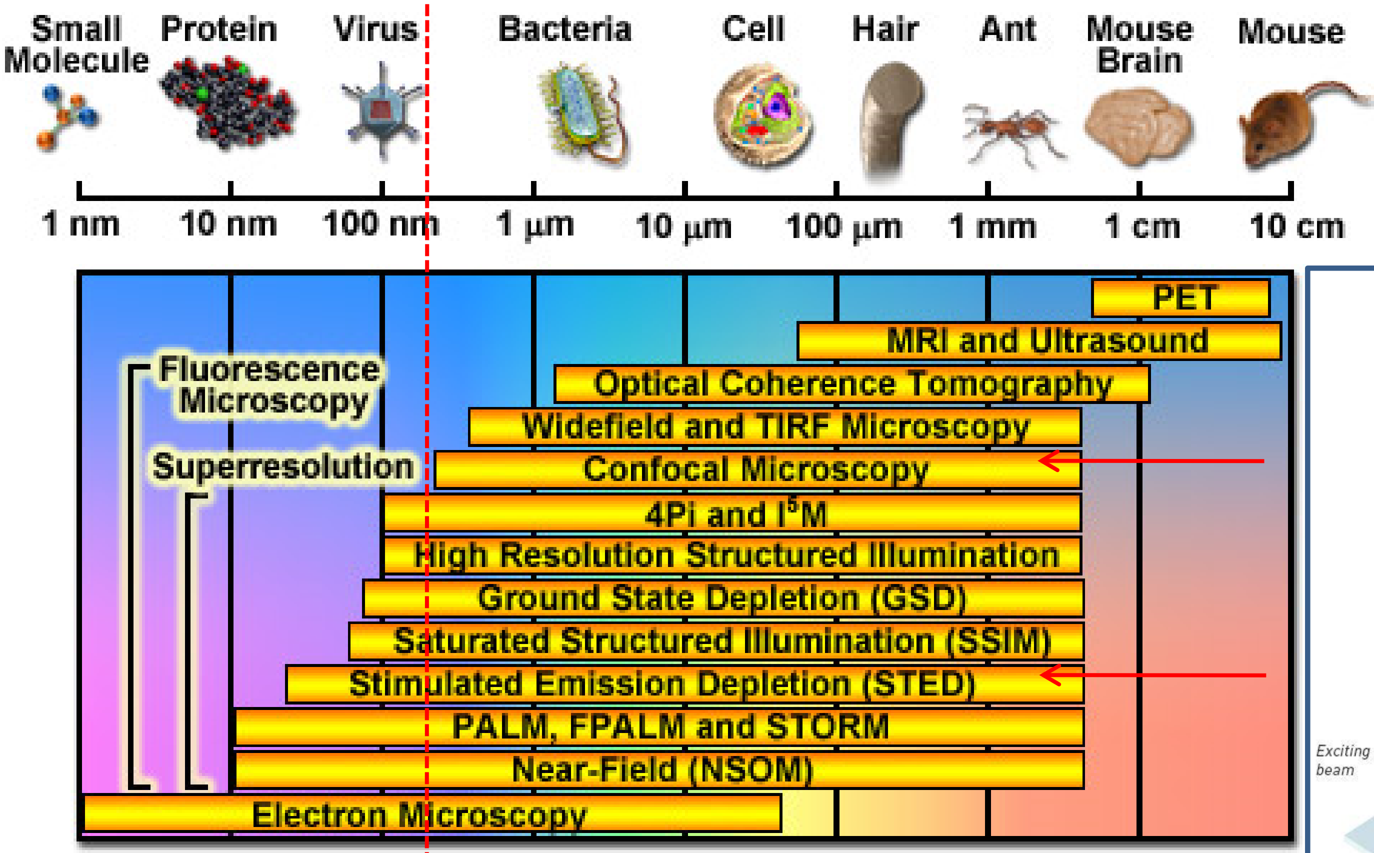

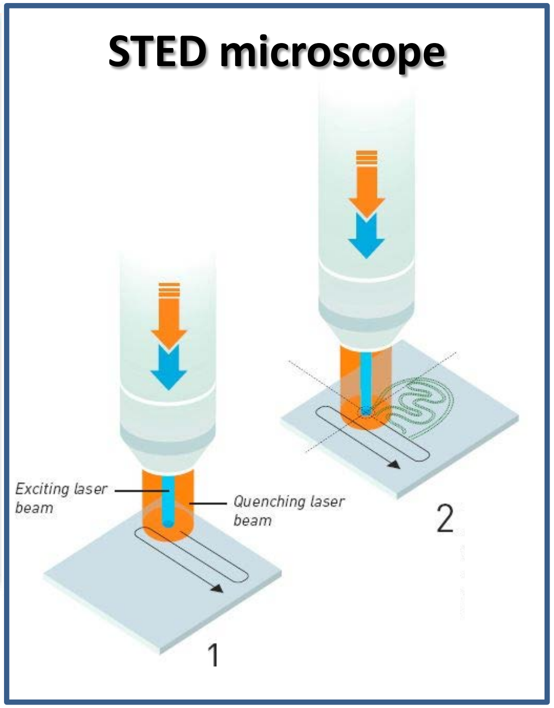

http://www.nobelprize.org/nobel_prizes/chemistry/laureates/2014/

Limit of resolution:

- **Human eye:** 0.1 mm.
- **Optical microscope:** 60-200 nm.
- **Scanning electron microscope (SEM):** 5-10 nm.
- **Transmission electron microscope (TEM):** 0.5 nm.

Ref: Carl Zeiss Microscopy Online Campus

Importance of neural interfacing

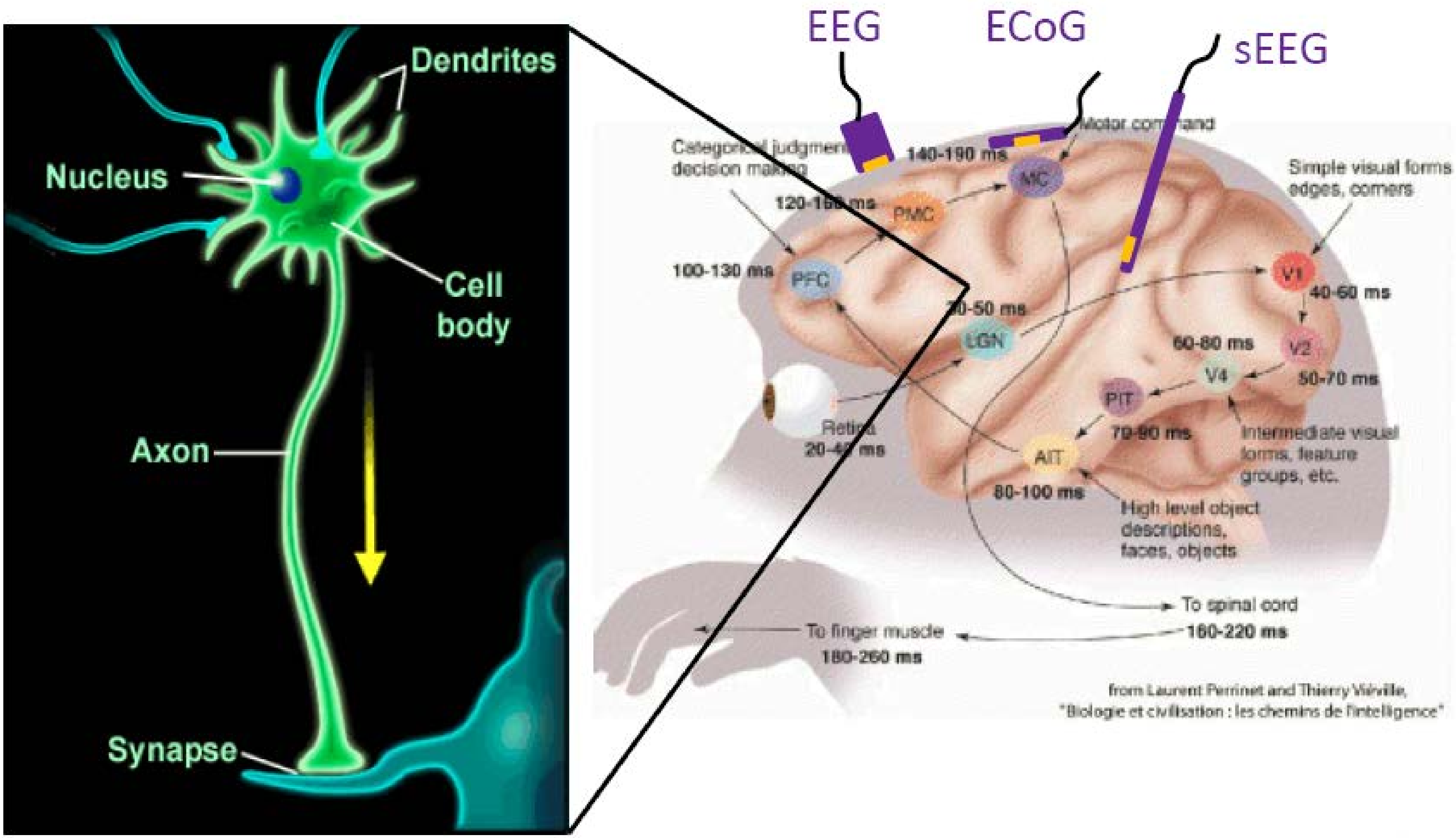

Epilepsy

- Affects 1-2% of world population
- Temporal lobe epilepsy (TLE) is most frequent form in adults
- TLE is often drug resistant

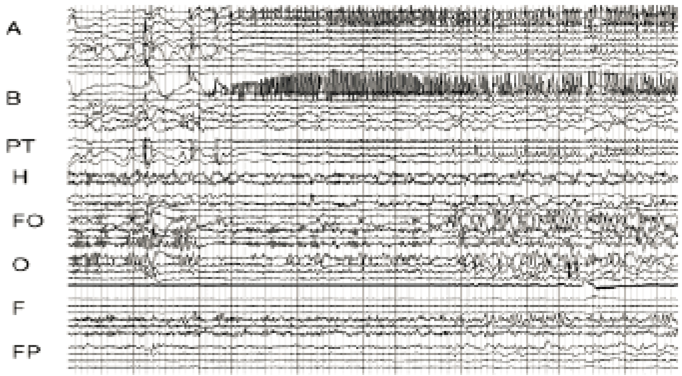

Key challenges:

- Improve electrode performance
- Make less invasive recordings

Deep brain stimulation for Parkinson's

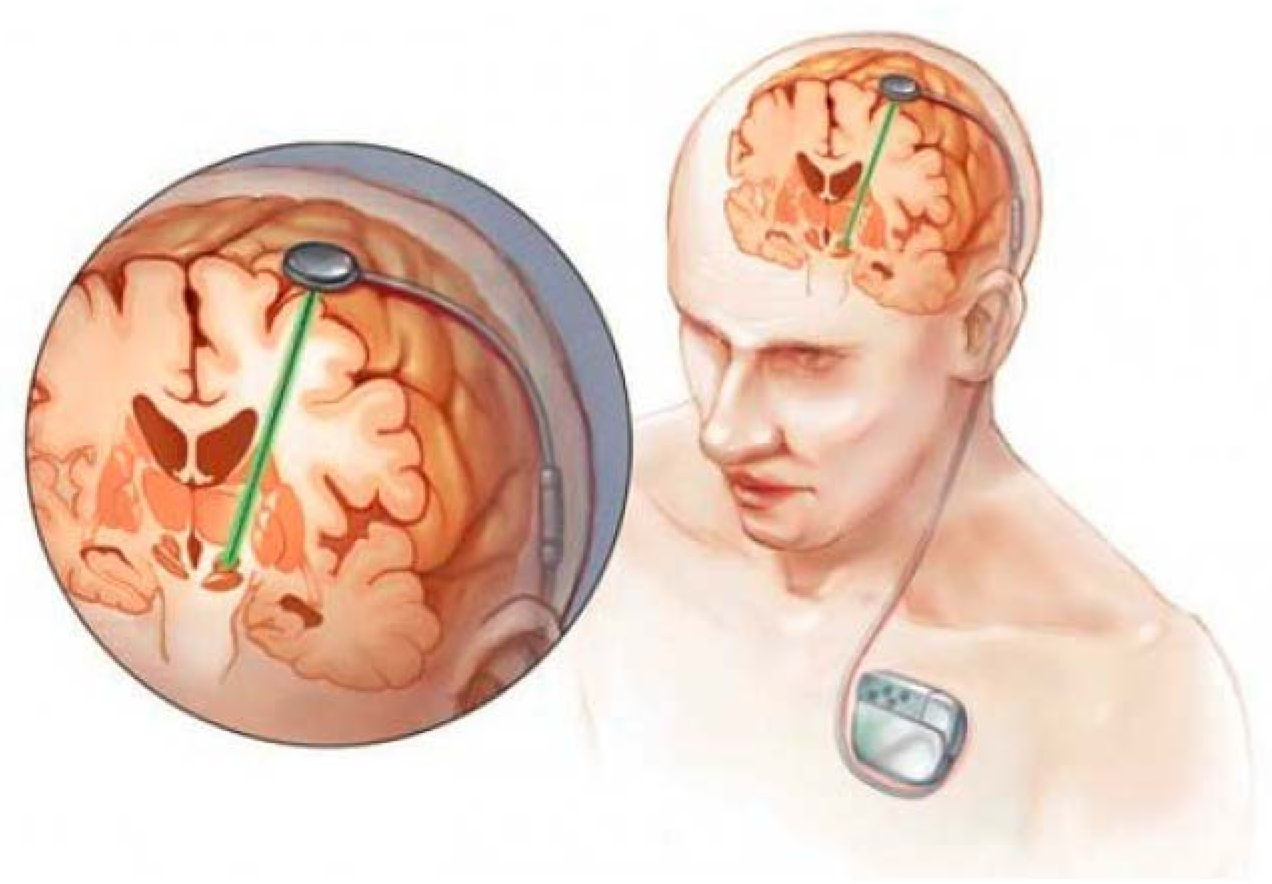

Implantable Electronic Medical Devices

- **Approved devices:**
  - Heart pacemakers – 600,000 per year
  - Cochlear implants (hearing) – 300,000 patients
  - Spinal cord stimulators (pain relief) – 15,000 per year
  - Deep brain stimulators (Parkinson's)
  - Phrenic nerve stimulators (assisted breathing)
  - Sacral nerve stimulators (bladder control)
  - Vagus nerve stimulators (epilepsy)
  - Retinal implants (vision)

Implantable defibrillator
(Medtronic)

Cochlear implant
(Cochlear)

- **In development:**
  - Functional electrical stimulation (standing and gait)
  - Brain Computer Interfaces (control of robotic limbs)
  - DBS (severe psychiatric conditions)
  - Vestibular prostheses (balance)
  - Vision prostheses (vision)
  - Cortical prostheses (epilepsy detection & suppression)

Artificial limbs controlled by the brain
(Penn Center for Brain Injury and Repair)

Conducting polymer microelectrodes record single neurons from brain surface

Levels of neural interfacing

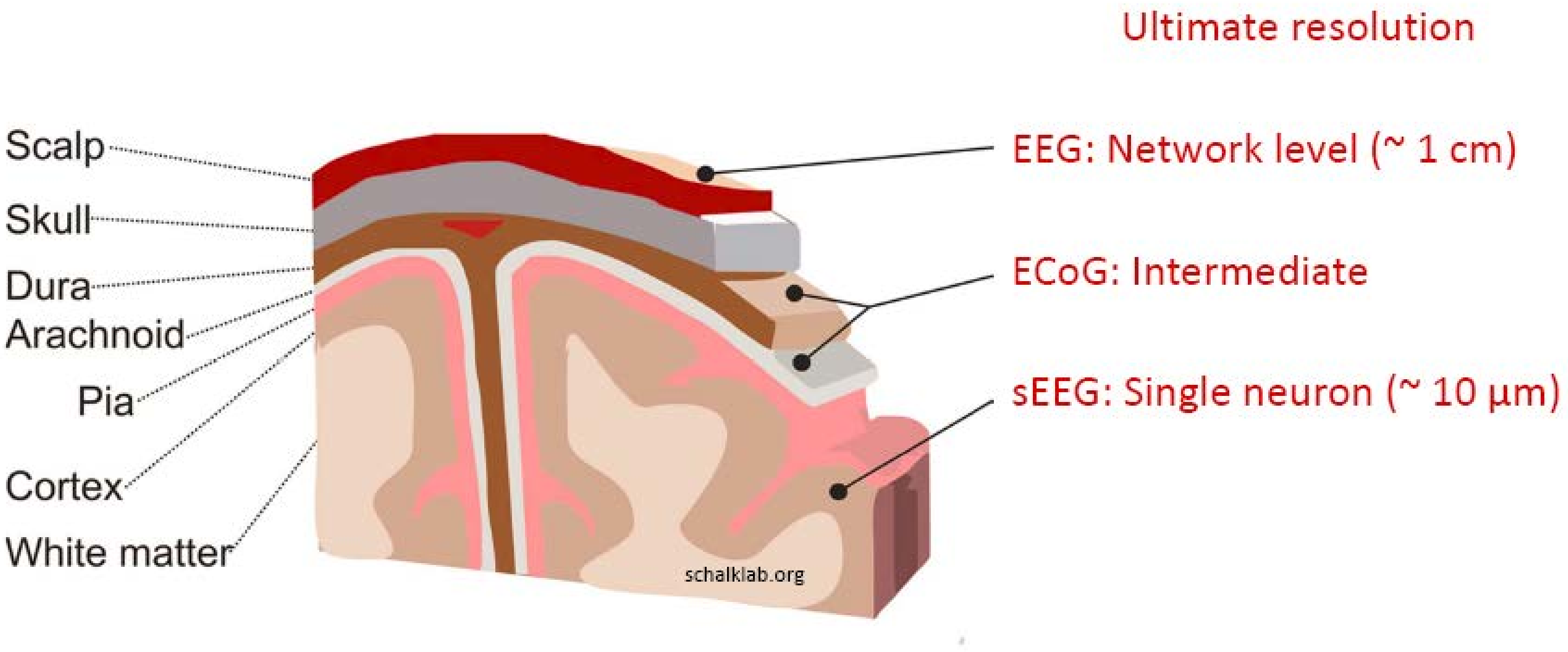

It was not considered possible to obtain single neuron recordings without penetrating the brain

State-of-the-art ECoG circa 2010

nature materials
ARTICLES
PUBLISHED ONLINE: 18 APRIL 2010 | DOI: 10.1038/NMAT2745

Rogers group (UIUC)

Dissolvable films of silk fibroin for ultrathin conformal bio-integrated electronics

Dae-Hyeong Kim and Jonathan Viventi *et al.**

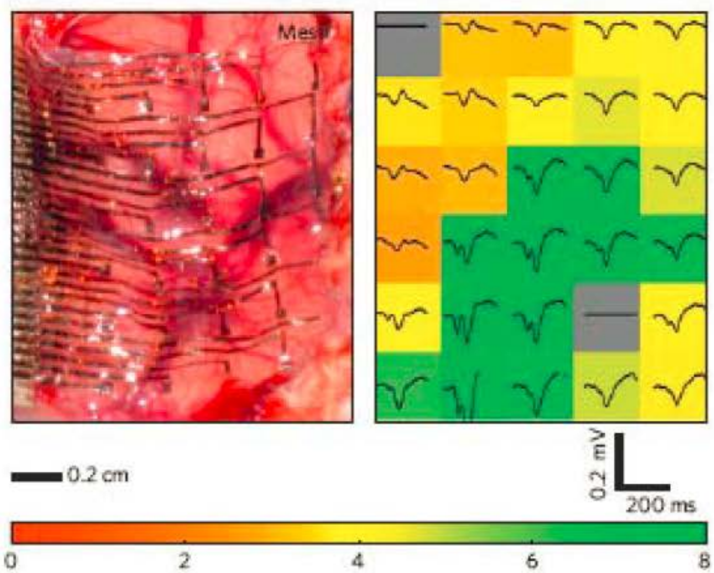

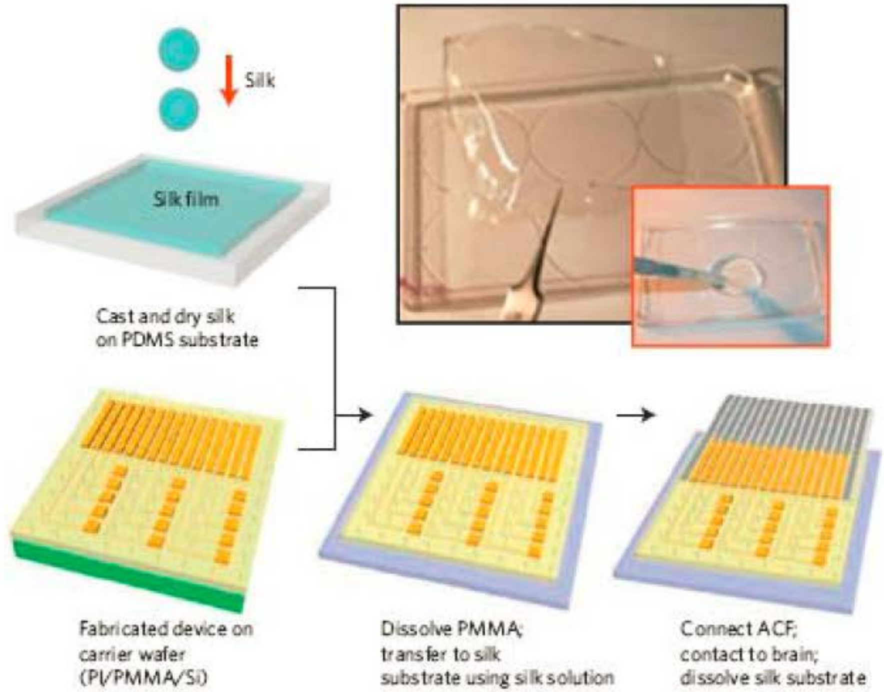

Conducting polymers improve neural interfaces

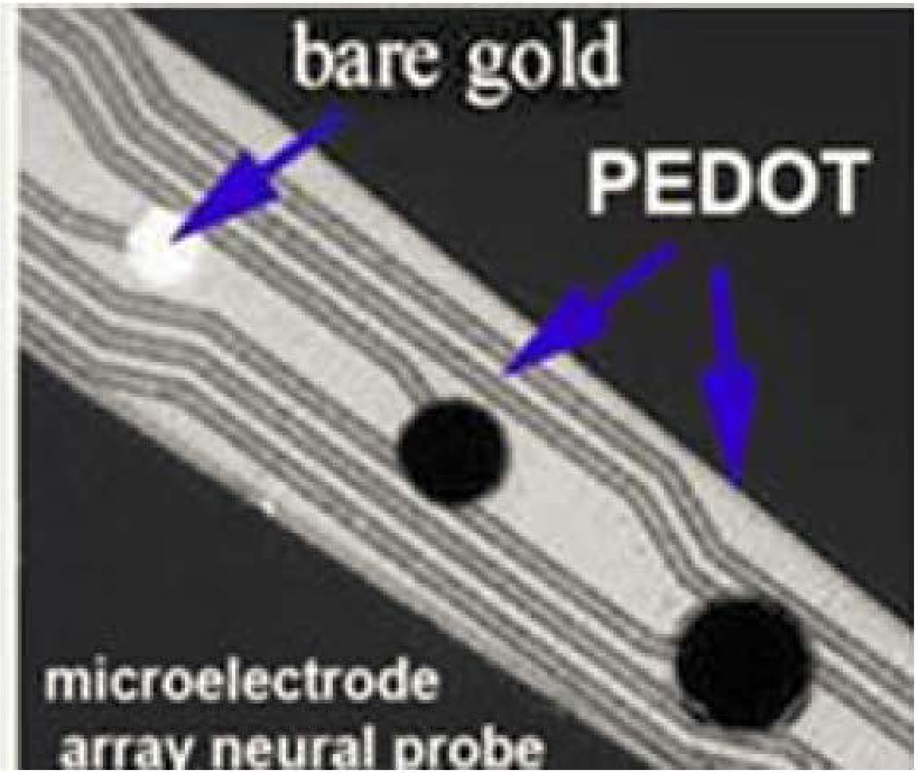

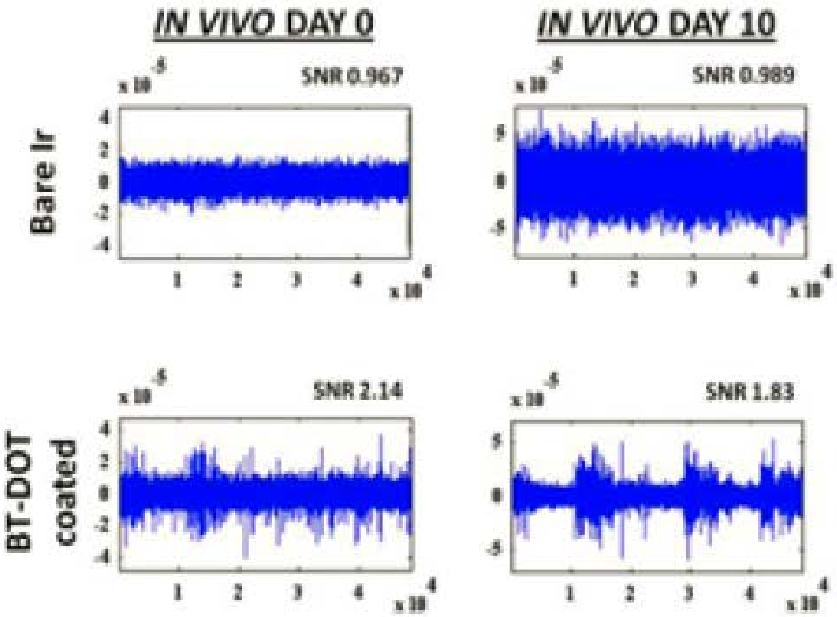

Electrochemical growth on pre-patterned metal electrodes

Work of Martin, Wallace, Inganäs, …

Conducting polymers lower interfacial impedance

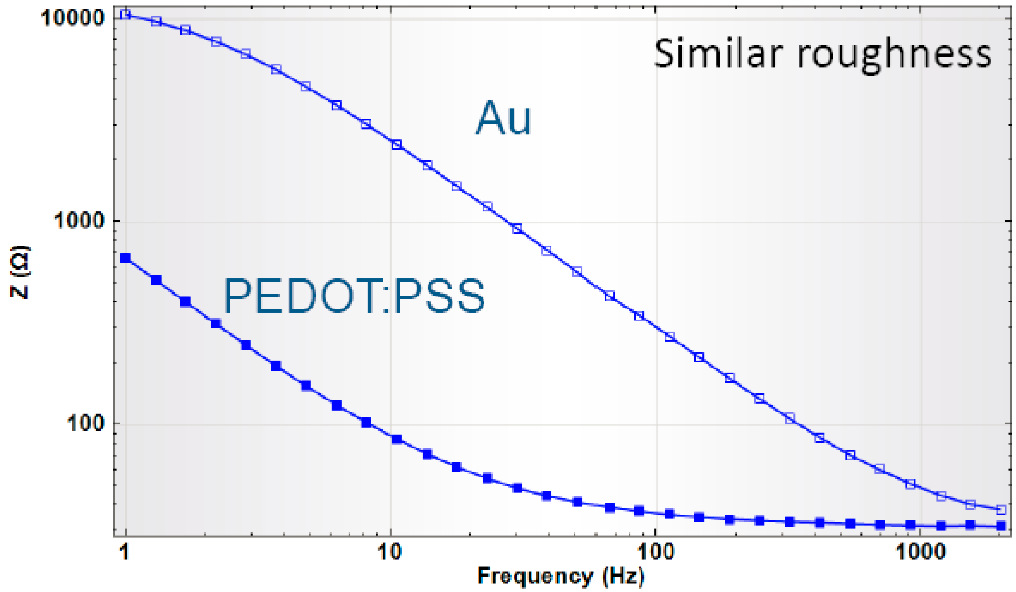

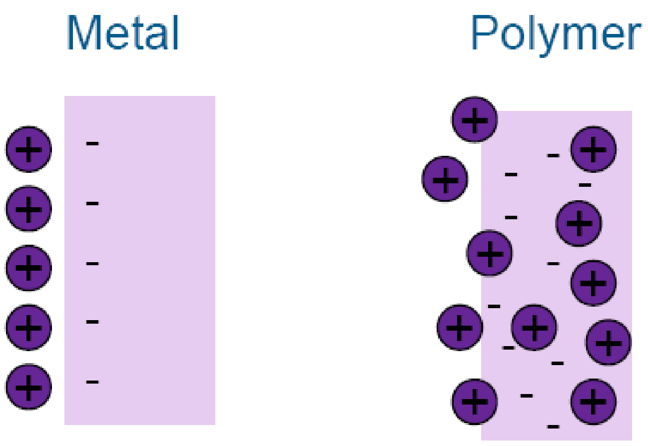

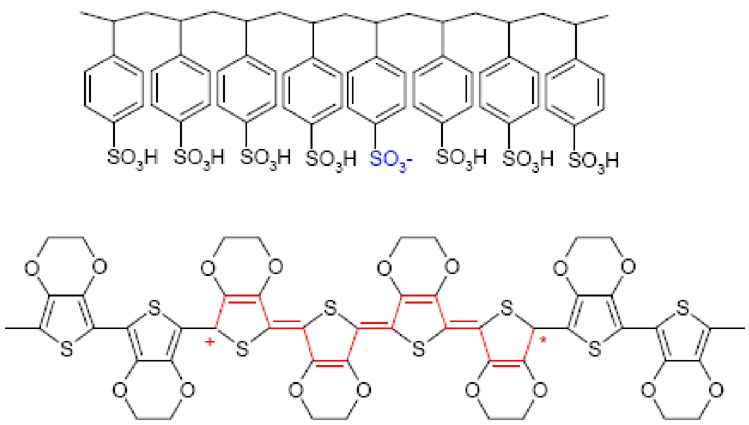

Different "nature" of capacitance across the electrode/electrolyte interface

Introduction of Electrical Stimulation and Recording

Various stages (resting state, depolarization and repolarization) of nerve cells during electrical stimulation:

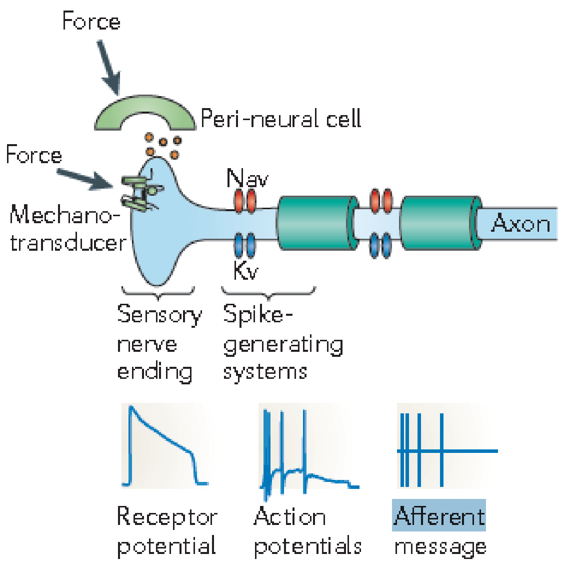

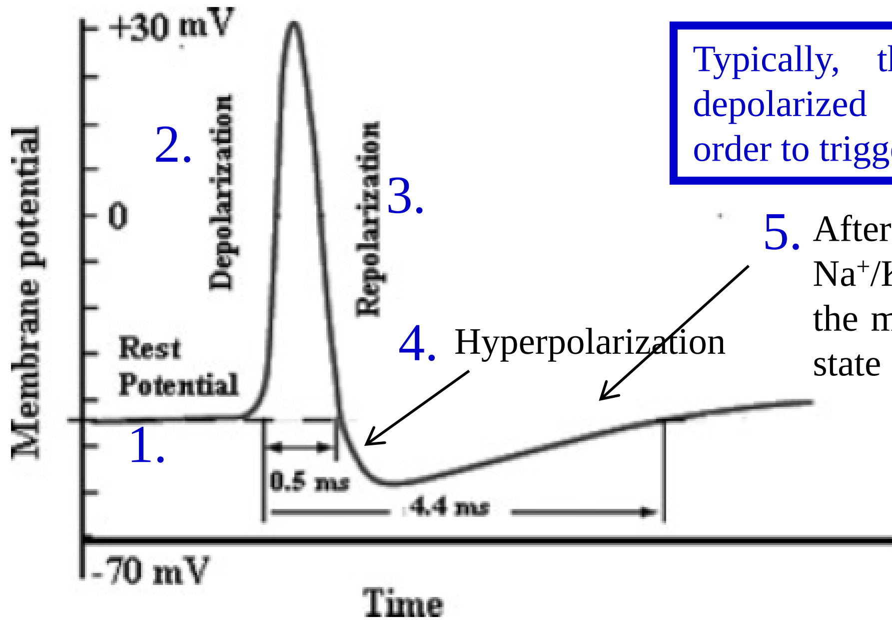

Typically, the membrane must be depolarized by about 10–20 mV in order to trigger an action potential.

5. After hyperpolarization, the Na^+/K^+ pump eventually brings the membrane back to its resting state of −70 mV.

1. Typical value of membrane potential (resting potential):
-60~ -100 mV

2. Depolarization:
More Na^+ channels are opened and the Na^+ influx drives the interior of the cell membrane up to about +30 mV.

3. Repolarization:
The membrane begins to repolarize back towards its resting potential as the K^+ channels open. The repolarization typically overshoots the resting potential to about −90 mV.

4. Hyperpolarization:
Hyperpolarization assures that the signal is always proceeding in one direction.

Nature Reviews 12 (2011) 139.
J Tissue Eng Regen Med 5 (2011) e17.

47

Charge Injection Limit

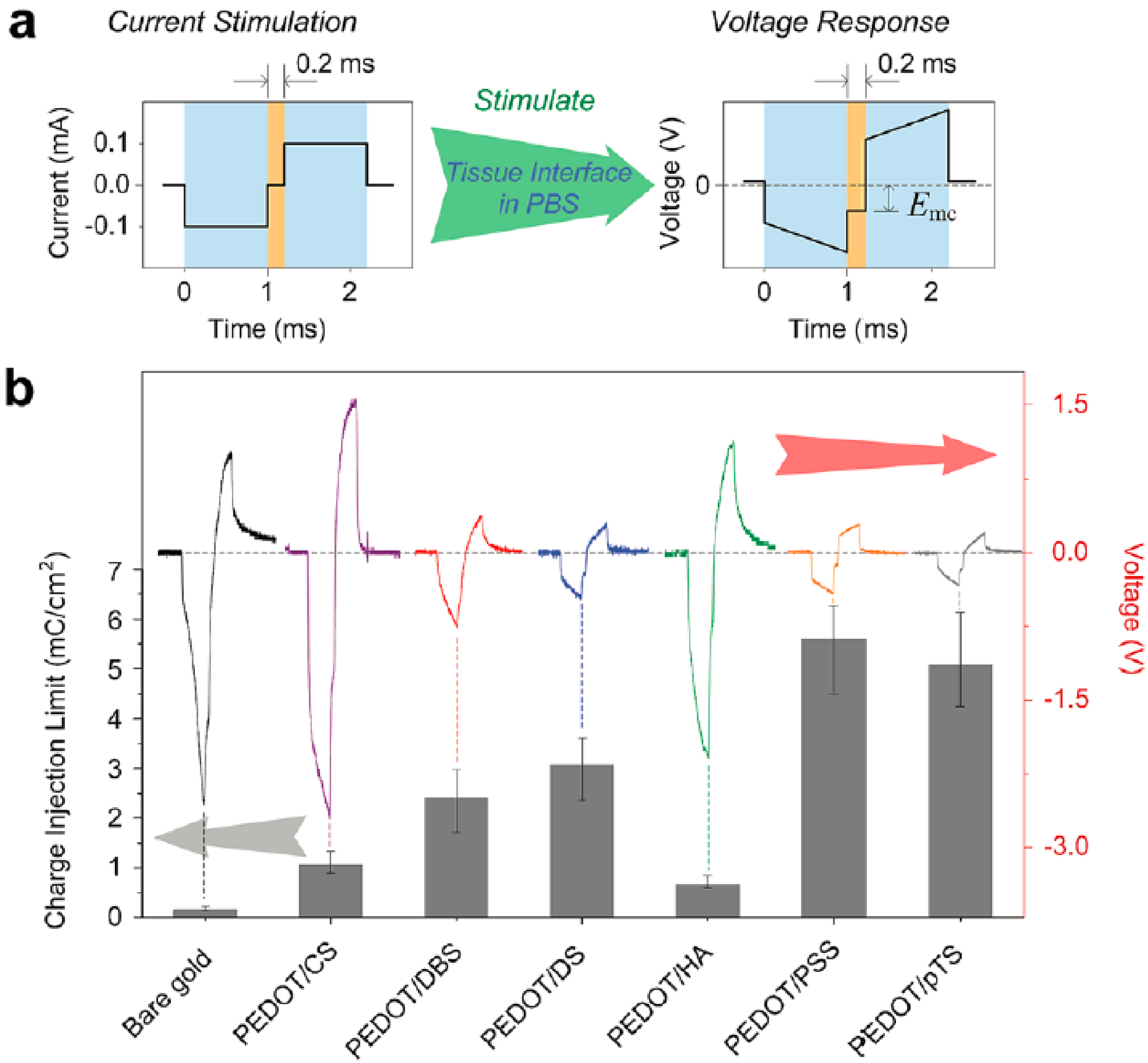

RSC Adv., 4 (2014) 47461

Conducting-Polymer Nanotubes for Controlled Drug Release (DC Martin)

PLGA electrospun
nanoscale fibers

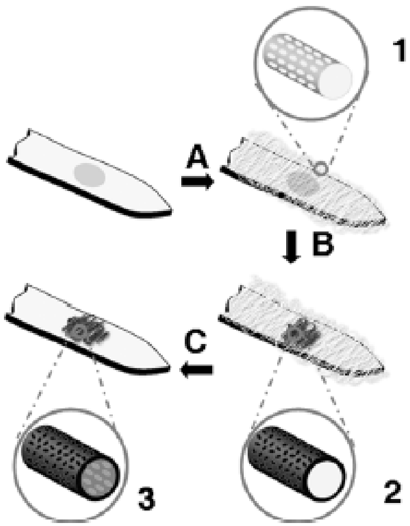

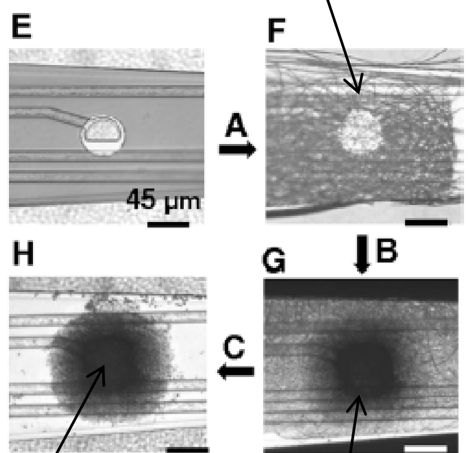

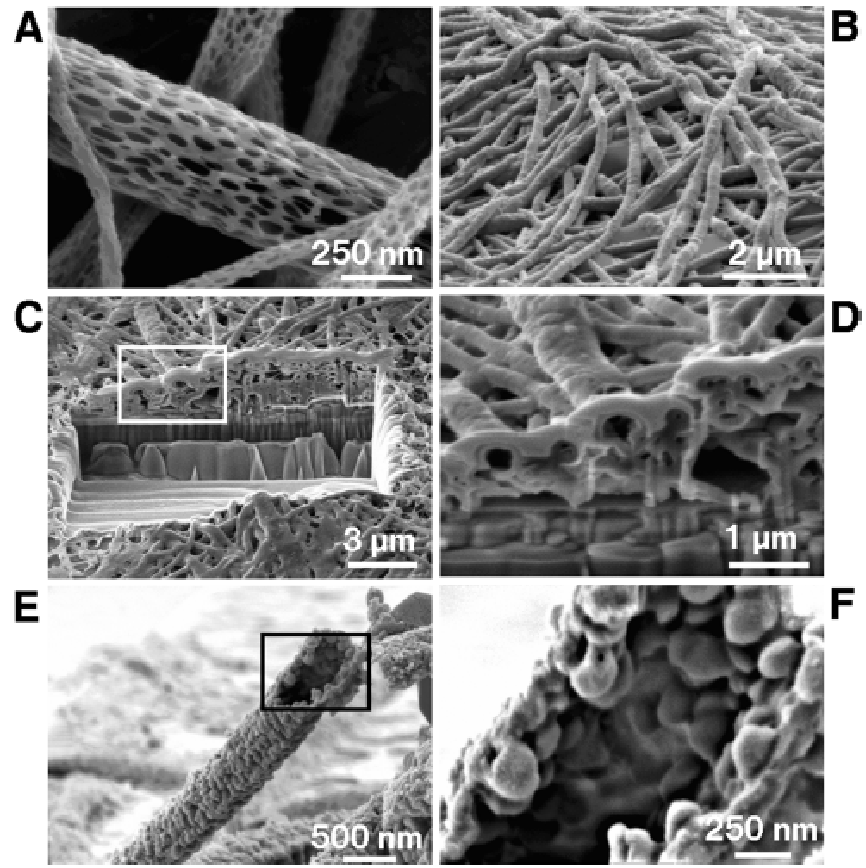

Removal of the core nanoscale
fiber templates

Electrochemical
deposition of PEDOT

Adv. Mater. 18 (2006) 405-409.

Cumulative Mass Release of Dexamethasone:

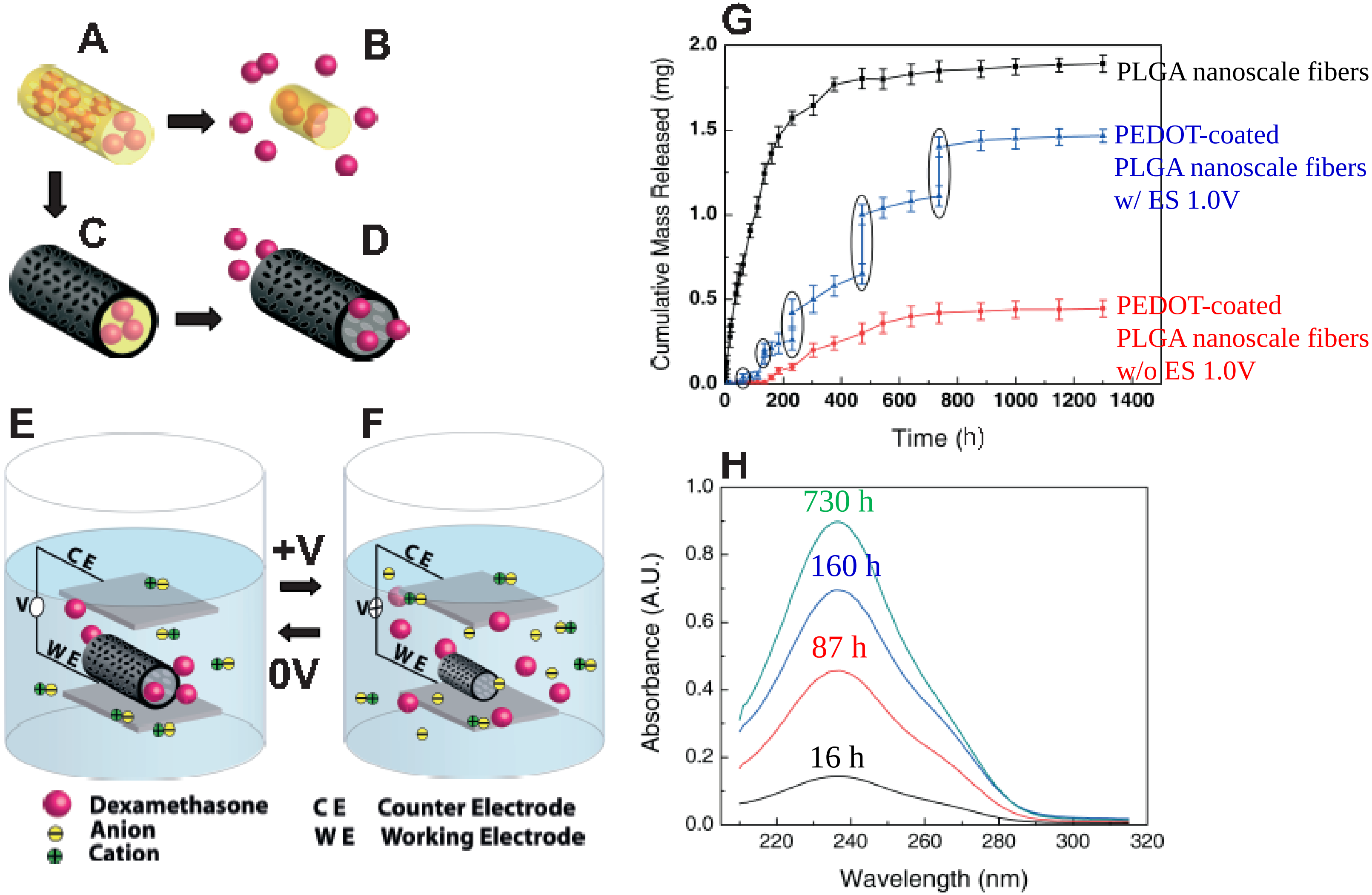

Adv. Mater. 18 (2006) 405-409.

Experimental and theoretical characterization of implantable neural microelectrodes modified with conducting polymer nanotubes

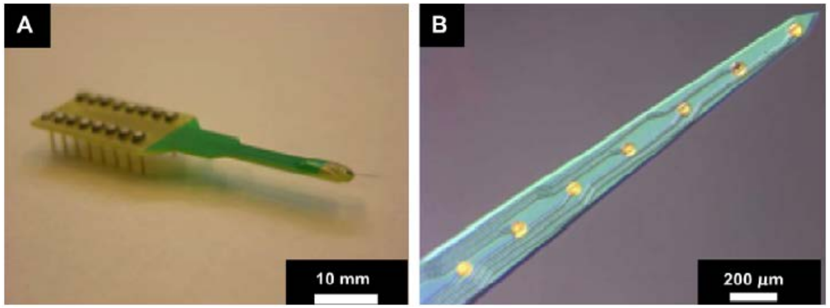

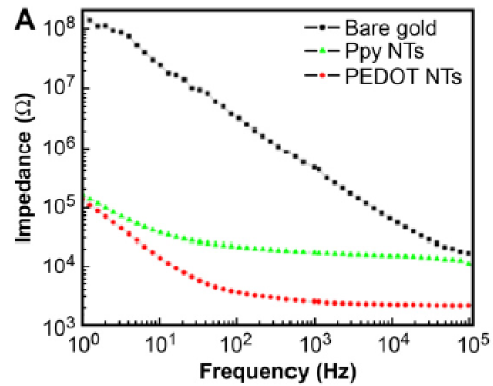

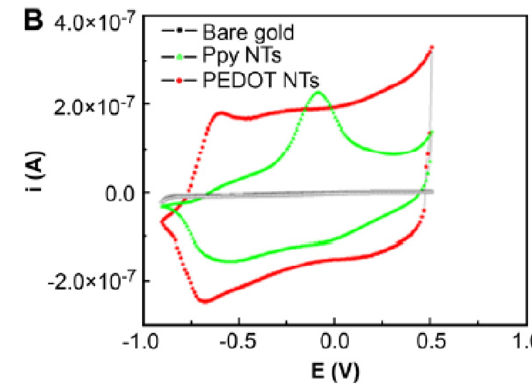

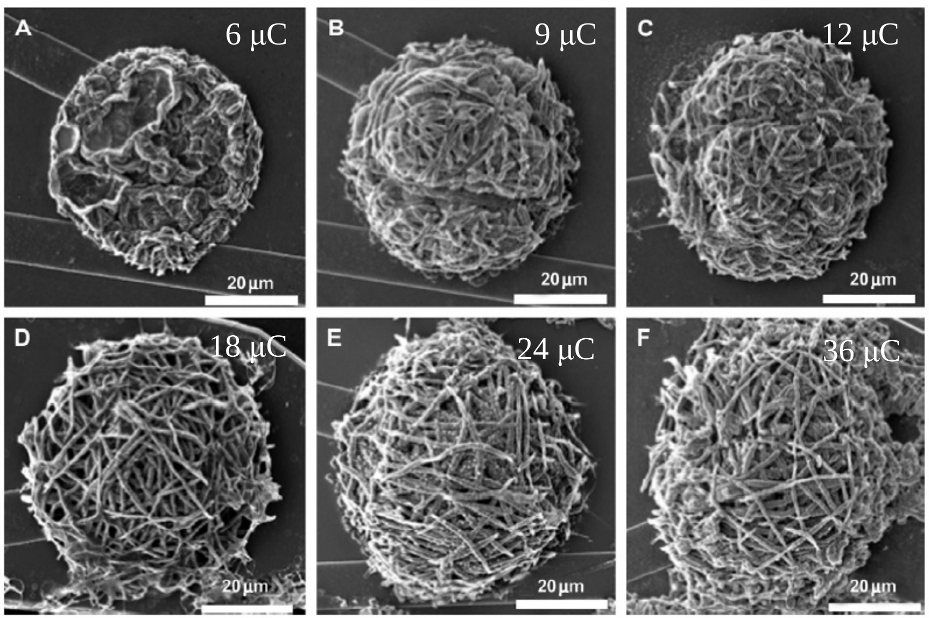

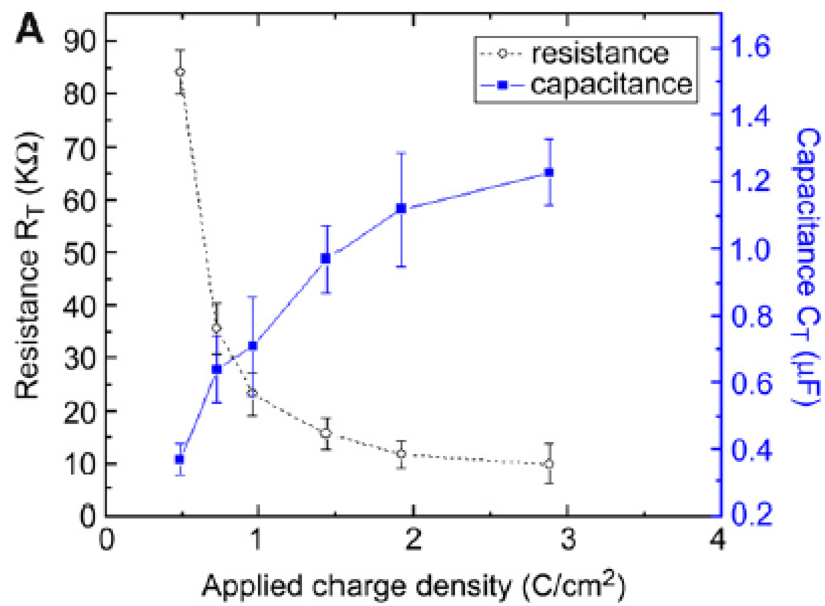

Diffusional pseudocapacitance (CT) and diffusional resistance (RT) for PPy NTs as a function of applied charge density

Biomaterials 29 (2008) 1273-1283.

Layered Carbon Nanotube-Polyelectrolyte Electrodes Outperform Traditional Neural Interface Materials (DC Martin)

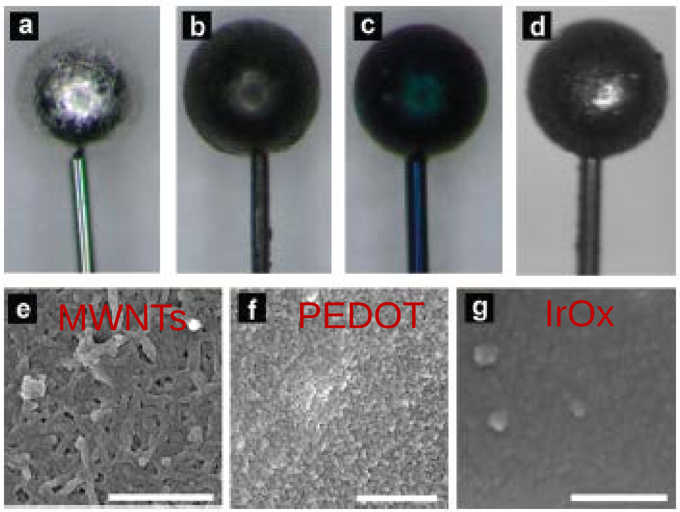

SEM images after 300 CV scanning cycles at a scan rate of 0.1 V/s.

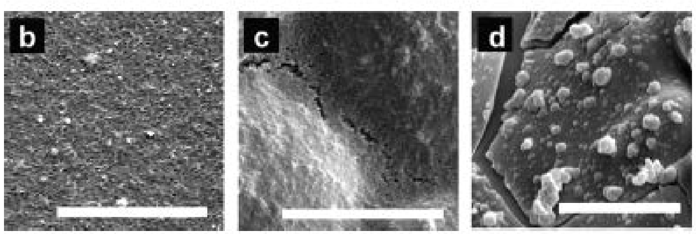

MWNTs PEDOT IrOx

(CV sweep between -0.9 and 0.5 V)

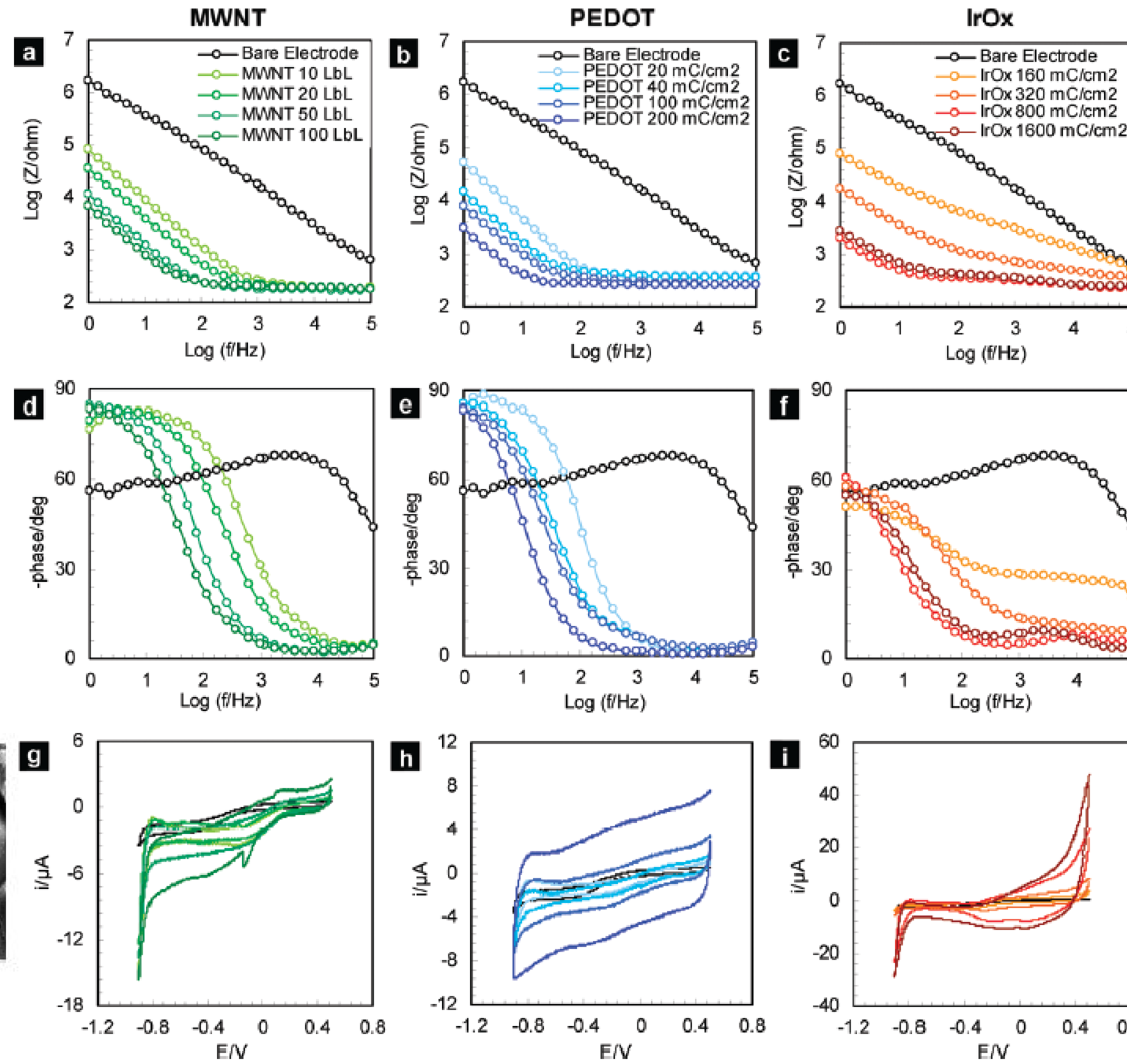

Nano Lett. 9 (2009) 4012-4018.

Charge storage capacity (CSC)

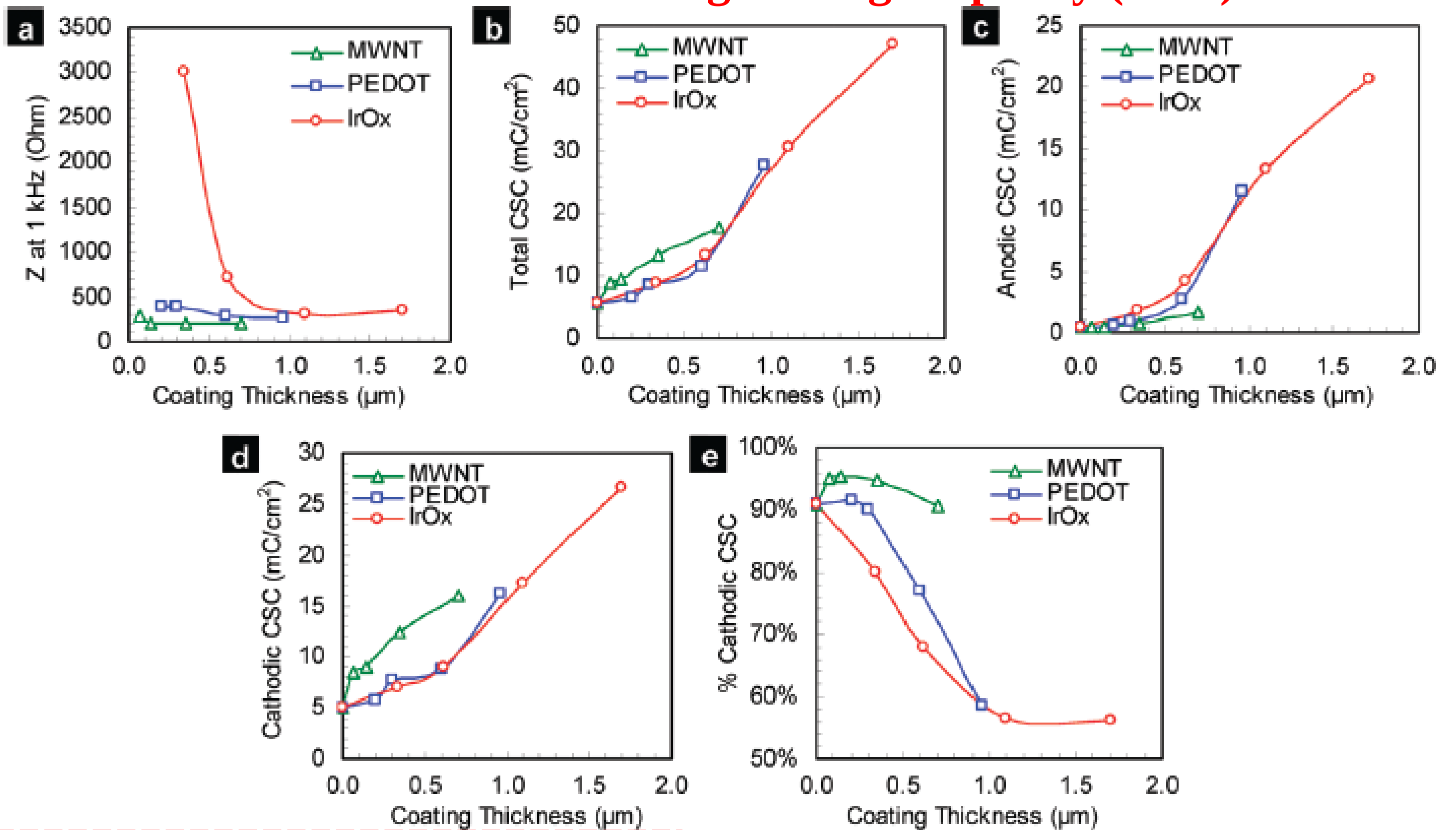

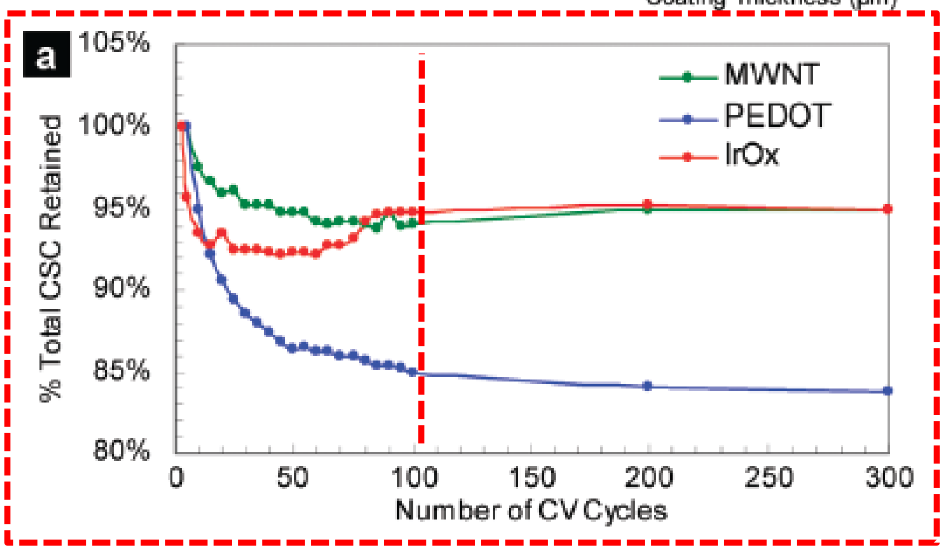

Electrical Stimulation Stability:

MWNT> IrOx> PEDOT

Nano Lett. 9 (2009) 4012-4018.

Multifunctional Nanobiomaterials for Neural Interfaces (DC Martin)

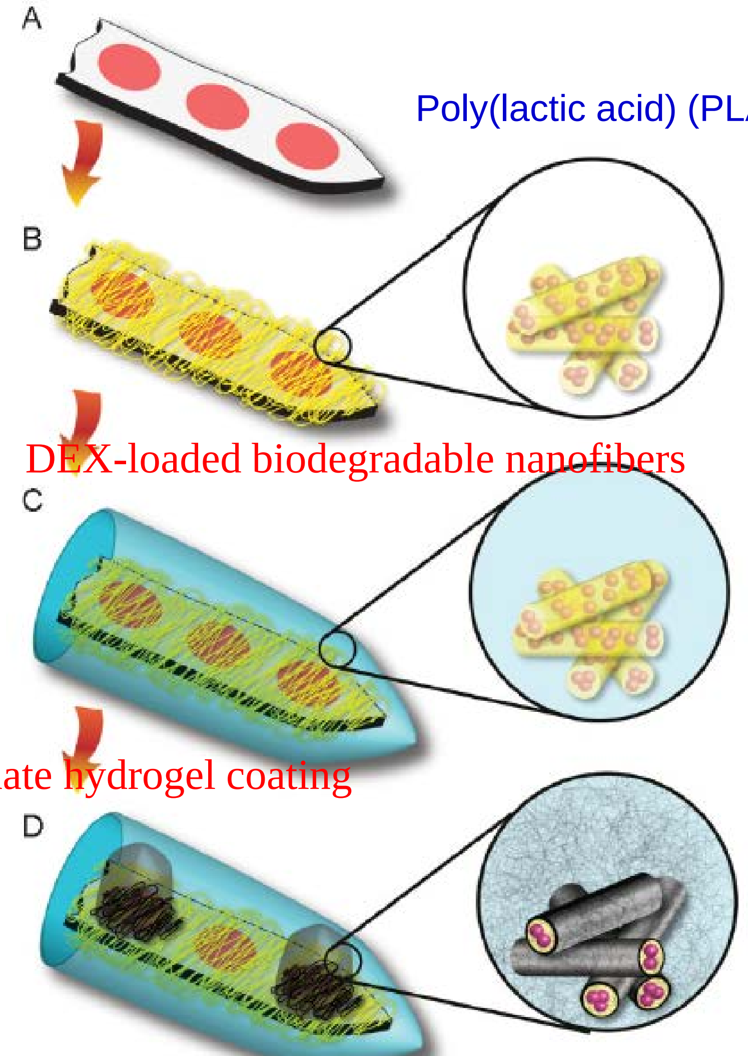

Poly(lactic acid) (PLA)

DEX-loaded biodegradable nanofibers

Alginate hydrogel coating

PEDOT on the electrode sites

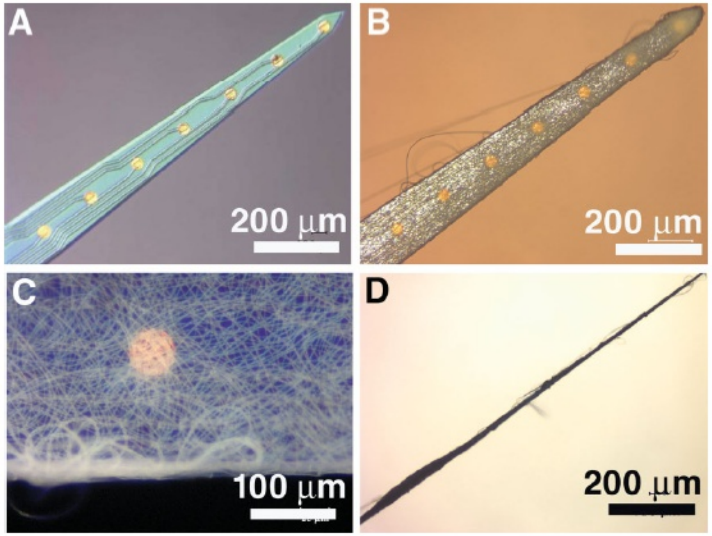

PLDL PLDL/DEX=10:1 PLLA/DEX=10:1

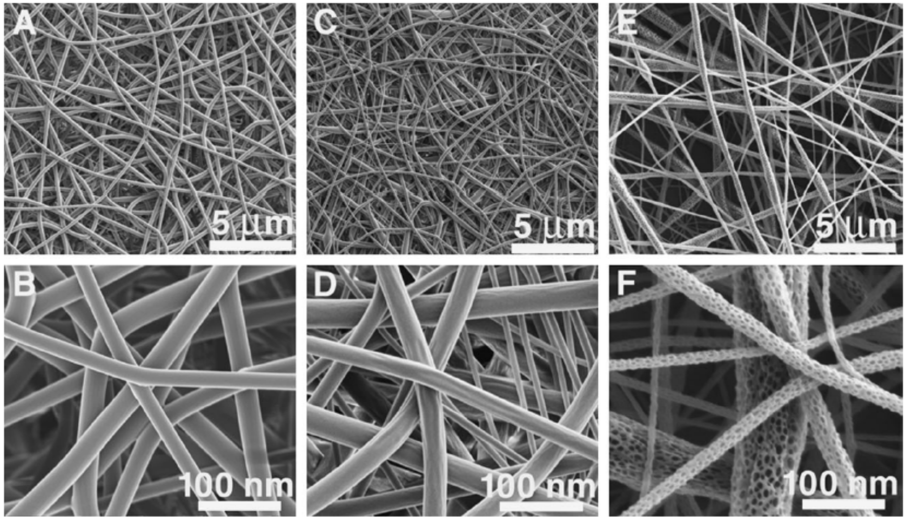

Adv. Funct. Mater. 19 (2009) 573-585.

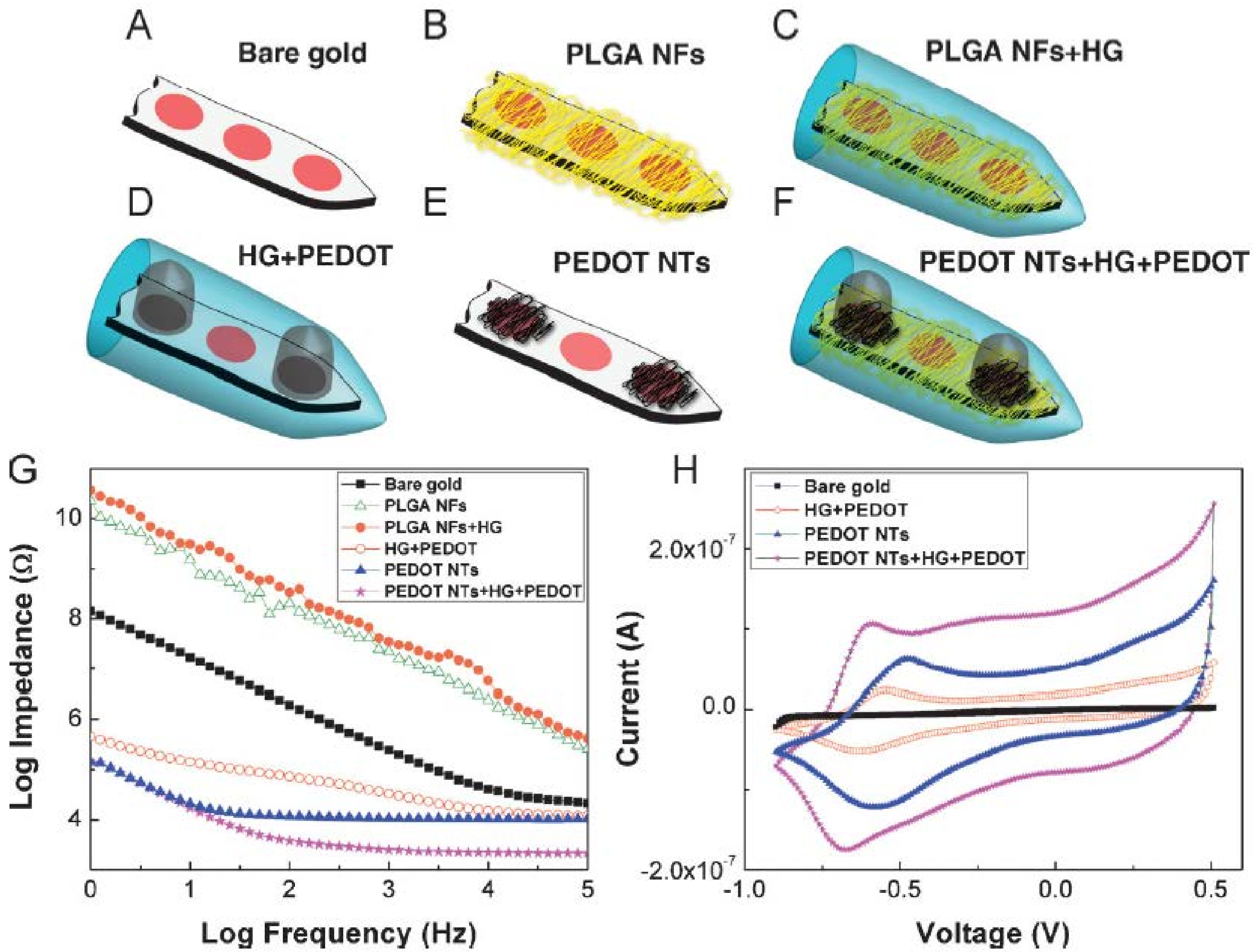

Adv. Funct. Mater. 19 (2009) 573-585.

Degradation of nanofibers in PBS solution

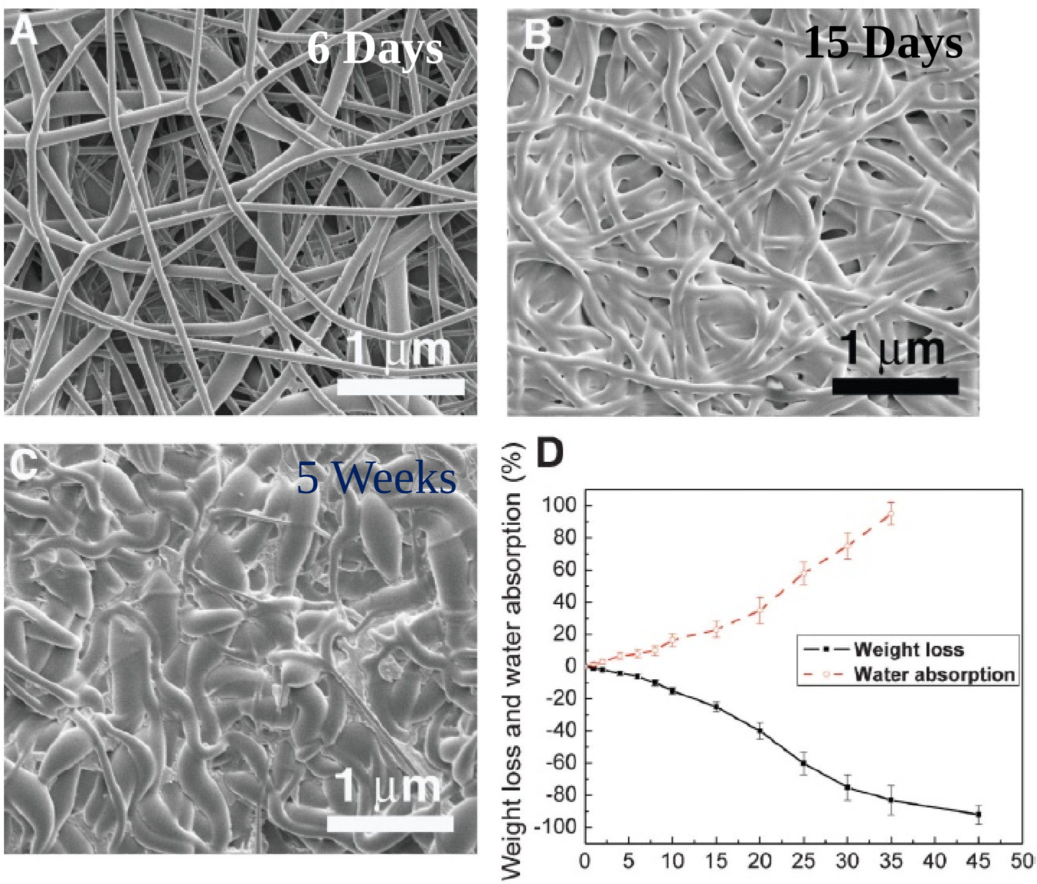

Adv. Funct. Mater. 19 (2009) 573-585.

Percentage cumulative mass release profiles of DEX-loaded polymers

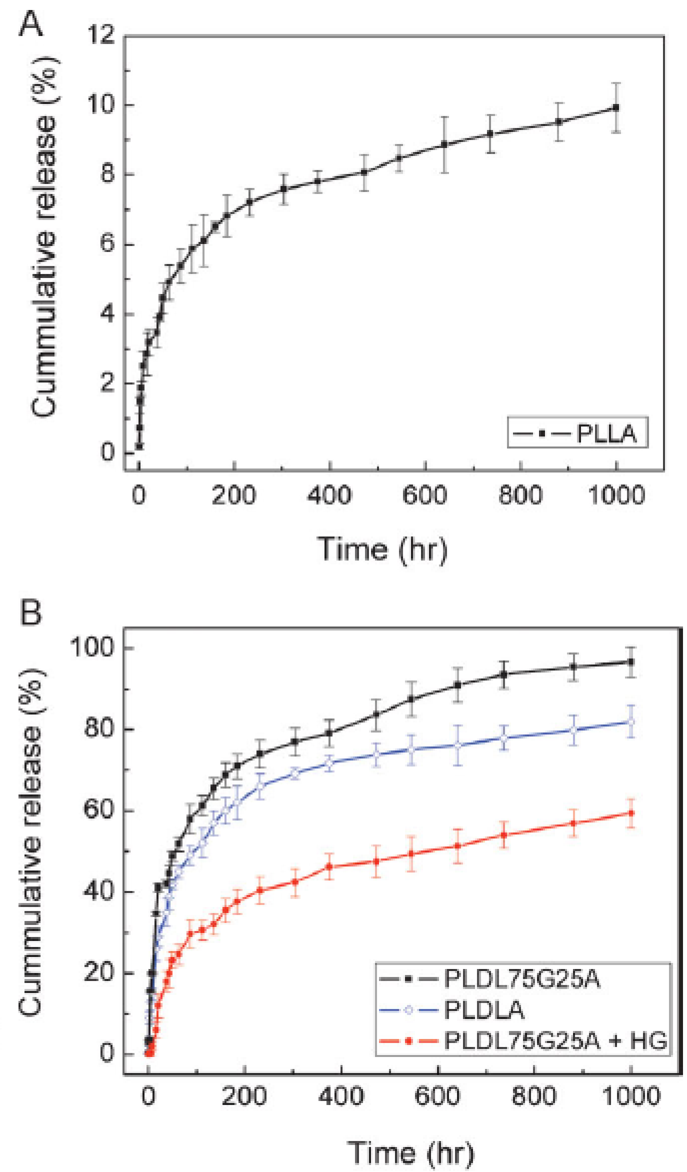

Conducting polymers on hydrogel-coated neural electrode provide sensitive neural recordings in auditory cortex (DC Martin)

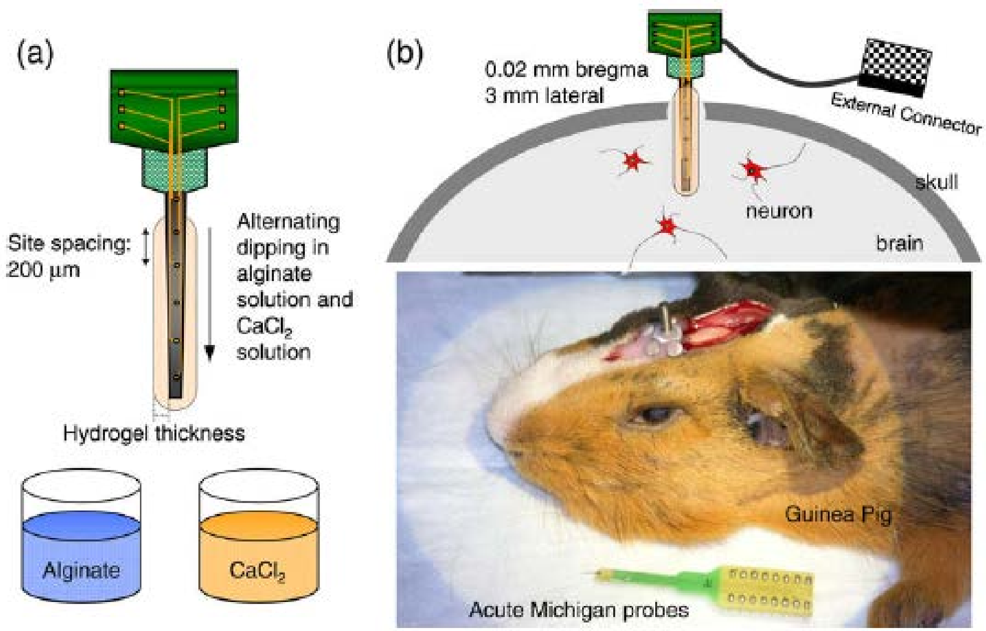

Table 1
Classification of signal to noise ratios.

Define	SNR range	Characteristics
High SNR	SNR > 4.0	Signals from clearly detectable units: easy to discriminated/analyzed from background noise
Medium SNR	4.0 > SNR > 3.5	Signals from active units: possible to be discriminated from background noise with some exceptions
Low SNR	SNR < 3.5	Signals from bad units: Difficult to be discriminated from background noise

Acta Biomaterialia 6 (2010) 57–62.

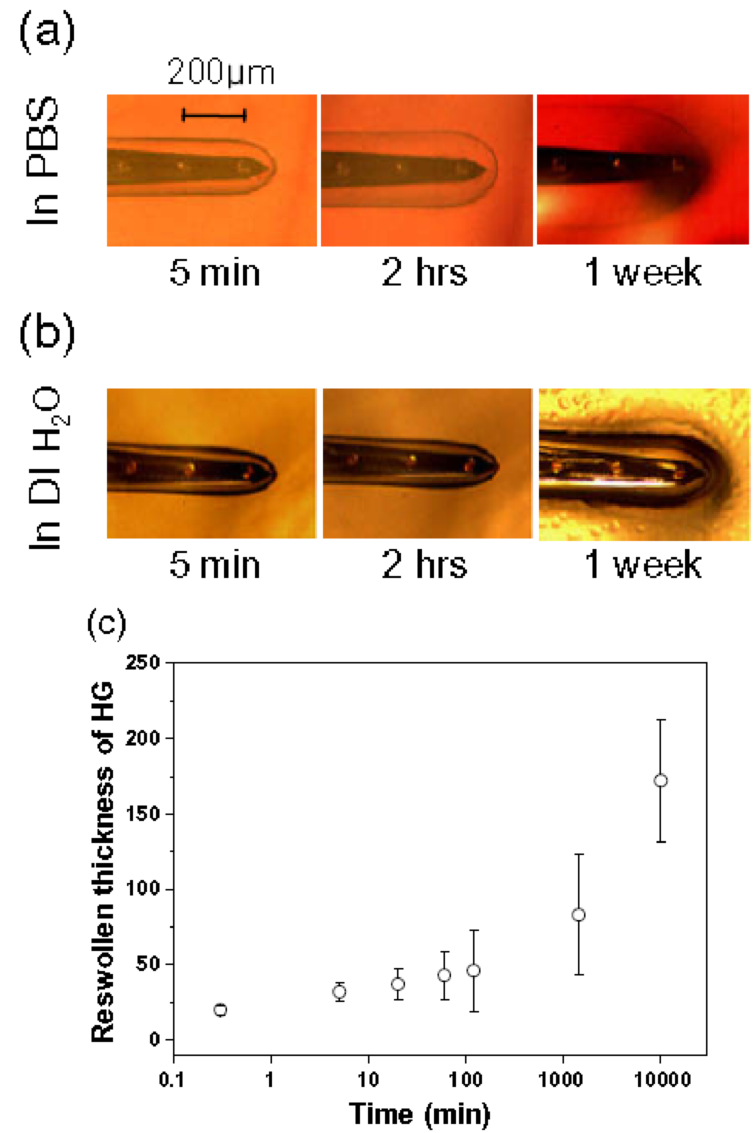

(Sensitivity)

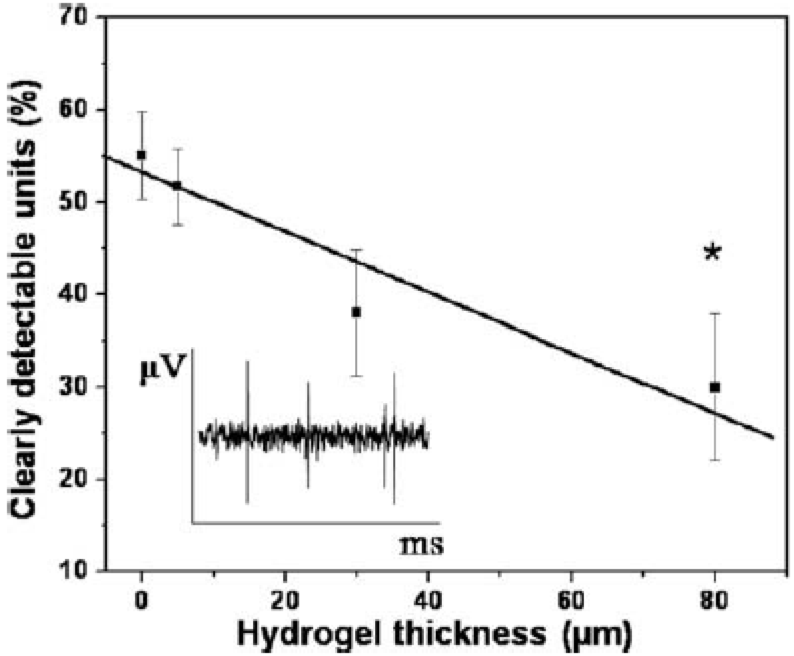

The average percentages of clearly detectable units as a function of the thickness of HG-coated electrodes in the auditory cortex with a 200 ms noise burst.

(Signal-to-noise ratio, SNR)

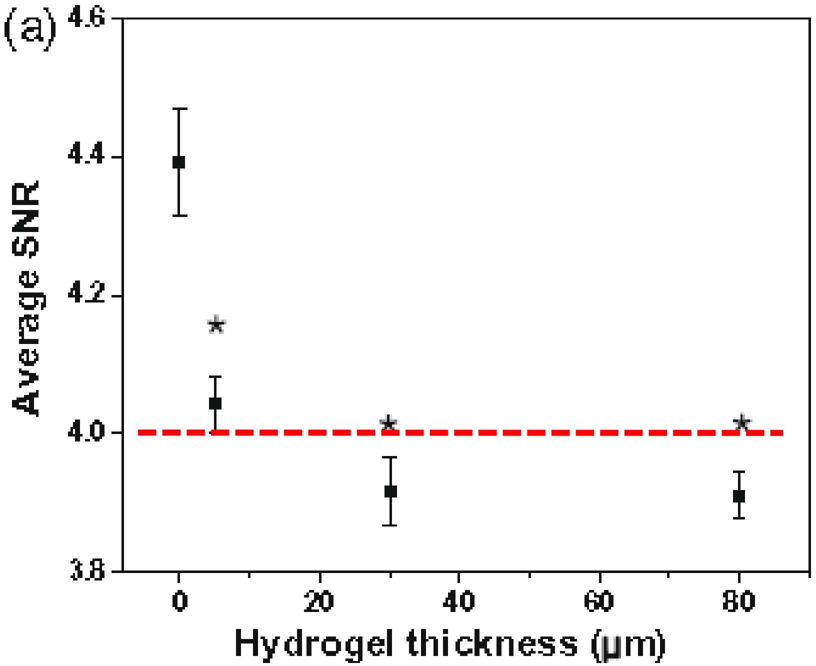

Average SNRs and signal quality as a function of hydrogel thickness.

Acta Biomaterialia 6 (2010) 57–62.

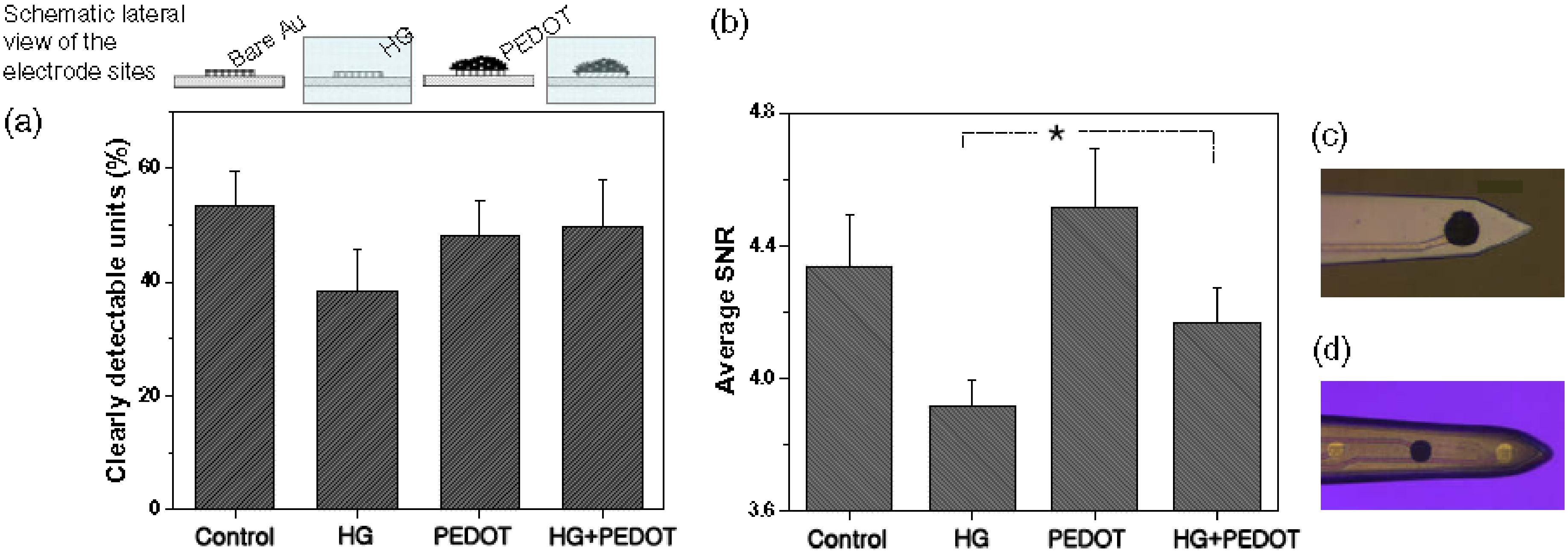

A significant loss in functionality determined by SNRs was observed with HG coatings as thin as 5 μm, while the number of clearly detectable units gradually decreased as a function of the HG coating thickness. The loss of functionality of the electrodes is due to the lack of neurons immediately around the electrodes sites.

PEDOT deposited on the electrode sites did not produce any increase in the number of clearly detectable units as compared with the bare electrodes, the PEDOT deposition improved the recording functionality of the HG-coated electrodes as measured by the SNR.

Acta Biomaterialia 6 (2010) 57–62.

Conducting-Polymer Nanotubes Improve Electrical Properties, Mechanical Adhesion, Neural Attachment, and Neurite Outgrowth of Neural Electrodes (DC Martin)

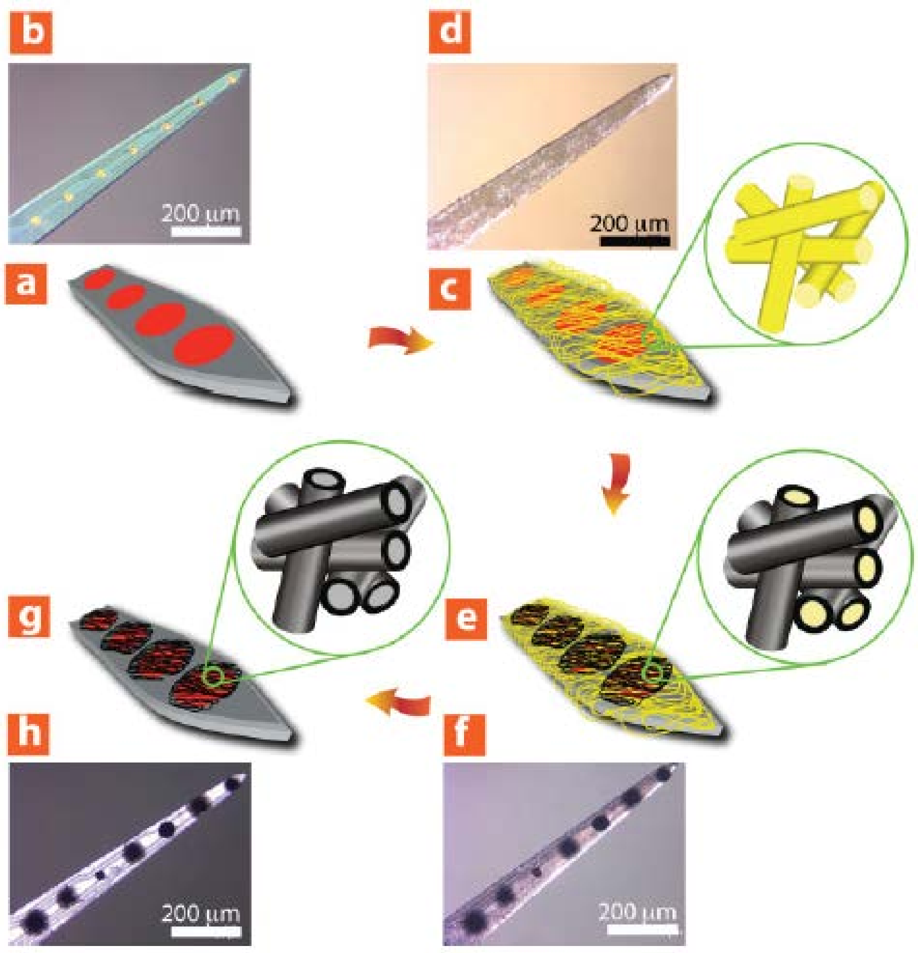

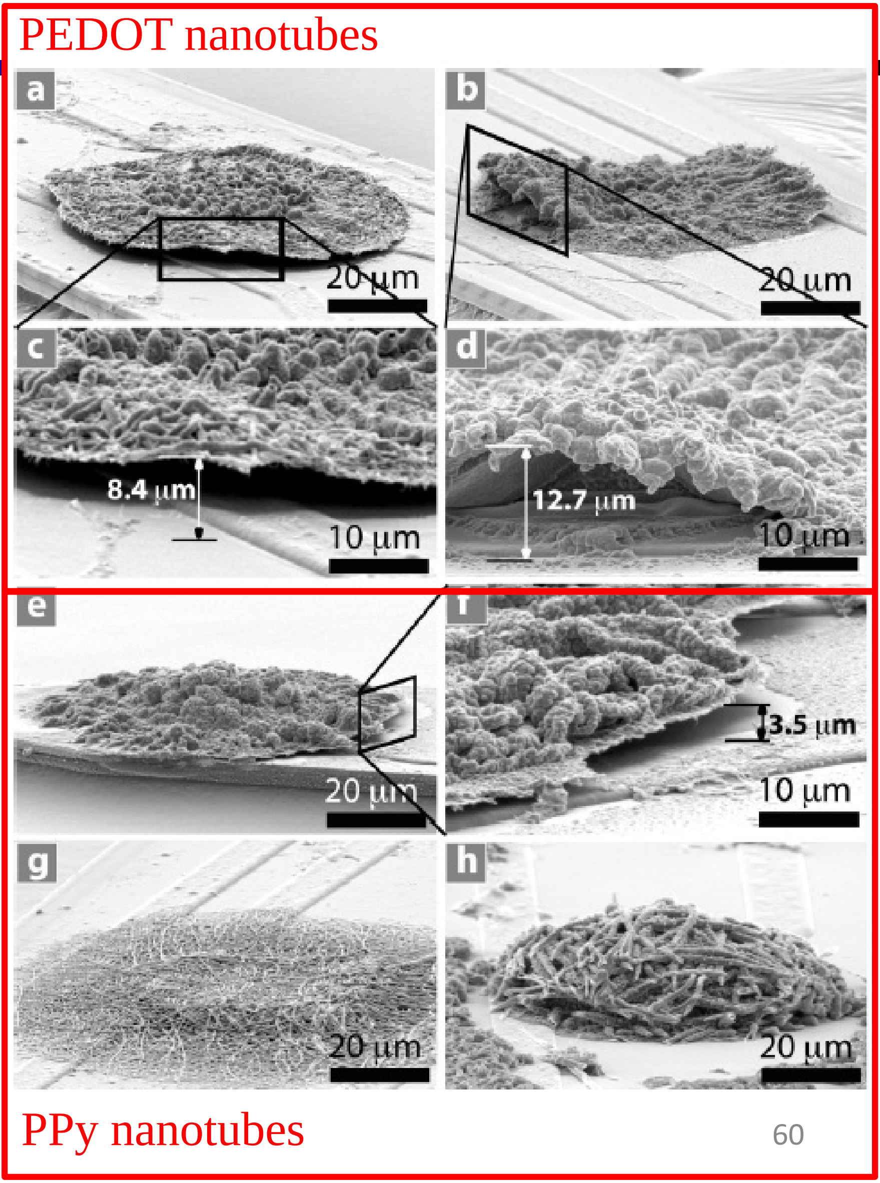

Small 6 (2010) 421–429.

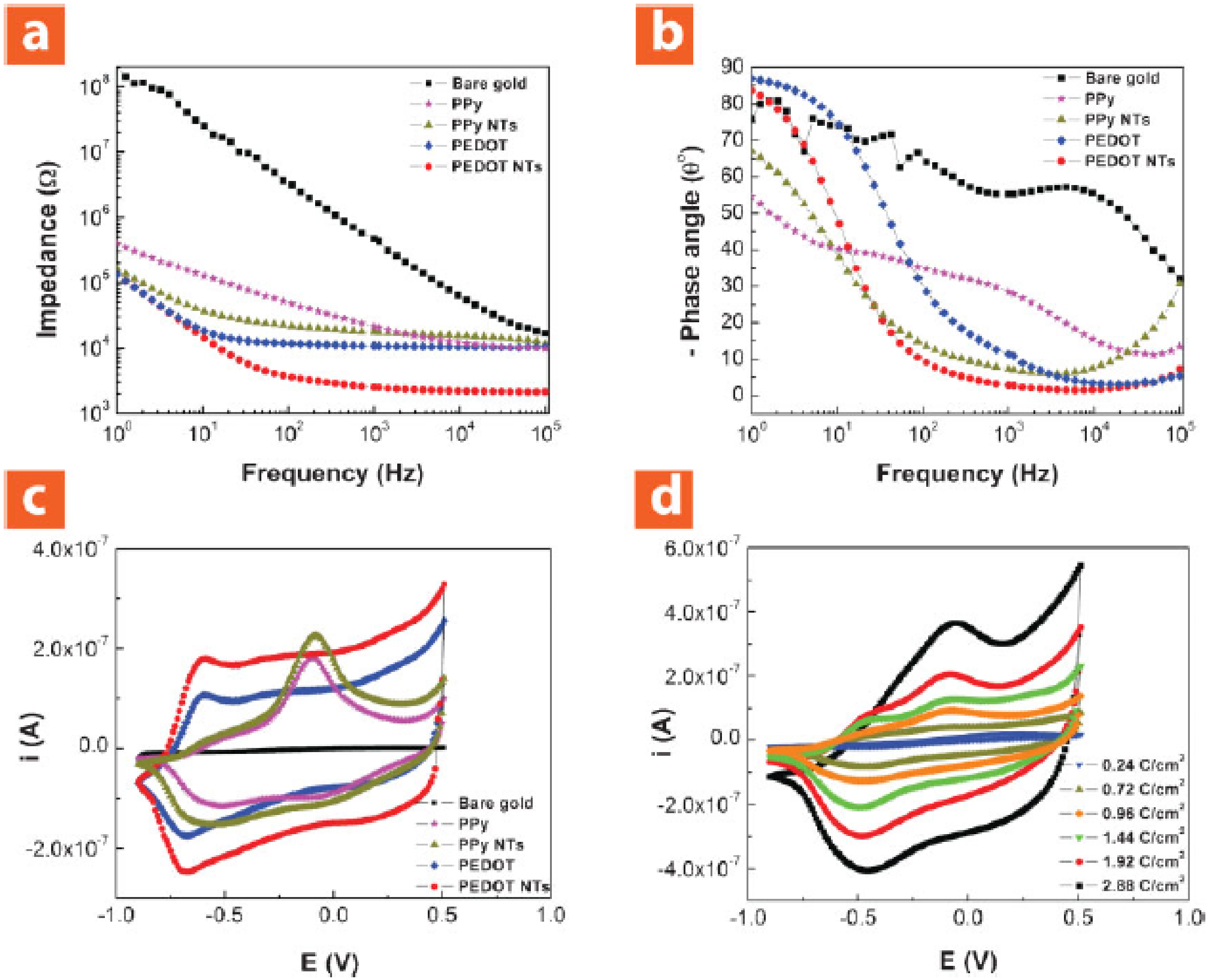

Small 6 (2010) 421–429.

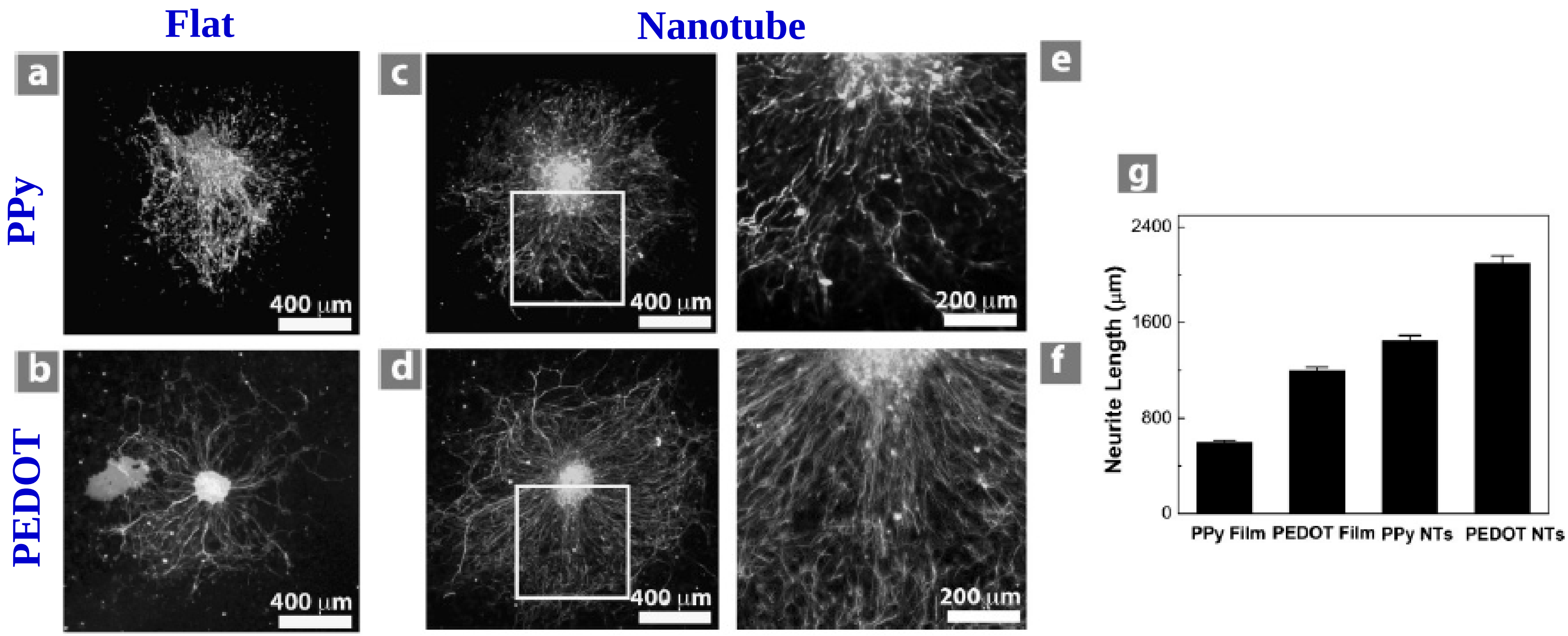

DRG explants cultured on conducting polymer films and nanotubes.

Small 6 (2010) 421–429.

Structural, chemical and electrochemical characterization of poly(3,4-Ethylenedioxythiophene) (PEDOT) prepared with various counter-ions and heat treatments (DC Martin)

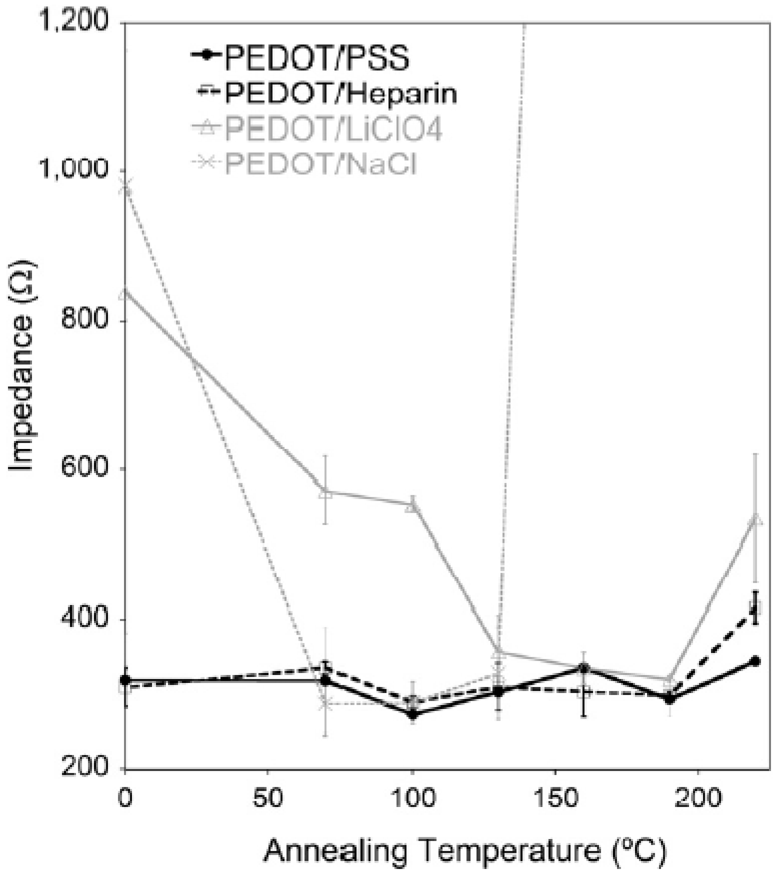

Table 1
Comparison of PEDOT films polymerized with different counter-ions and annealed.

Counter-ion	Molecular weight	d_{100} spacing	1 kHz impedance and CSC before annealing	1 kHz impedance and CSC after annealing 1 h at 160 °C
PSS	~70,000 Da	~1.3 nm	319 Ω 26.1 mC/cm^2	335 Ω 14.7 mC/cm^2
Heparin	12,000–15,000 Da		309 Ω 20.9 mC/cm^2	304 Ω 11.2 mC/cm^2
$LiClO_4$	106.4 Da		839 Ω 8.6 mC/cm^2	335 Ω 11.3 mC/cm^2
NaCl	58.4 Da	1.27 nm	981 Ω 19.3 mC/cm^2	3168 Ω 12.7 mC/cm^2

Thermal annealing
→ Impedance and CSC decrease

Polymer 52 (2011) 1302–1308.

Manipulating location, polarity, and outgrowth length of neuron-like pheochromocytoma (PC-12) cells on patterned organic electrode arrays

☆ PEDOT microelectrode array system☆

Lab Chip, **11**, 3674 (2011).

Live/Dead assay: Live (green)/ Dead (Red)

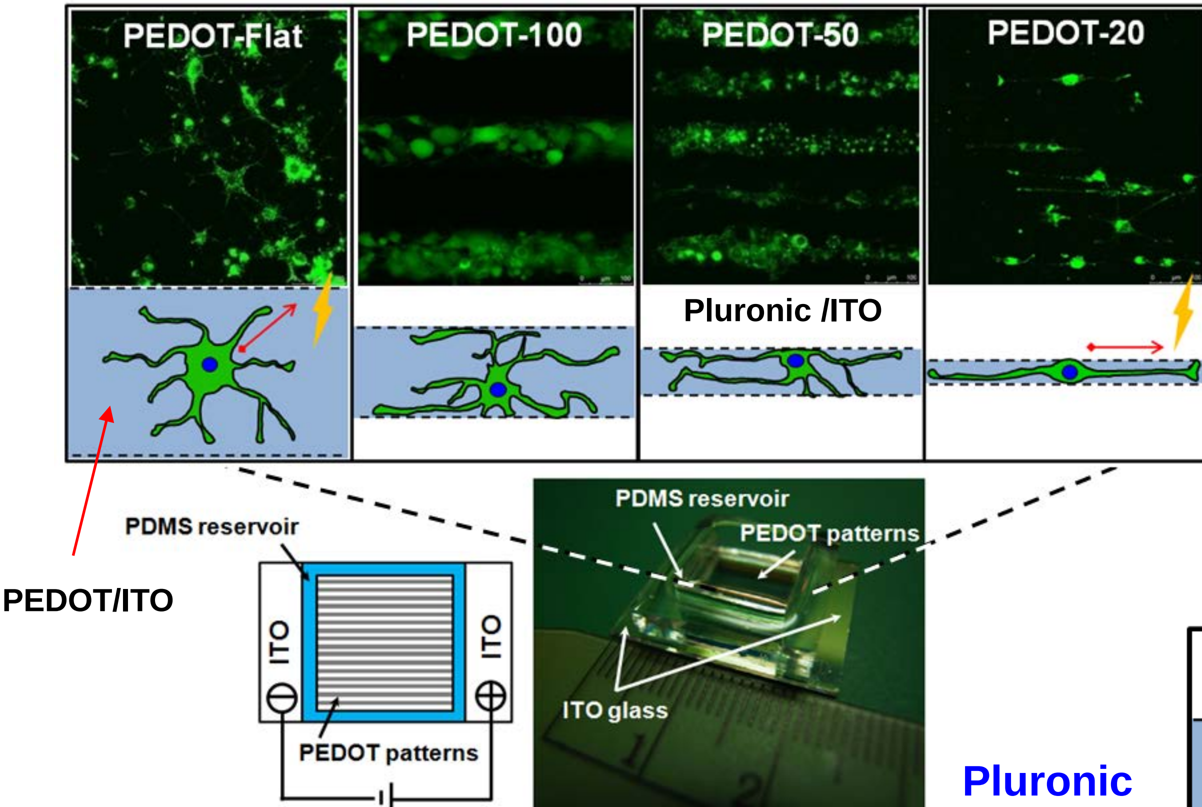

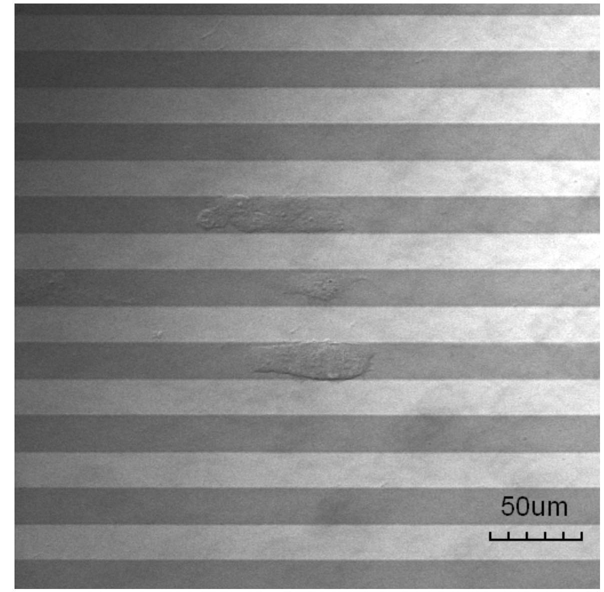

Pluronic

1. Contact attraction: PEDOT:PSS
2. Contact repulsion: $(PEO)_m/(PPO)_n/(PEO)_m$
3. Chemoattraction. (NGF)
4. Electrical Stimulation

Topview　　Cross-section

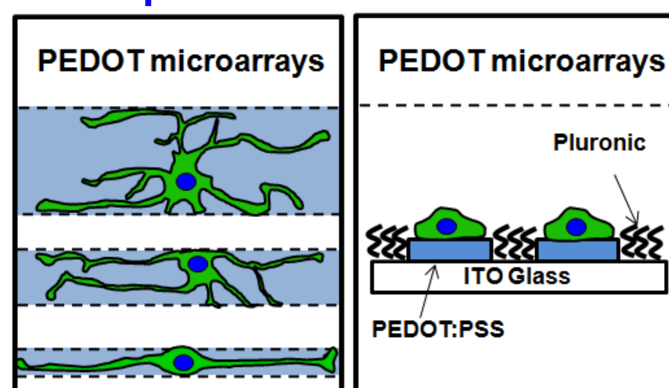

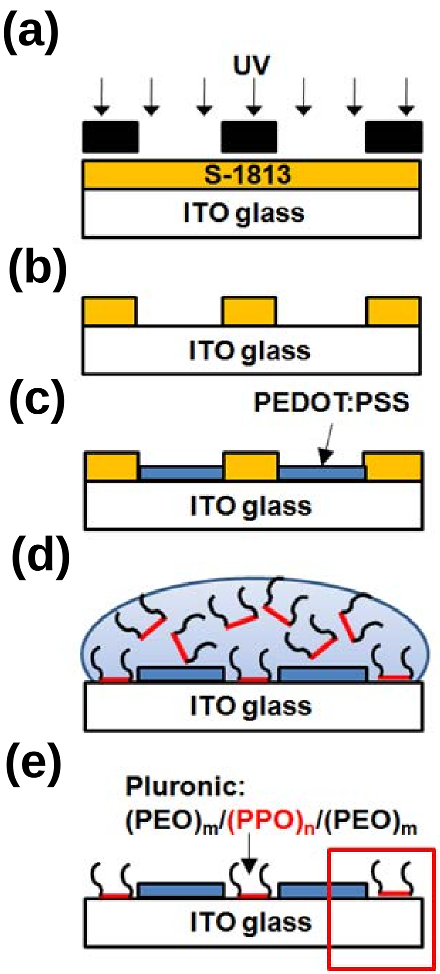

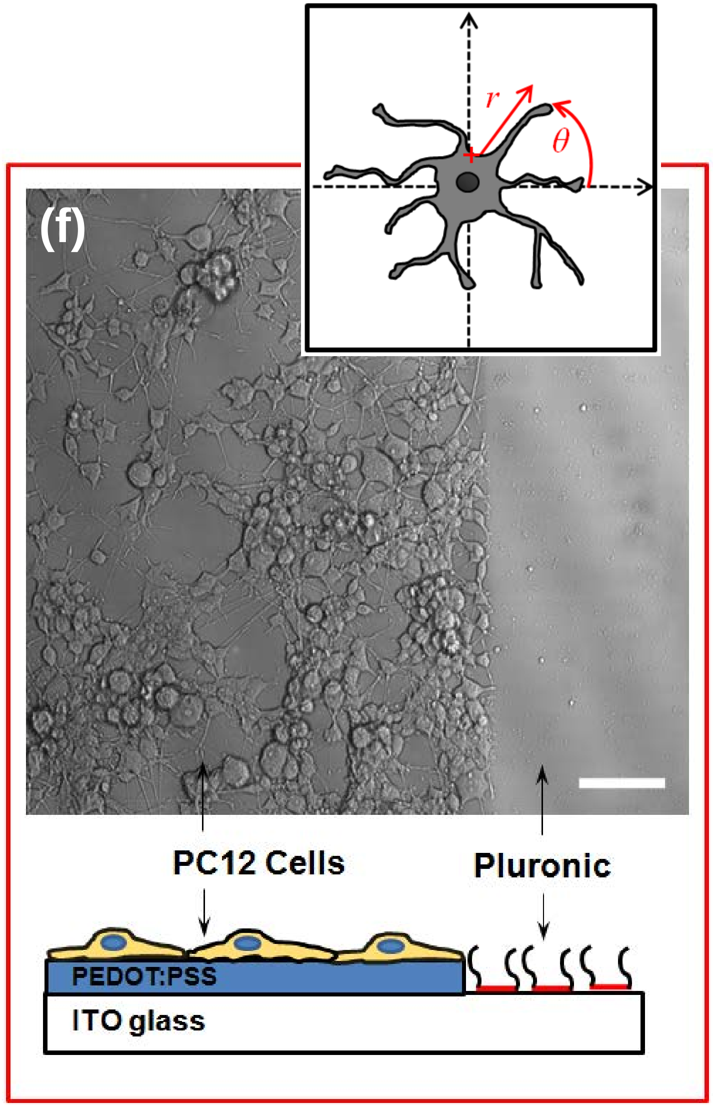

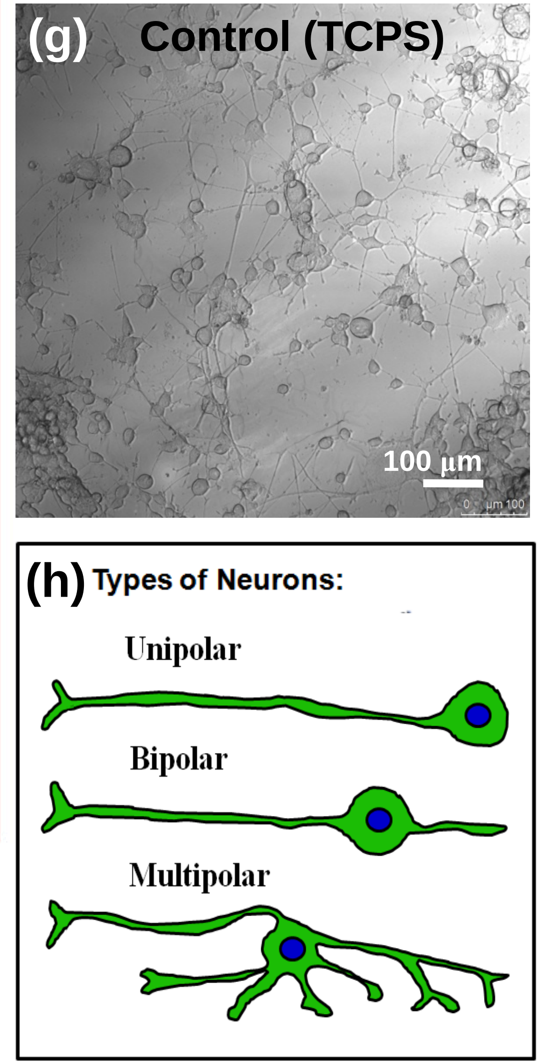

(a-e) Schematic representation of the fabrication of PEDOT microelectrode arrays with anti-adhesive Pluronic F108 coatings.

Lab Chip, **11**, 3674 (2011).

	Unipolar (% of Cells)	Bipolar (% of Cells)	Multipolar (% of Cells)	Average number of neurites per cell	Median neurite length (µm)	Polar order parameter (S)
Control	4	18	78	3.7	91	-0.05±0.36
PEDOT-Flat	6	14	80	3.2	98	-0.08±0.36
PEDOT-100	26	22	52	2.7	60	0.22±0.36
PEDOT-50	8	54	38	2.4	66	0.68±0.24
PEDOT-20	24	72	4	1.8	88	0.97±0.07
PEDOT-Flat-ES[a]	6	12	82	3.5	119	-0.07±0.36
PEDOT-20-ES[a]	20	74	6	1.8	143	0.97±0.06

[a]Electrical Stimulation (ES)

Polar order parameter (S)=$(2\langle\cos^2\theta\rangle-1)$

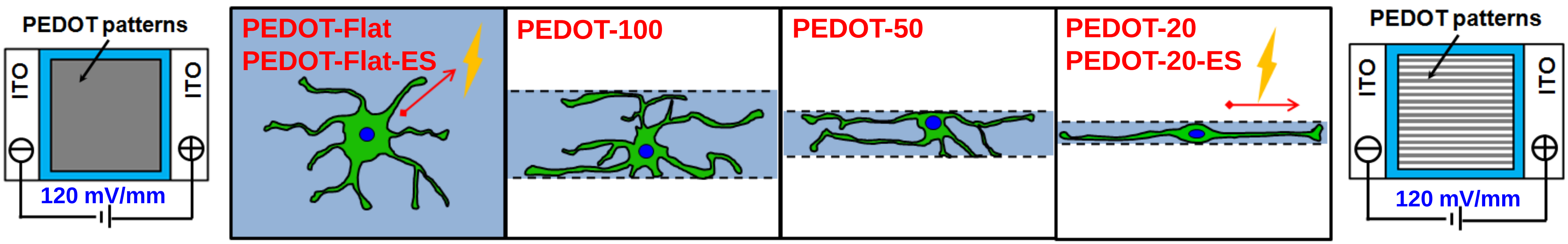

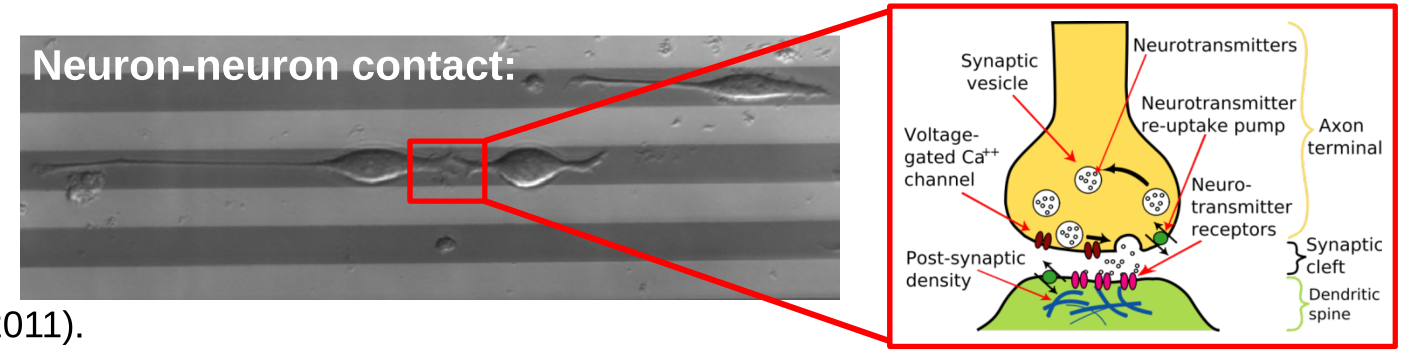

Lab Chip, **11**, 3674 (2011).

Cytoskeleton Morphology and Focal Adhesion of PC12 cells on PEDOT-Flat and PEDOT-20 microelectrode arrays

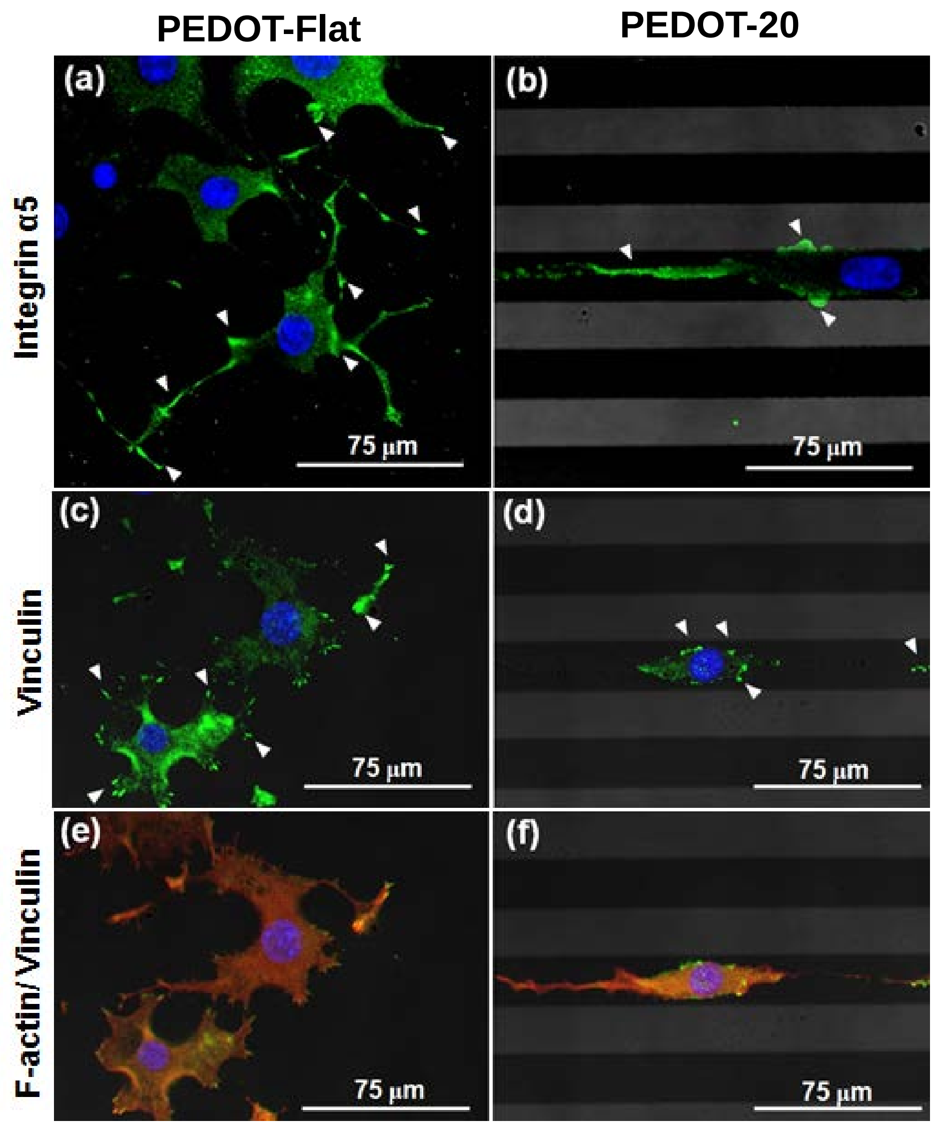

F-actin (red)/ vinculin (green)/ nucleus (blue)

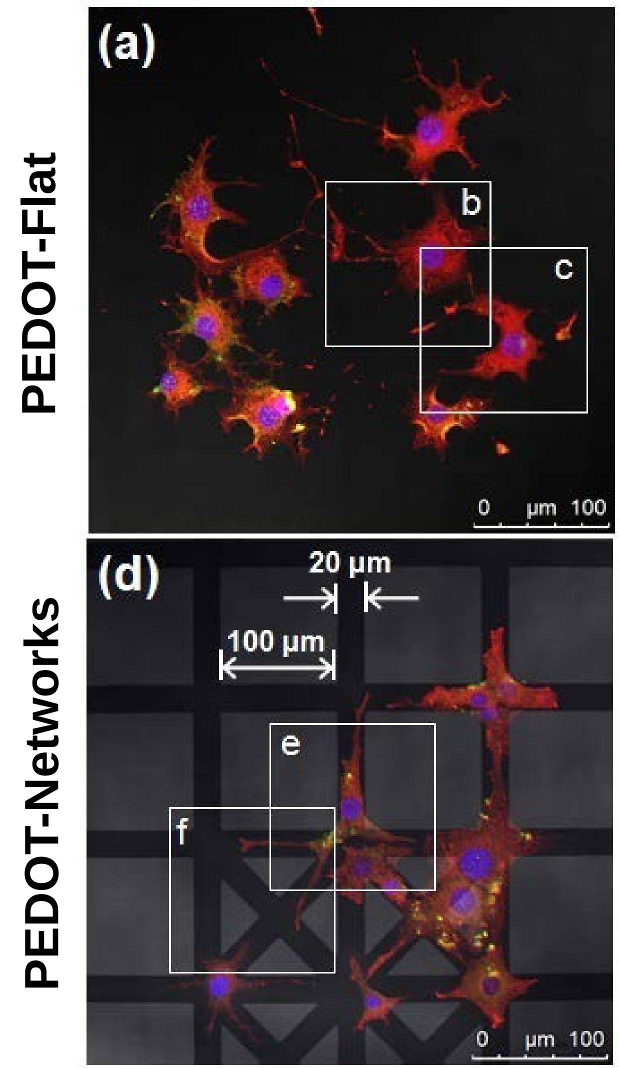

Lab Chip, **11**, 3674 (2011).

Electrically tunable organic bioelectronics for spatial and temporal manipulation of neuron-like pheochromocytoma (PC-12) cells

☆ Graphene-PEDOT microelectrode array system☆

BBA General Subject, **1830**, 4321 (2013)

Electrical Stimulation (ES) Condition:

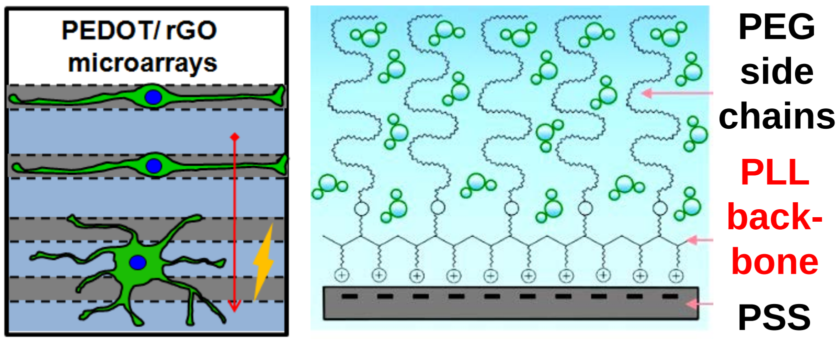

Raman Image

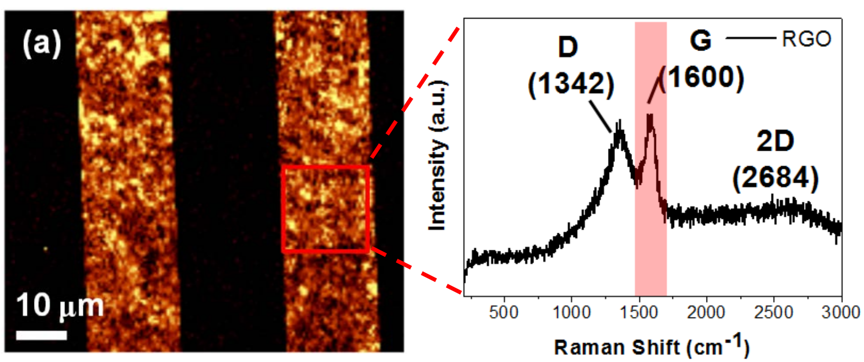

Reduced graphene oxide (rGO)

1. **Contact attraction:** rGO
2. **Contact repulsion:** PLL-*g*-PEG/PEDOT:PSS
3. **Chemoattraction.** NGF
4. **Electrical Stimulation**

ES for Spatiotemporal Control by DC voltage

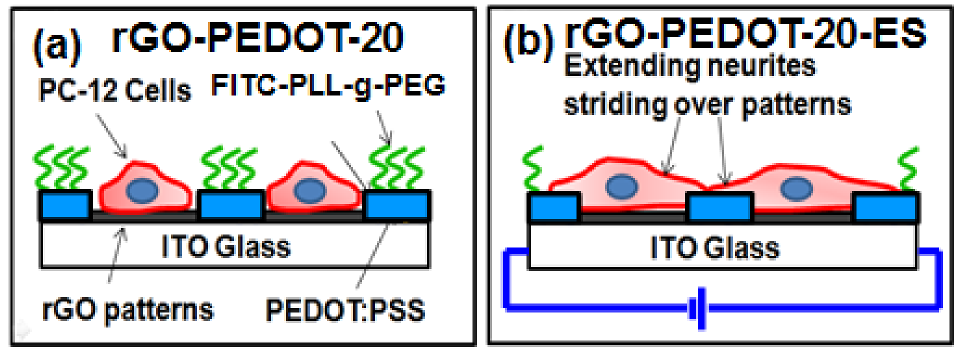

DC voltage of 120 mV mm^{-1}

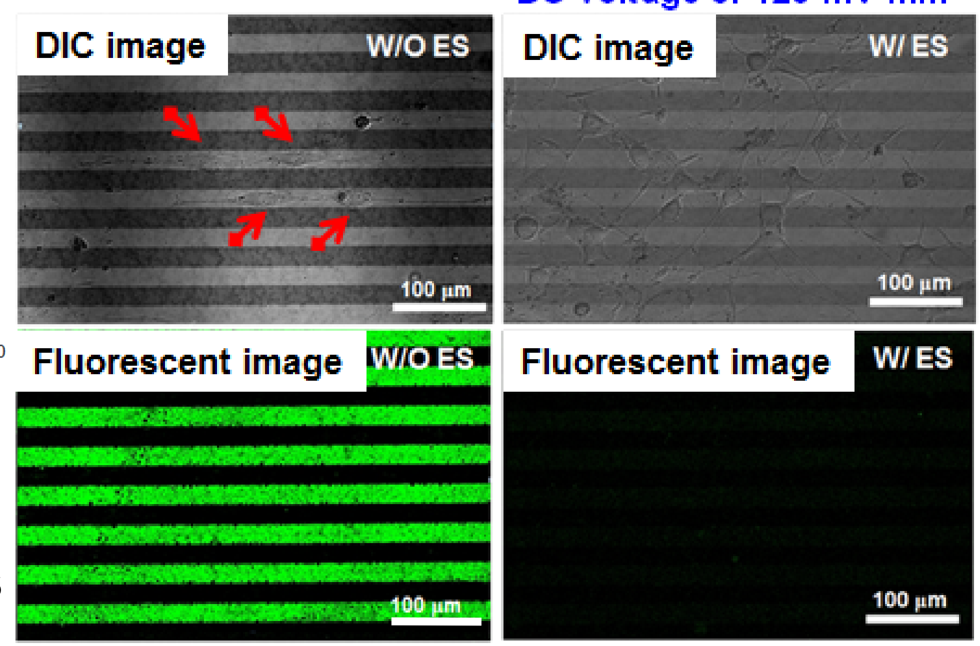

rGO-Flat rGO-PEDOT-20

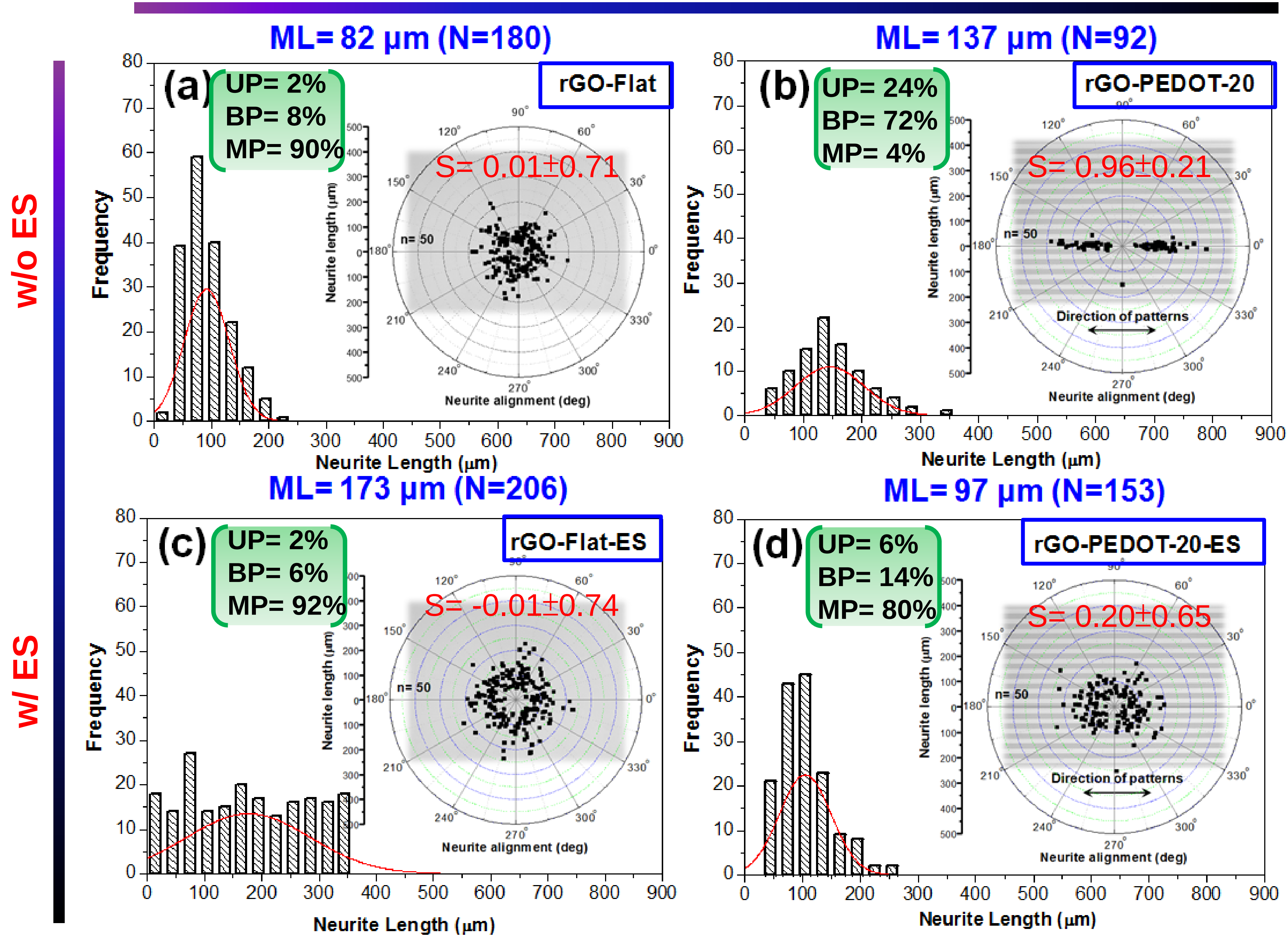

PC-12 Cell type: Unipolar (UP); Bipolar (BP); Multipolar (MP)

Microelectrode Array (MEA)-System

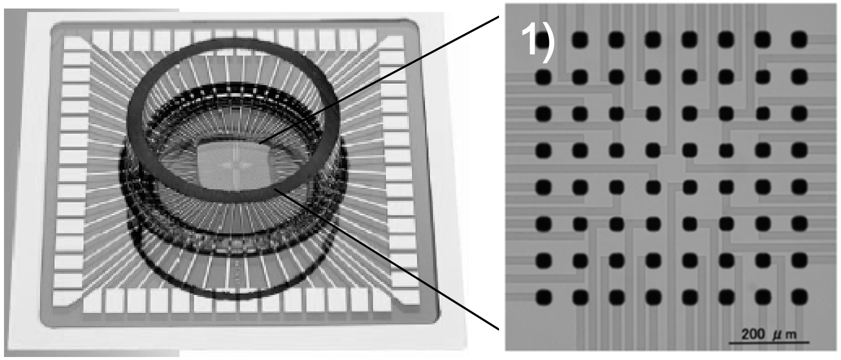

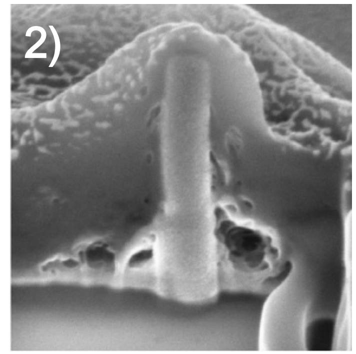

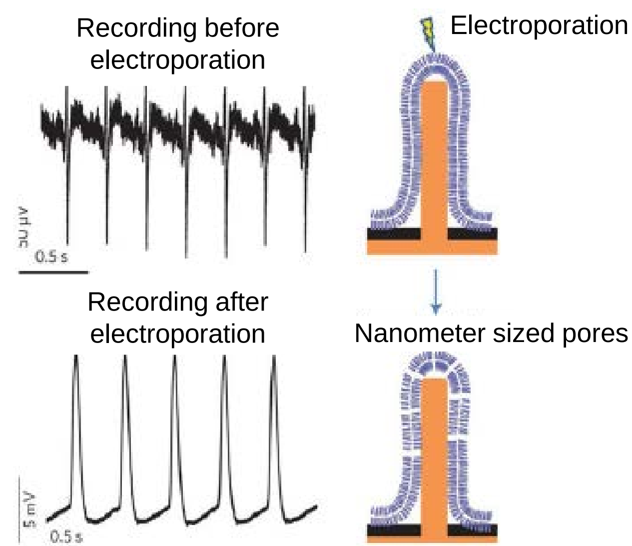

BI Materials **Vertical Nanorods**

TiN electrodes, SiN isolator, contact pads and tracks transparent (ITO), with internal reference electrode, electrode grid 8x8, 60 electrodes, electrode spacing 200µm, electrode diameter 30µm, warranty: 6 months.

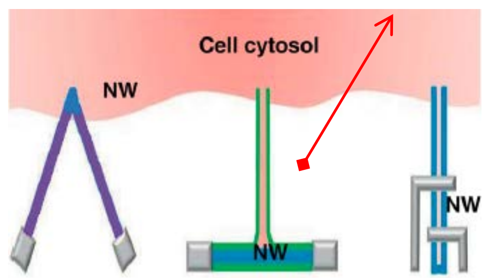

Retina

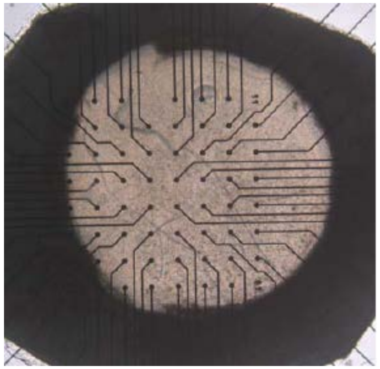

Brain Mapping

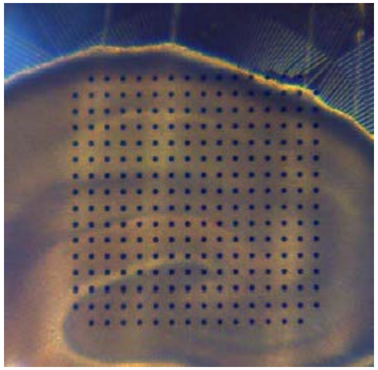

Neuronal cells

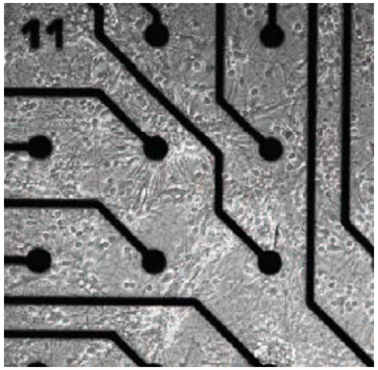

Stem cells

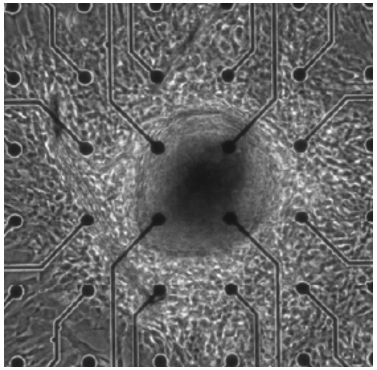

Organotypic cultures

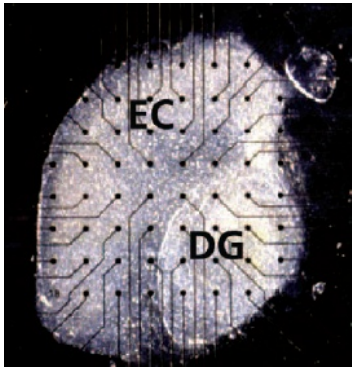

multichannel systems

Probe Mechanotransduction (PM)

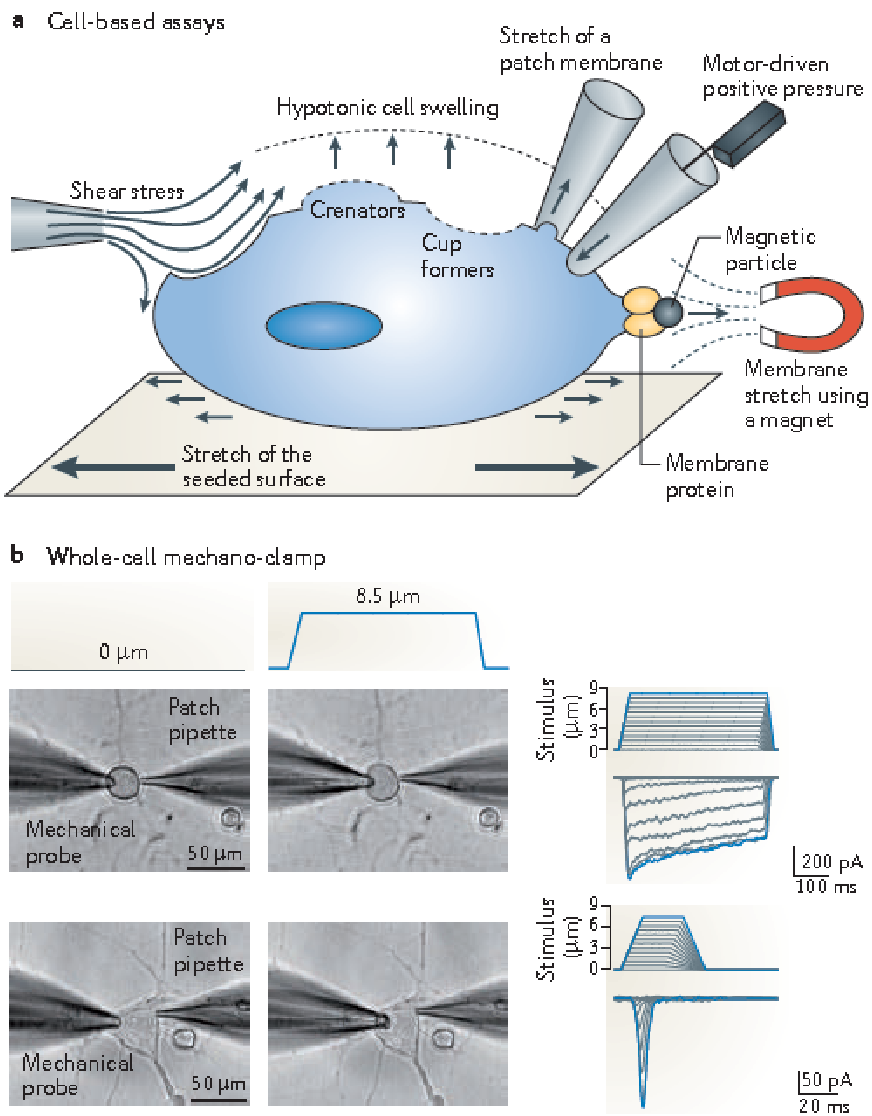

Nature Reviews 12 (2011) 139.

Electric Cell-Substrate Impedance Sensing (ECIS)

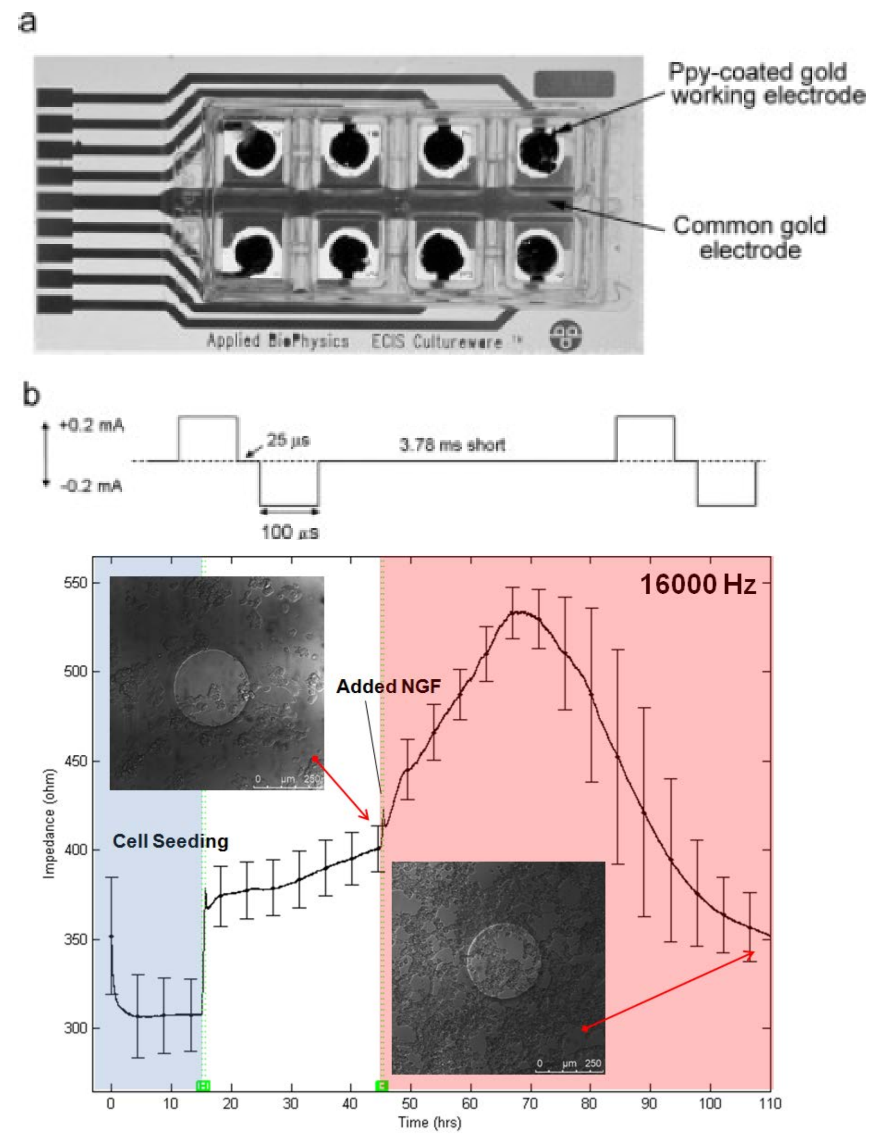

BI coated MEA-system for in vitro and in vivo

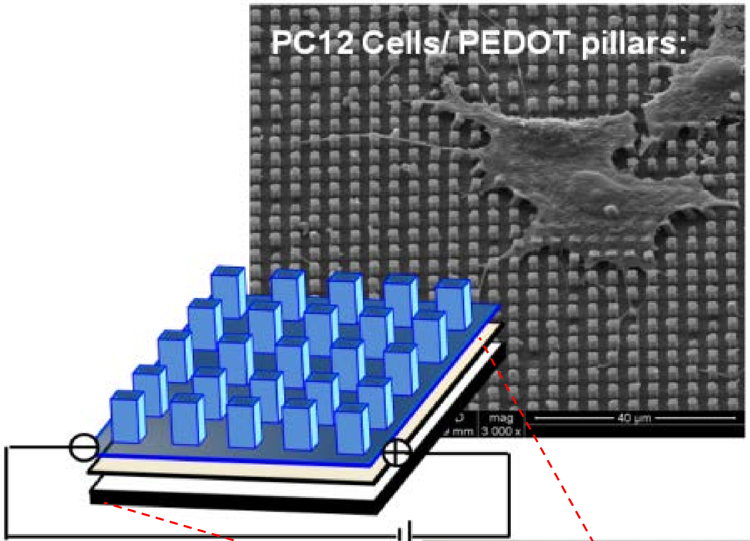

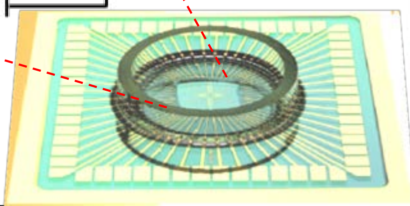

1. Action potential
2. Field potential
3. Electrocardiogram

4. Probe Mechanotransduction-FET :

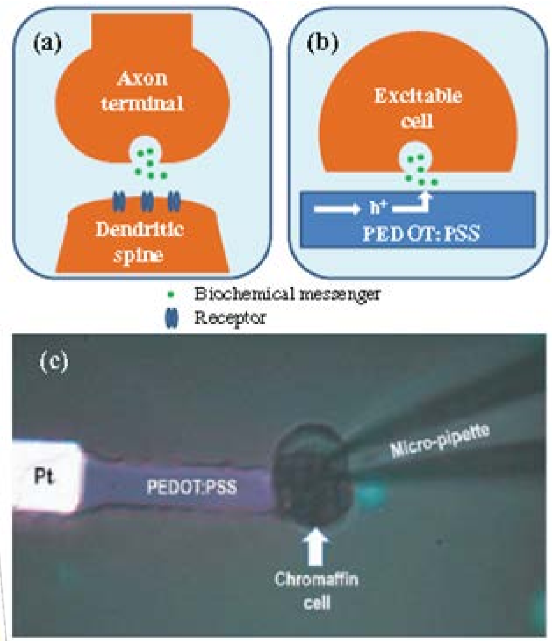

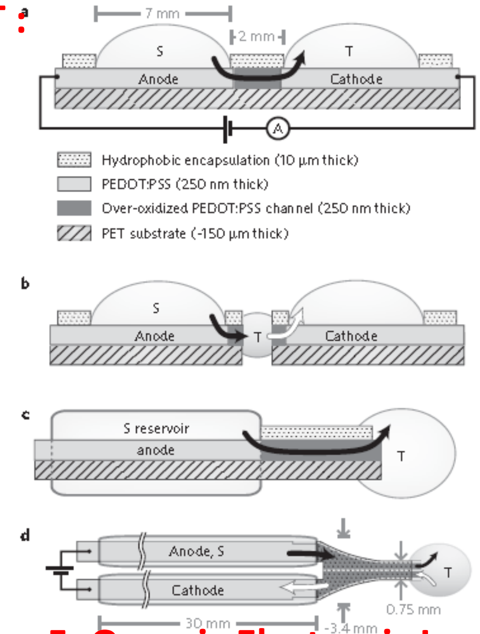

5. Organic Electronic Ion Pump (OEIP):

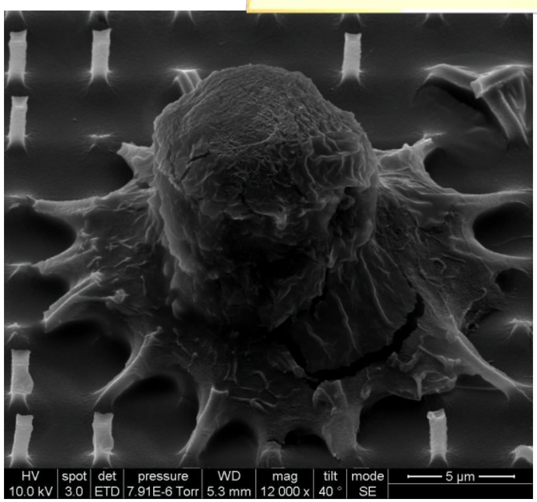

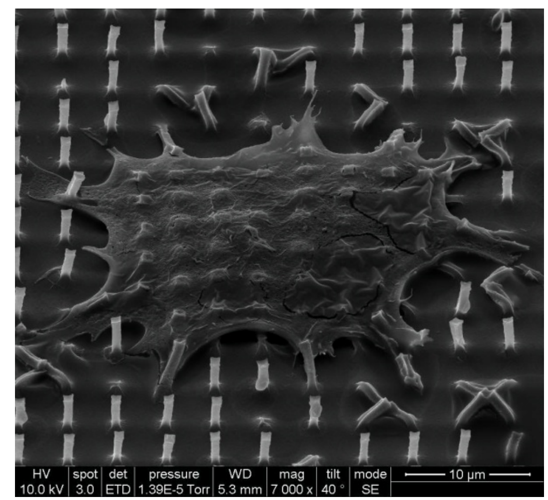

MCF7 cells/ PEDOT Nanorod Arrays

Ultra-conformable PEDOT:PSS microelectrodes

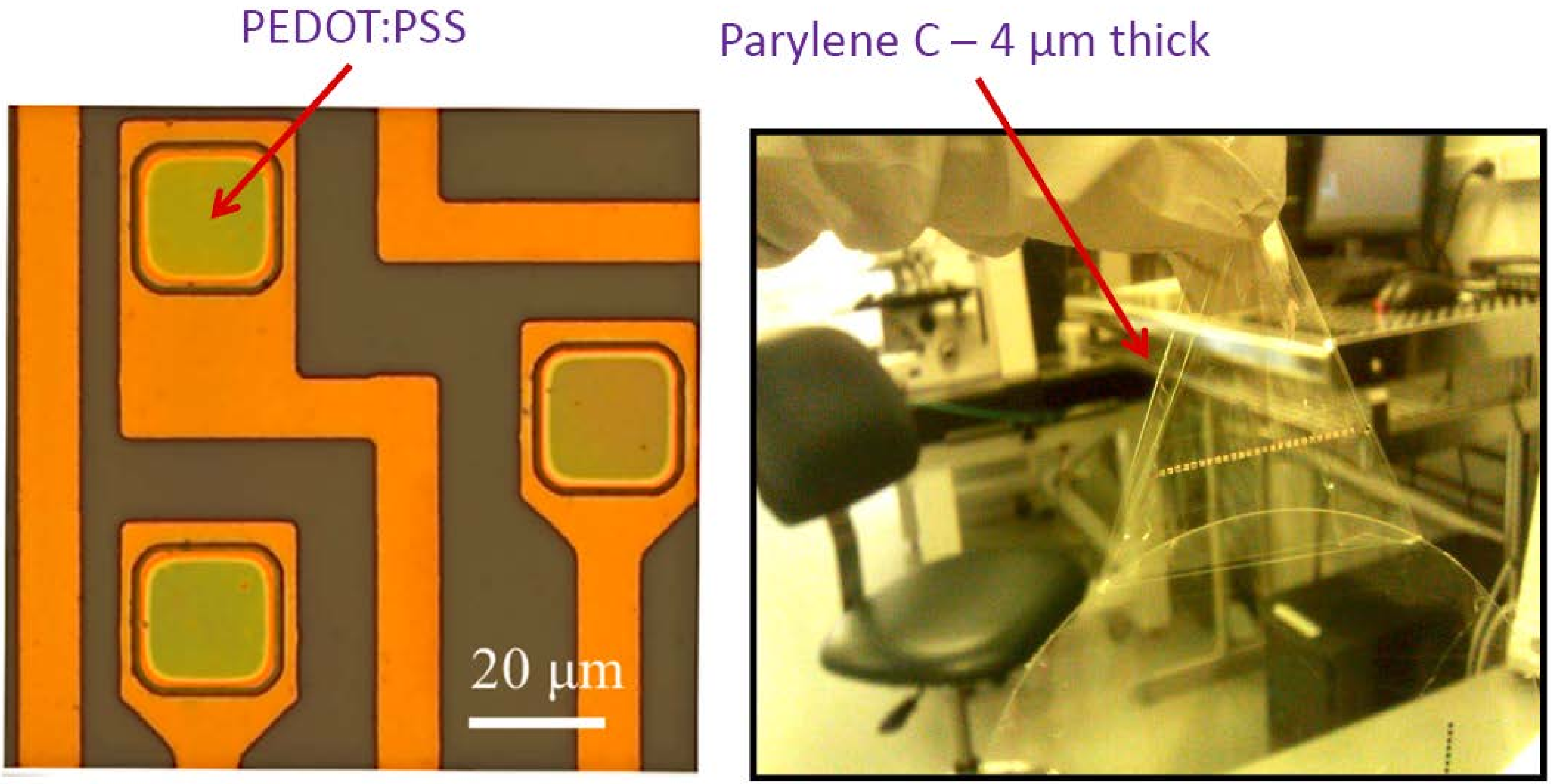

D. Khodagholy, T. Doublet, M. Gurfinkel, P. Quilichini, E. Ismailova, P. Leleux, T. Herve, S. Sanaur, C. Bernard, and G.G. Malliaras, Adv. Mater. 36, H268 (2011).

Ultra-conformable ECoG arrays

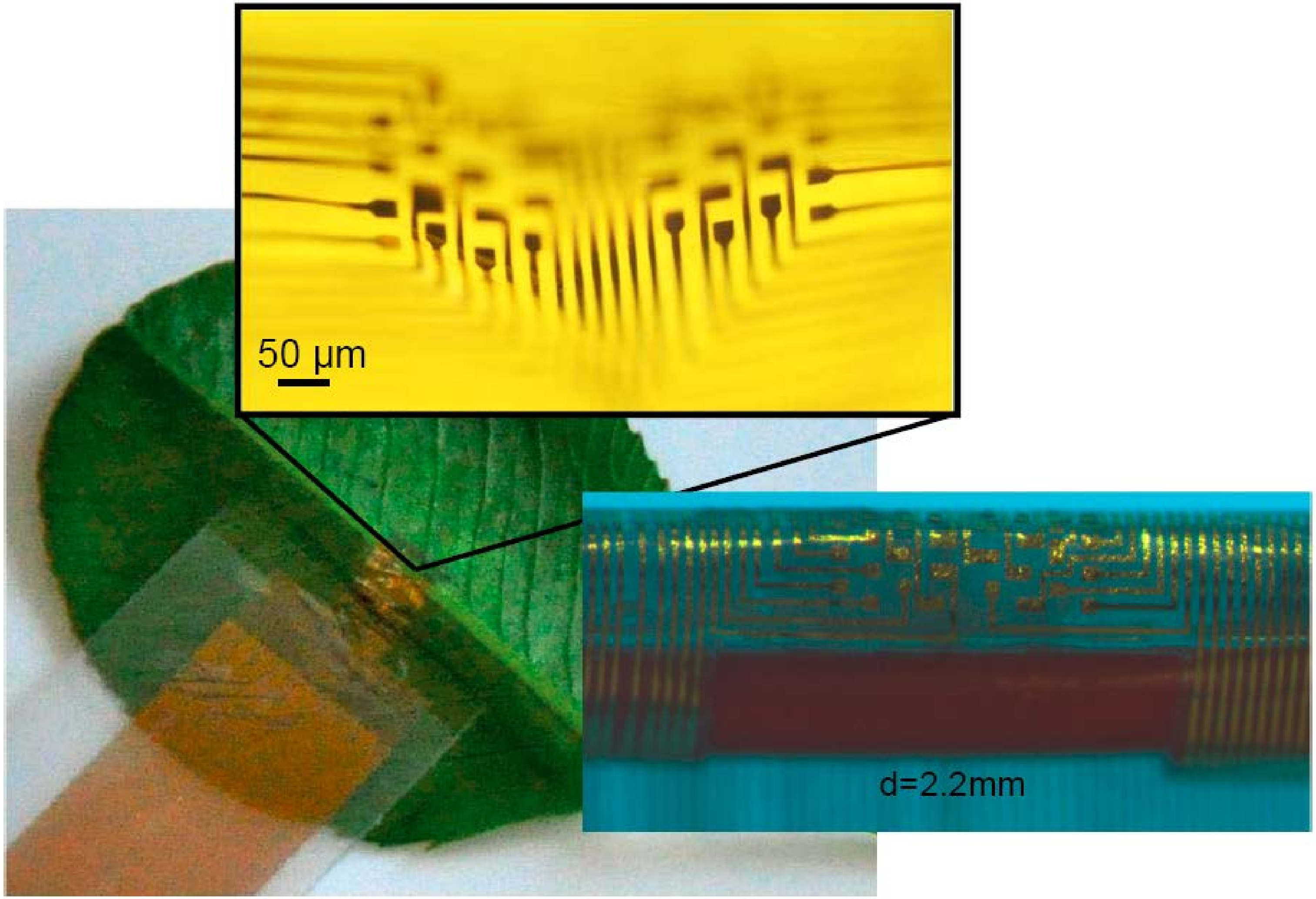

D. Khodagholy, T. Doublet, M. Gurfinkel, P. Quilichini, E. Ismailova, P. Leleux, T. Herve, S. Sanaur, C. Bernard, and G.G. Malliaras, Adv. Mater. 36, H268 (2011).

PEDOT:PSS electrodes outperform Au electrodes

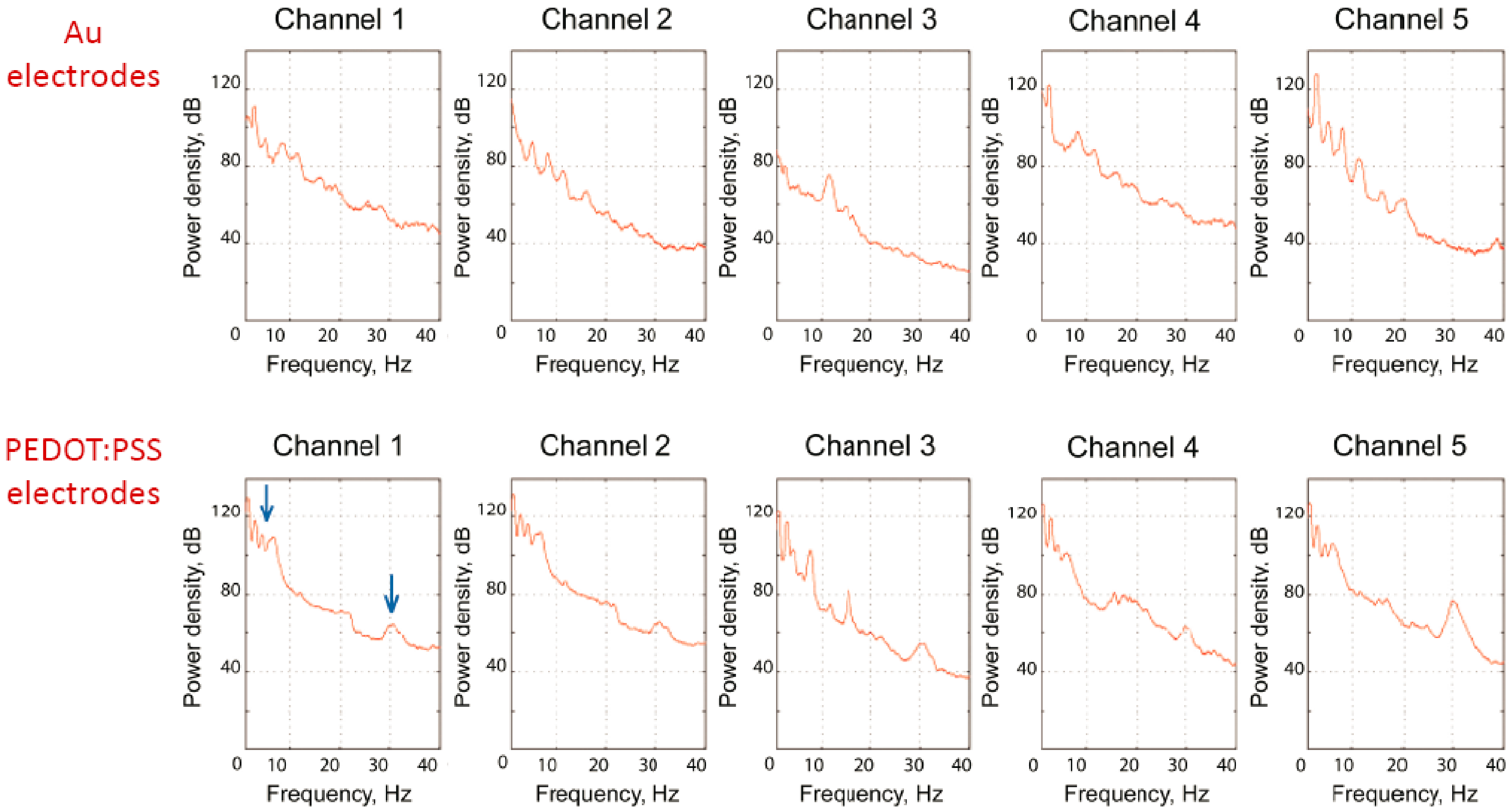

D. Khodagholy, T. Doublet, M. Gurfinkel, P. Quilichini, E. Ismailova, P. Leleux, T. Herve, S. Sanaur, C. Bernard, and G.G. Malliaras, Adv. Mater. 36, H268 (2011).

Detection of single neurons from brain surface

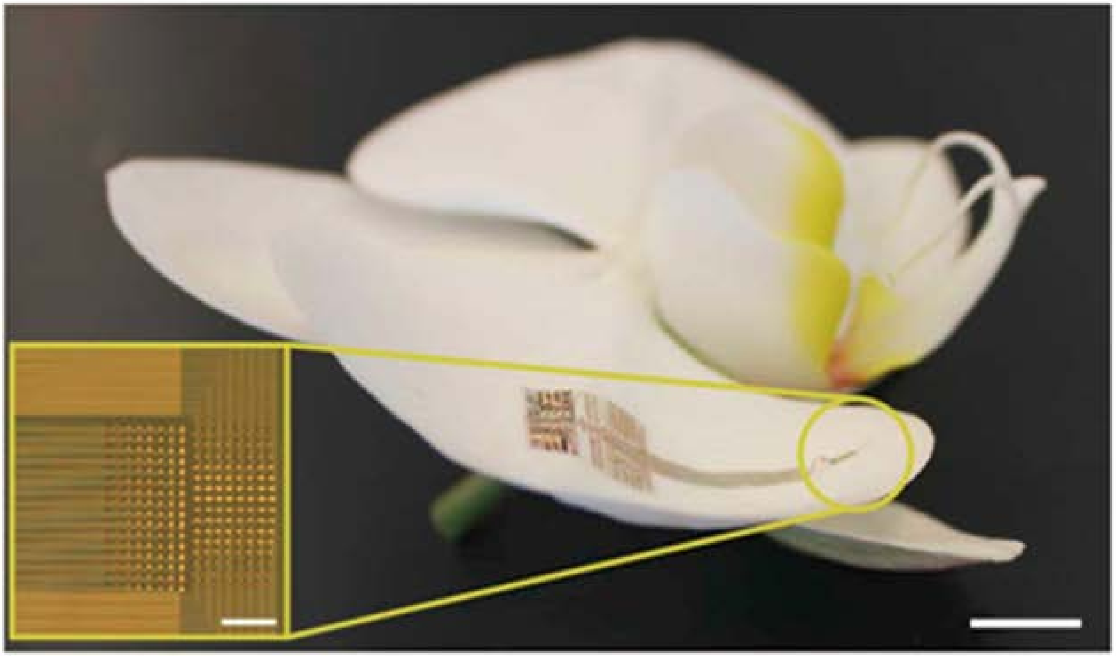

256 electrodes, 10 x 10 μm² with 30 μm inter-electrode spacing

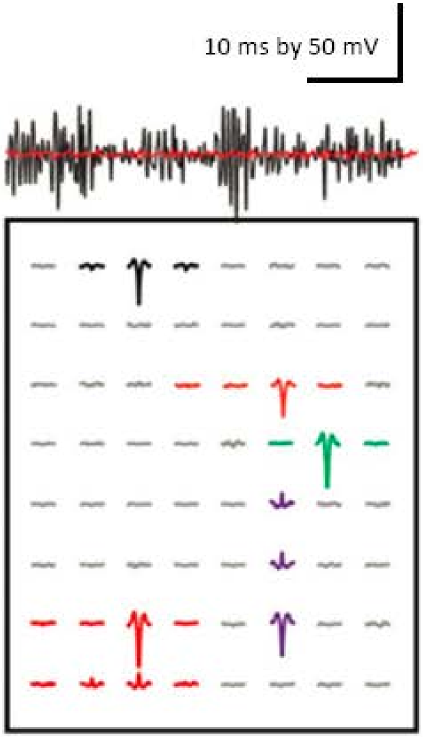

Electrocorticography in rats

D. Khodagholy, J.N. Gelinas, T. Thesen, W. Doyle, O. Devinsky,
G.G. Malliaras and G. Buzsáki, Natrure Neurosci. 18, 310 (2015)

Translation to the clinic

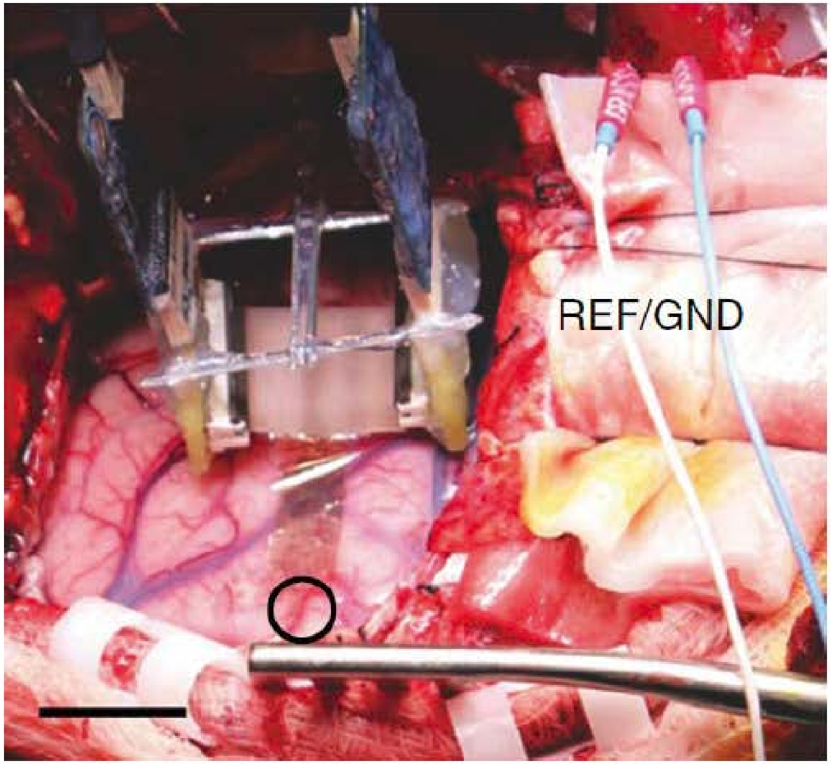

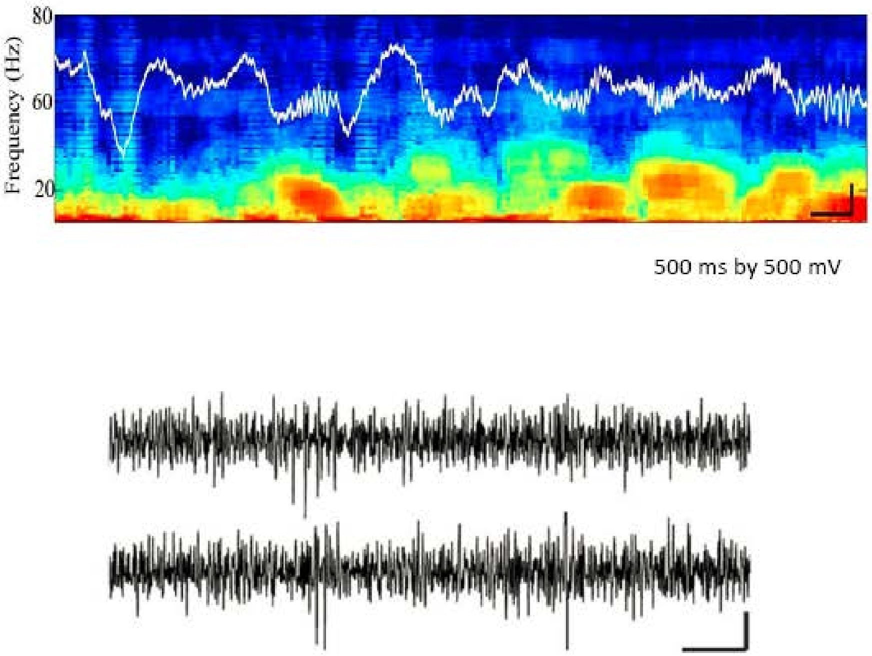

Acute recordings in human patients

D. Khodagholy, J.N. Gelinas, T. Thesen, W. Doyle, O. Devinsky,
G.G. Malliaras and G. Buzsáki, Natrure Neurosci. 18, 310 (2015)

Organic electrochemical transistors (OECTs) record brain activity with record-high SNR

Field-effect transistors for neural recordings

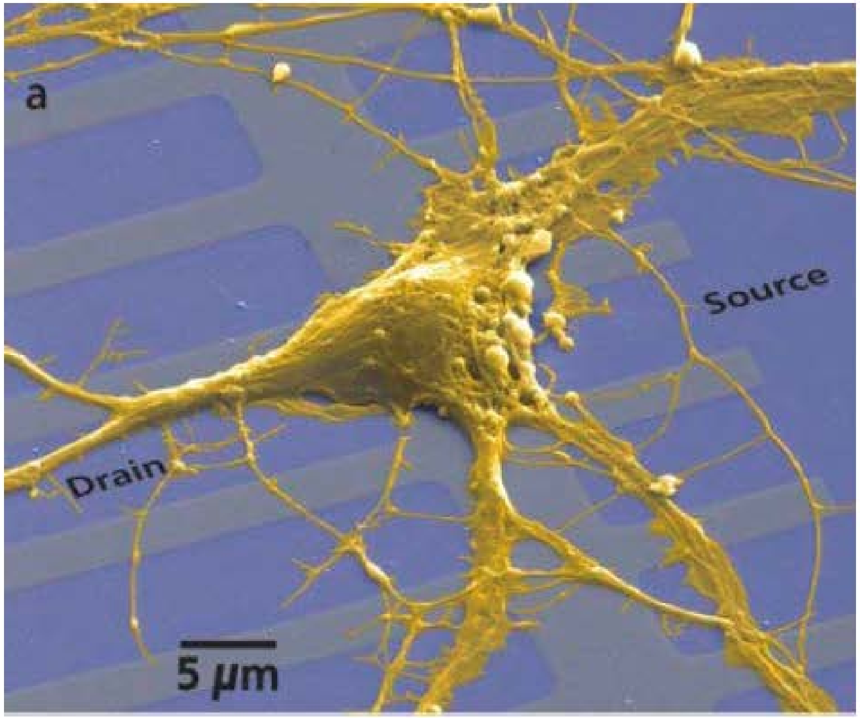

Fromherz group, MPI

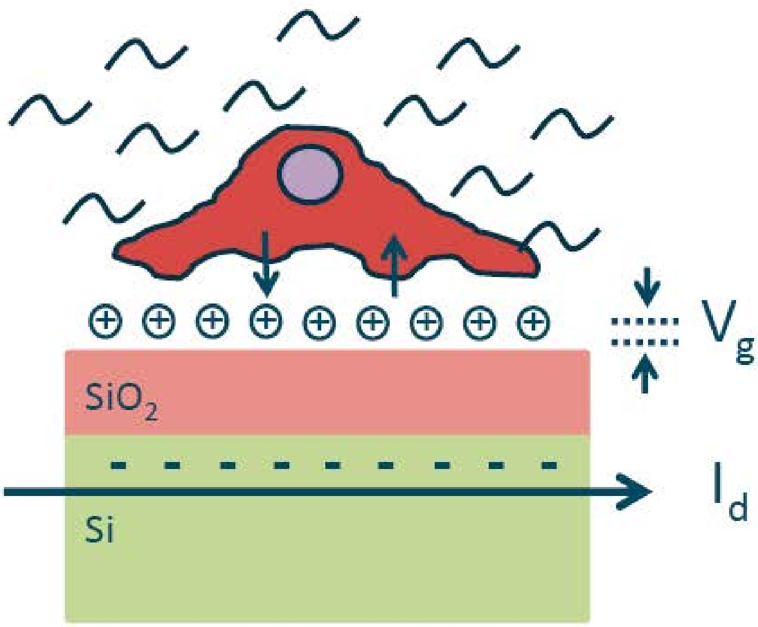

Field-effect transistor (FET)

$C'_{max} = 5\ \mu F/cm^2$

Organic Field-effect Transistors (OFET)

(a)

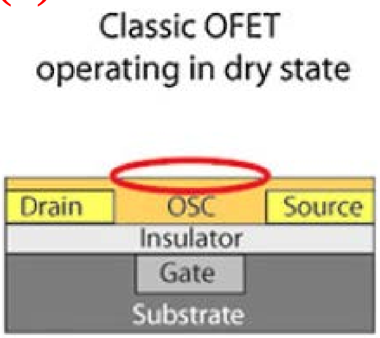

(c)

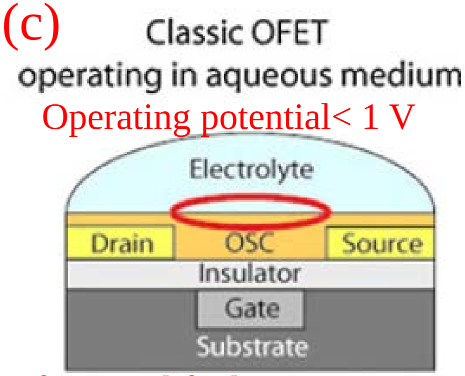

Operating potential< 1 V

Surface modified OSC can increase sensitivity

Detection limit= 1 nM for DNA

(b)

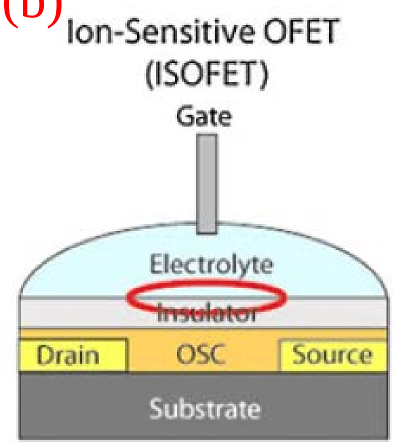

Operating potential> 10 V

Detection limit= 0.01-25 mM

(d)

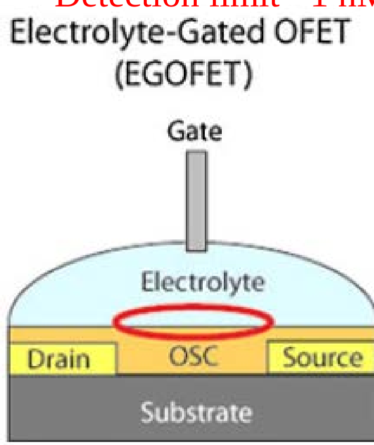

Operating potential< 1V

Faster response than OECT

In OFET, the gate is separated from the semiconductor by an insulator. Different dielectrics can be used, e.g. vacuum, oxides, polymers, self-assembled monolayers.

Characterization:

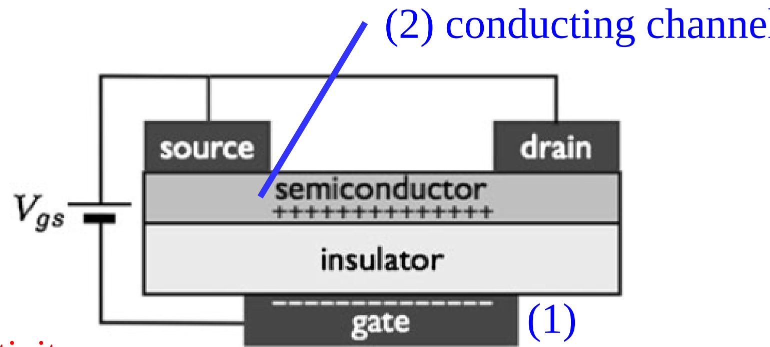

When the gate is negatively (positively) polarized in a p-channel (n-channel) device, free holes (electrons) in the semiconductor are drawn toward the semiconductor-insulator interface to compensate an equivalent negative (positive) charge at the gate-insulator interface.

The gate voltage required to switch the transistor from its “off” to its “on” state, i.e. to establish a conducting transistor channel, is called the threshold voltage.

Electrolyte-gated Organic Field-effect Transistors (EGOFETs)

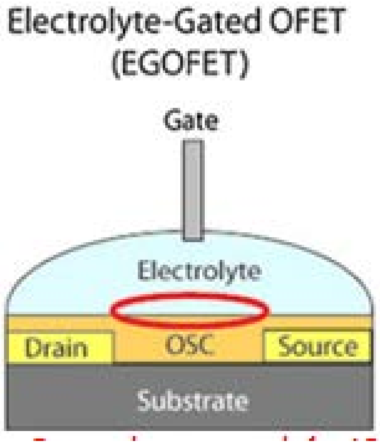

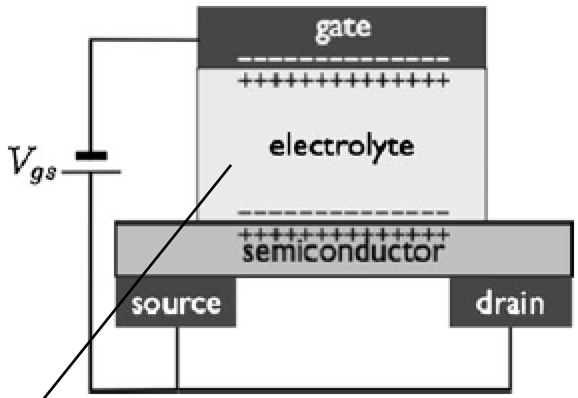

In a p-channel EGOFET device, upon positive polarization of the gate, the anions of the electrolyte migrate away from the electrolyte–semiconductor interface, while cations are attracted toward the electrolyte–gate interface, resulting in the formation of an electrical double layer (EDL) at both interfaces.

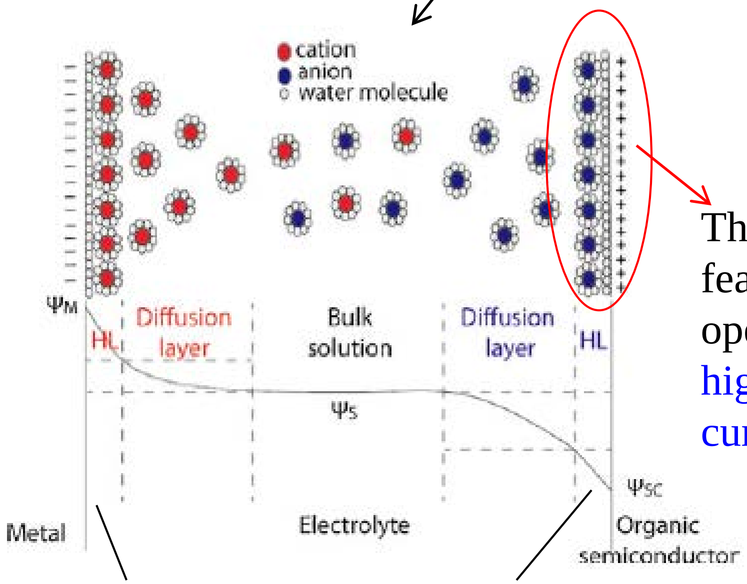

Helmholtz layer (HL)

The thin EDL (0.01 nm) can be compare to a capacitor featuring high capacitance, which enables the transistor to be operated at very low potentials. Furthermore, it generates a higher charge density, thus higher mobility and output currents.

Centimeter-Long and Large-Scale Micropatterns of Reduced Graphene Oxide Films: Fabrication and Sensing Applications

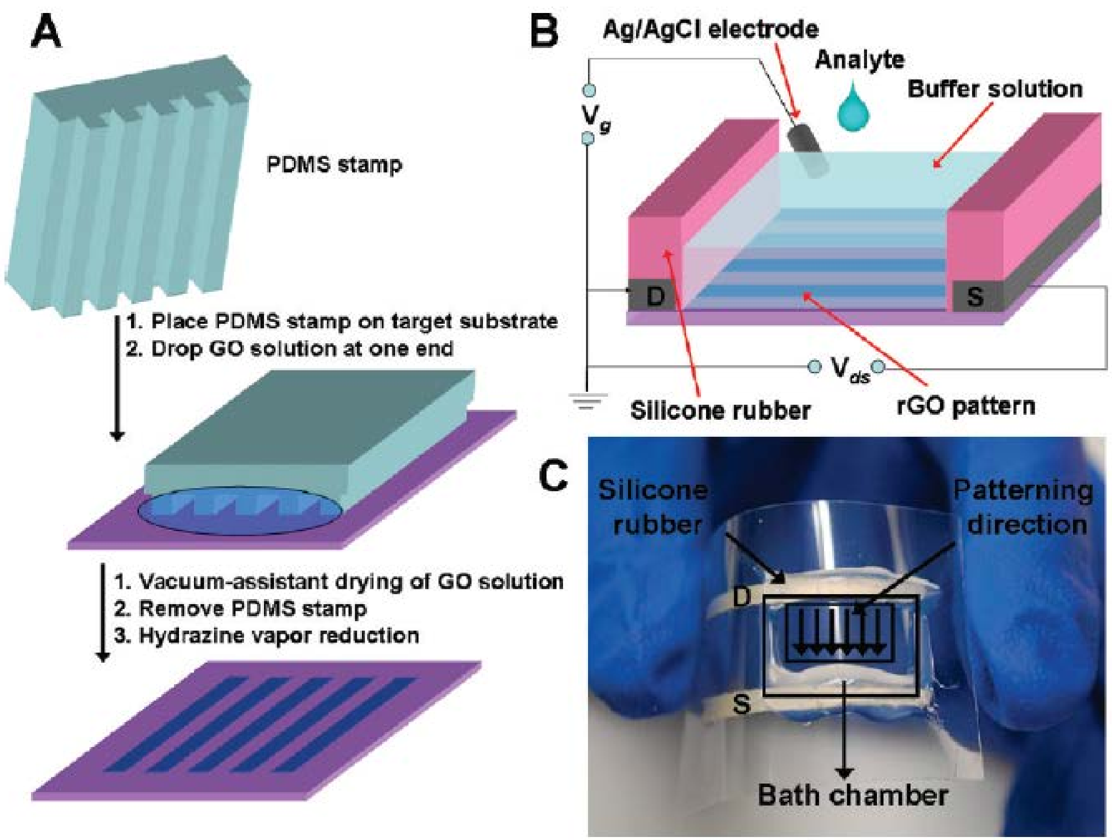

Schematic illustration of the experimental setup of front-gate FET for sensing application.

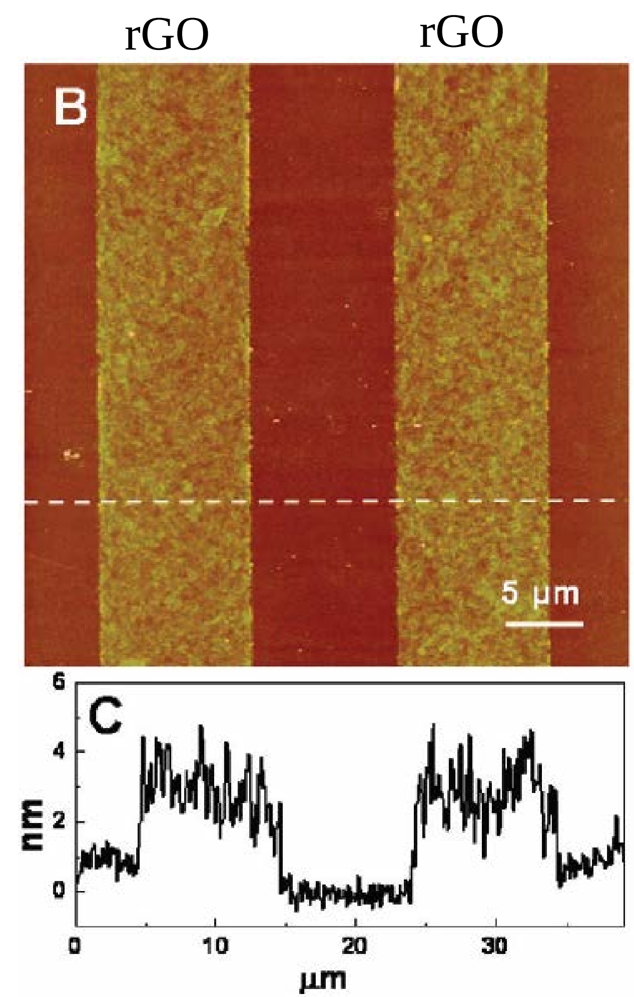

ACS Nano 2010, 4, 3201.

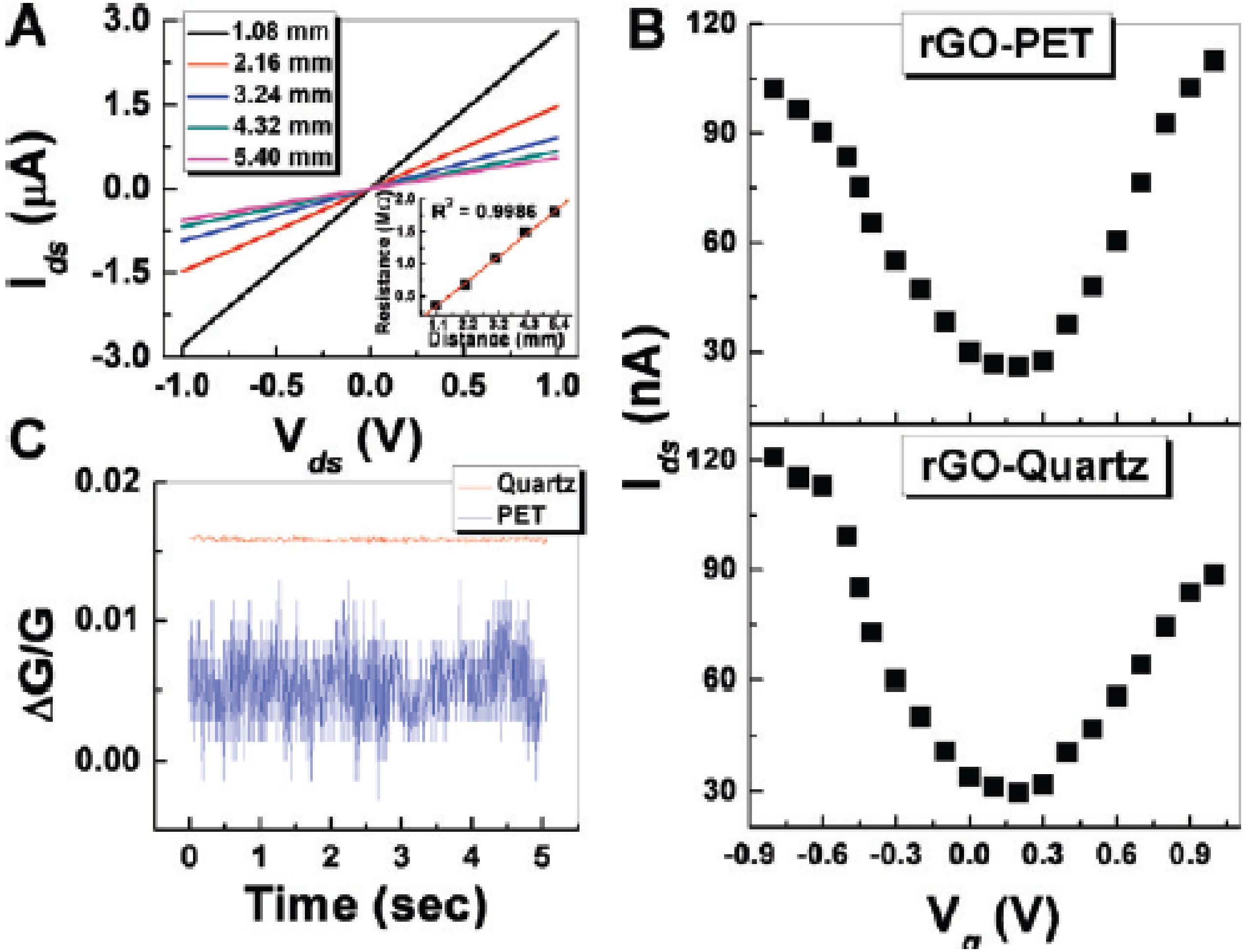

V_{ds} = 400 mV

Current noise on rGO-quartz and rGO-PET devices. The distance between the drain and source electrodes in the devices in panels B and C is fixed at 1 cm.

ACS Nano 2010, 4, 3201.

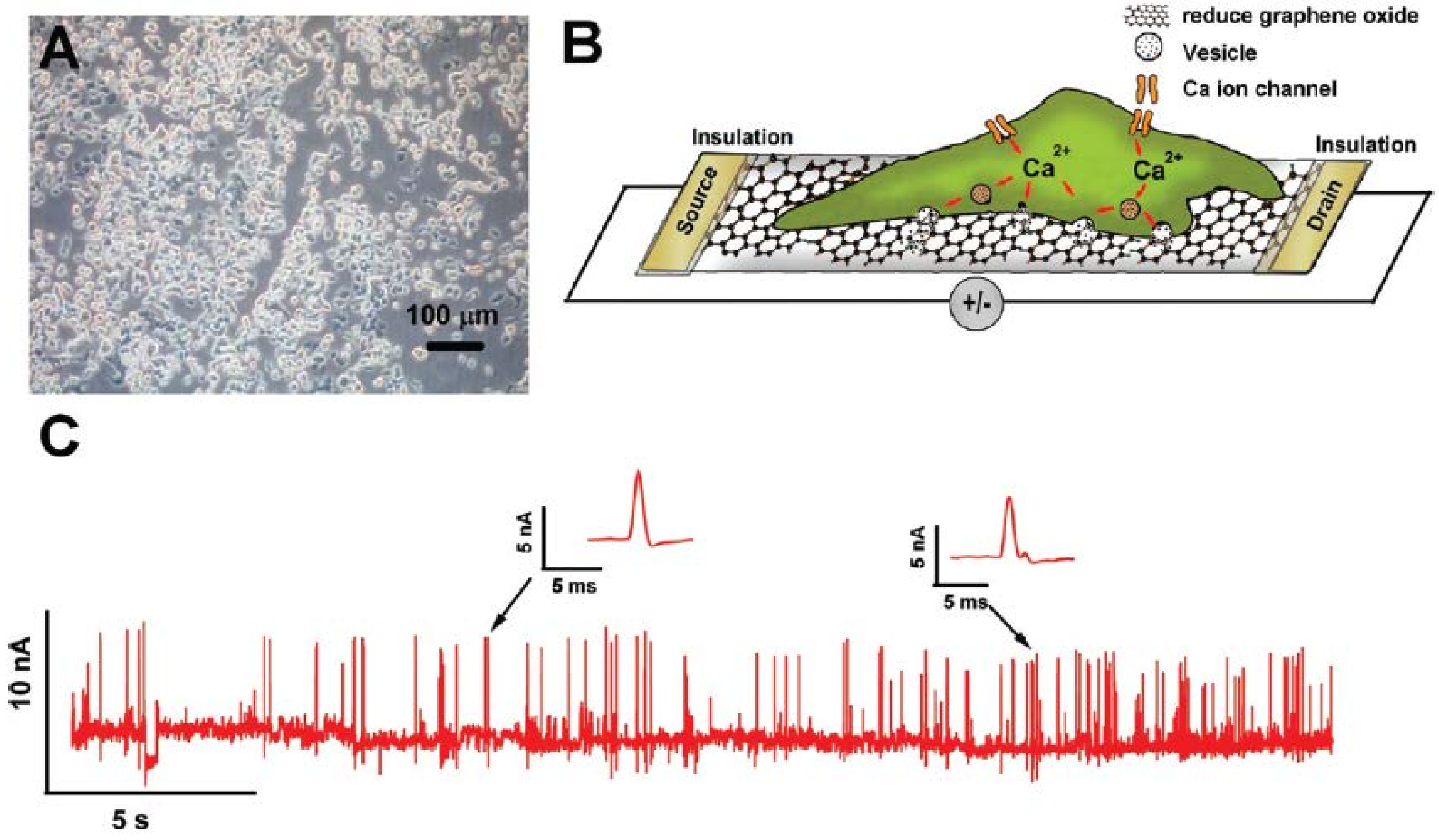

Real-time response of rGO-PET FET to the vesicular secretion of catecholamines from PC12 cells stimulated by high K^+ solution. V_{ds}= 100 mV, V_g = 0 V. The distance between the drain and source electrodes in the device is fixed at 1 cm.

ACS Nano 2010, 4, 3201.

The organic electrochemical transistor (OECT)

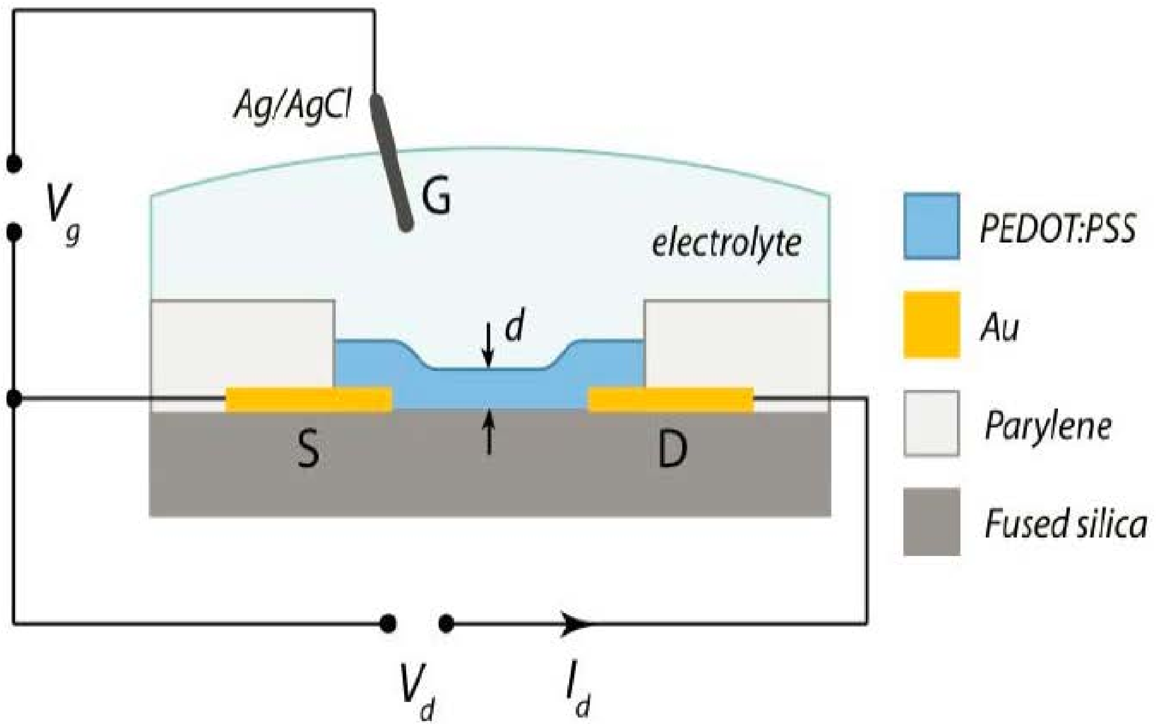

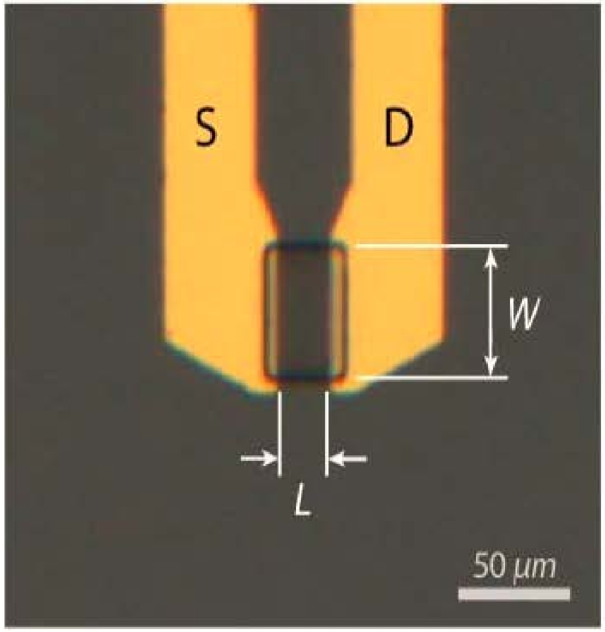

No insulator between channel and electrolyte

First OECT: H.S. White, G.P. Kittlesen, and M.S. Wrighton, *J. Am. Chem. Soc. 106, 5375 (1984).*

Volumetric response of capacitance in PEDOT:PSS

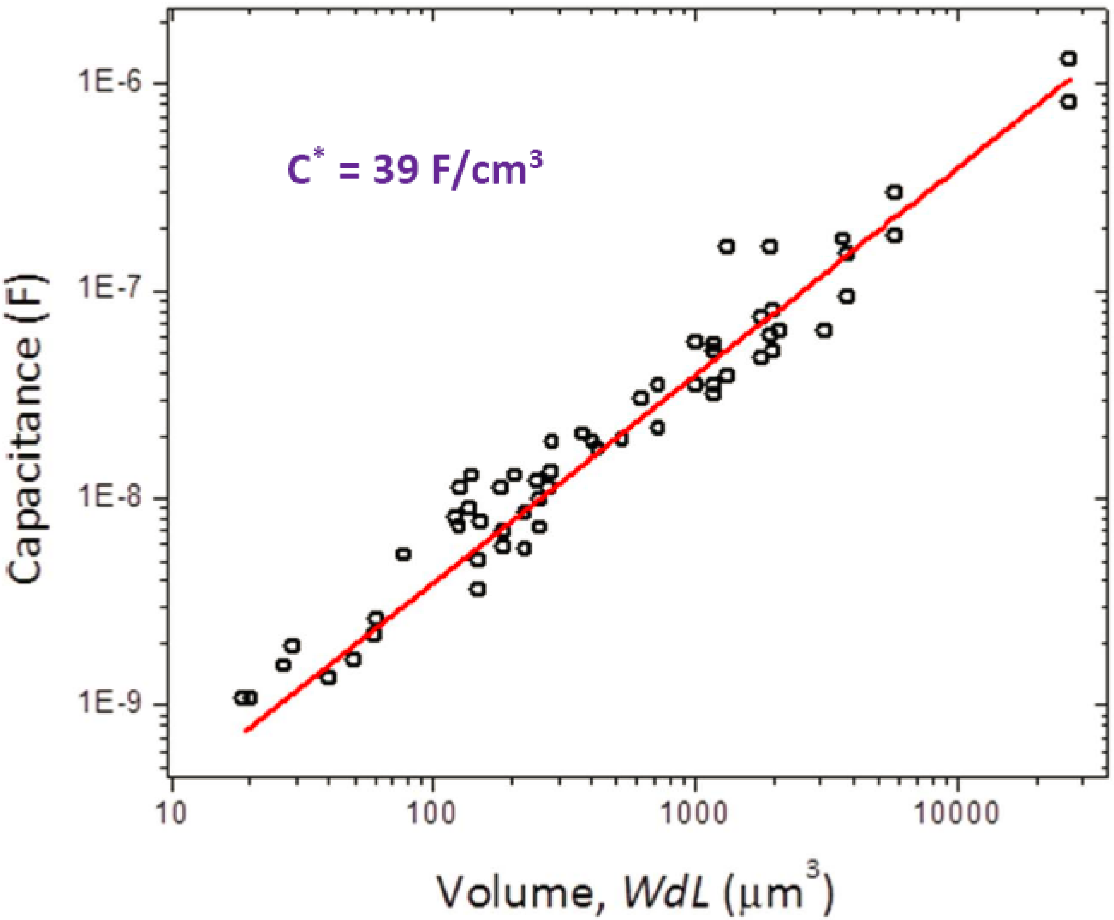

For d=130 nm:
$C' = 500\ \mu F/cm^2$

100× larger than double layer capacitance

J. Rivnay, P. Leleux, M. Ferro, M. Sessolo, A. Williamson, D.A. Koutsouras, D. Khodagholy, M. Ramuz, X. Strakosas, R.M. Owens, C. Benar, J.-M. Badier, C. Bernard, and G.G. Malliaras, SCIENCE Advances 1, e1400251 (2015).

Device model

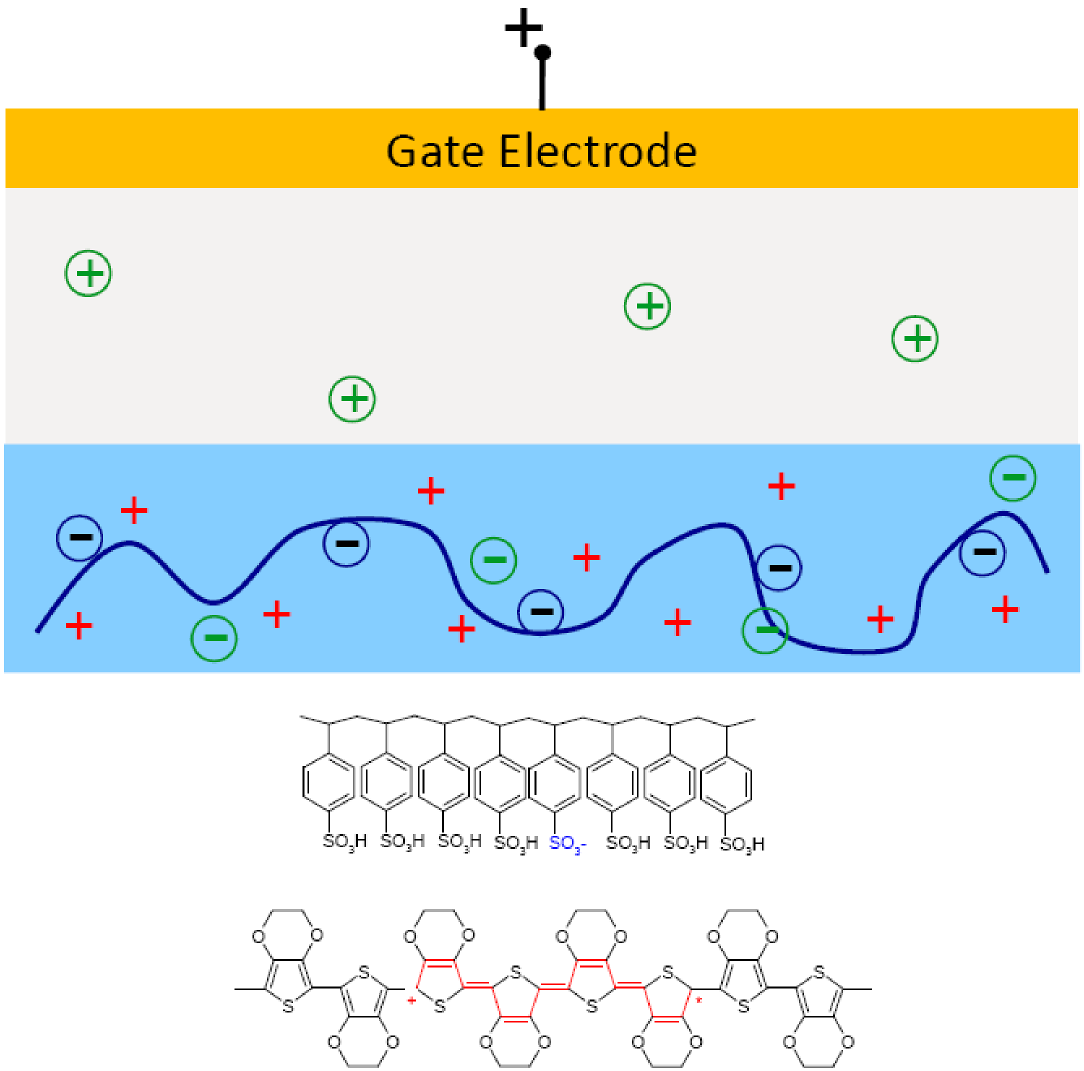

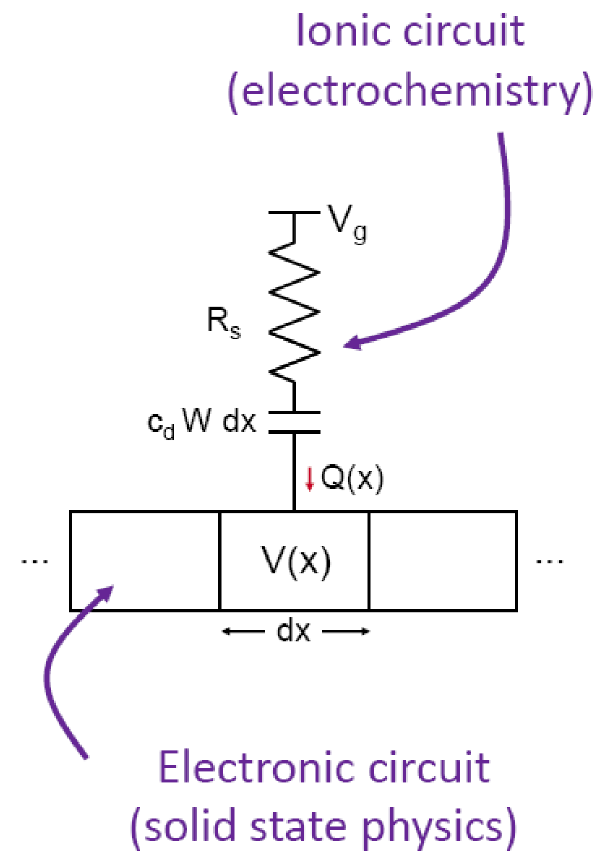

D.A. Bernards and G.G. Malliaras,
Adv. Funct. Mater. 17, 3538 (2008)

Characteristics of OECTs

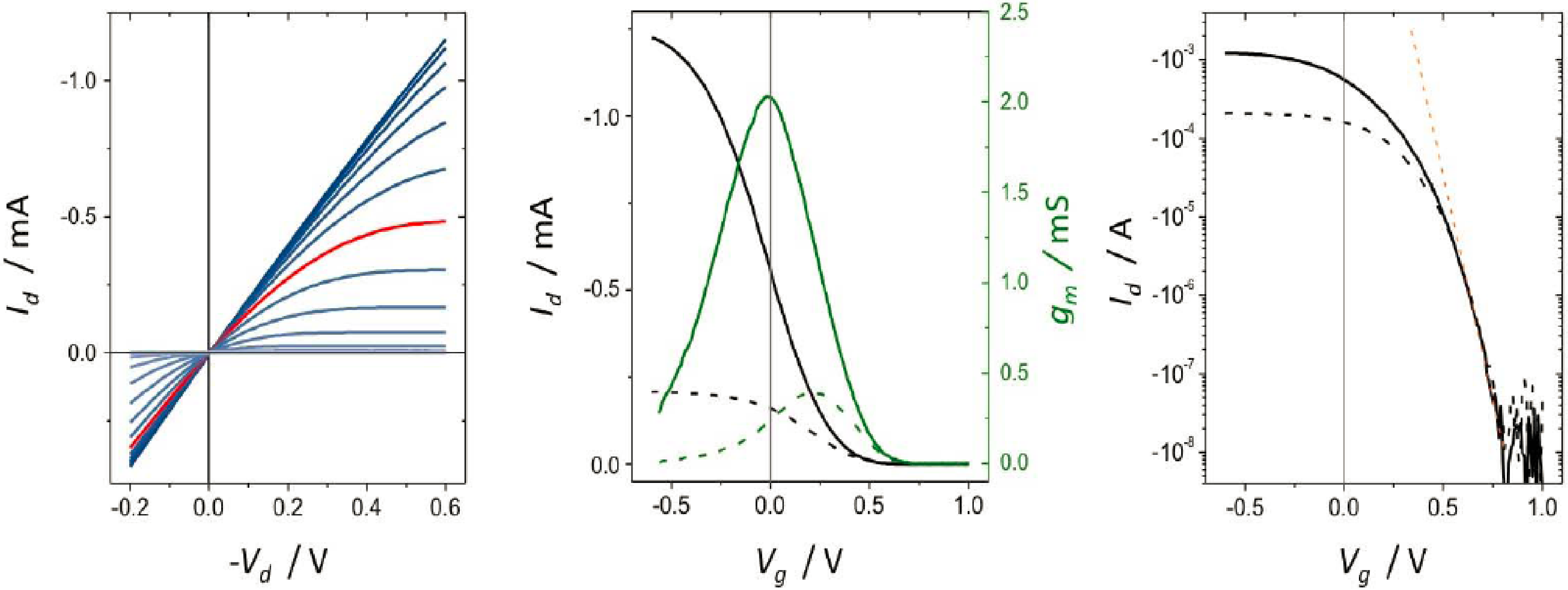

J. Rivnay, P. Leleux, M. Sessolo, D. Khodagholy, T. Hervé, M. Fiocchi, G. G. Malliaras, Adv. Mater. 25, 7010 (2013).

High transconductance OECTs

Active material	Dielectric material	W (μm)	L (μm)	$\|V_G\|$ (V)	$\|V_D\|$ (V)	g_m (μS)	g_m/W (S m^{-1})	$g_m/\|V_D\|$ (μS V^{-1})
Aqueous electrolyte								
PEDOT:PSS (best)	NaCl	10	10	0.2	0.6	4,020	402	6,700
PEDOT:PSS (typical)	NaCl	10	5	0.275	0.6	2,700	270	4,500
Graphene[17, (18)]	PBS + NaCl	40	20	0.25	0.1	420	11	4,200
Diamond[19]	PBS + KCl (*in vitro*)	~20	~5-20	0.22	0.2	18	0.9	90
Silicon[20]	SiO_2/TiO_2 (*in toto*)	20	20	0.25	0.25	15	0.75	60
Silicon NW[21]	SiO_2, PBS	20	2	~0.4	0.03	5	0.25	167
Ionic liquid/gel, solid electrolyte								
ZnO[22]	IL (DEME/TFSI)	200	500	1.2	0.1	160	0.8	1,600
ZnO NW[23]	Solid electrolyte ($PVA/LiClO_4$)	0.018	0.94	~1.5	0.5	2.79	155	5.58
Organic semiconductor: P3HT[24, (15)]	IL (EMIM/TFSI) gel (PS-PEO-PS)	100	20	~4	1	50	0.5	50
Solid-state								
ZnO[25, (26)]	Al_2O_3	50	1	5.1	4	1,400	28	350
Graphene[27, (28,29)]	SiO_2 (BG); Y_2O_3 (TG)	2.7	0.31	~1.2	2	1,863	690	932
III-V NW: n-InAs NW[30, (31)]	SiN_x	0.05	2	0.56	1	97.5	1,950	98
III-V Bulk: GaN/InAlN[32, (33,34)]	SiN_x	NR	0.06	1.75	2	NR*	1,105	NR
Carbon nanotube (mat)[35, (36)]	HfO_2	10	1.5	~1	0.5	50	5	100
Organic semiconductor: DNTT[37, (38,39)]	AlO_x/SAM	10	1	~2	2	12	1.2	95
Silicon NW[40]	SiO_2	0.01	0.8-2	~2-4	NR	2	200	NR

D. Khodagholy, J. Rivnay, M. Sessolo, M. Gurfinkel, P. Leleux, L.H. Jimison, E. Stavrinidou, T. Herve, S. Sanaur, R.M. Owens, and G.G. Malliaras, Nature Comm. 4, 2133 (2013).

In vivo recordings using transistors

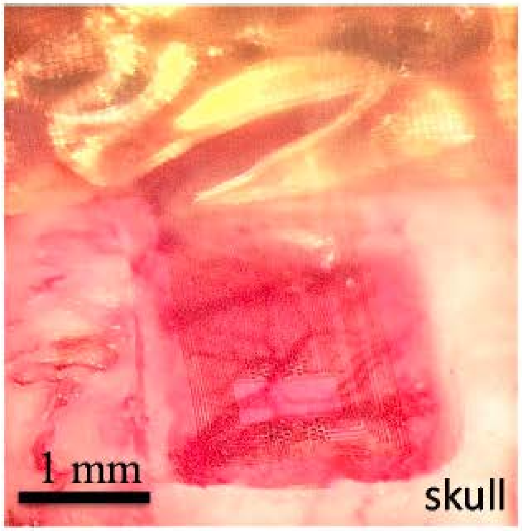

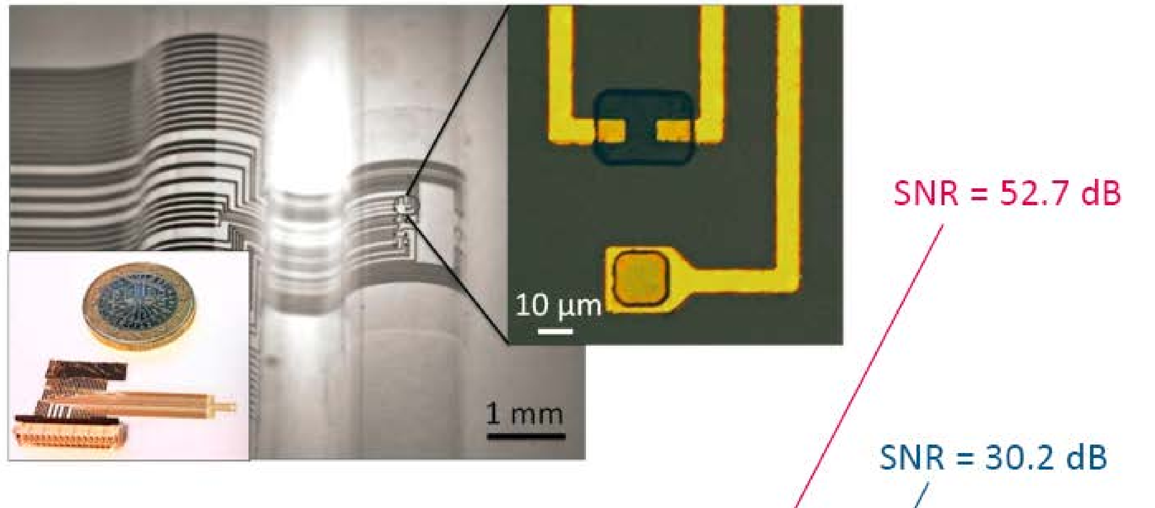

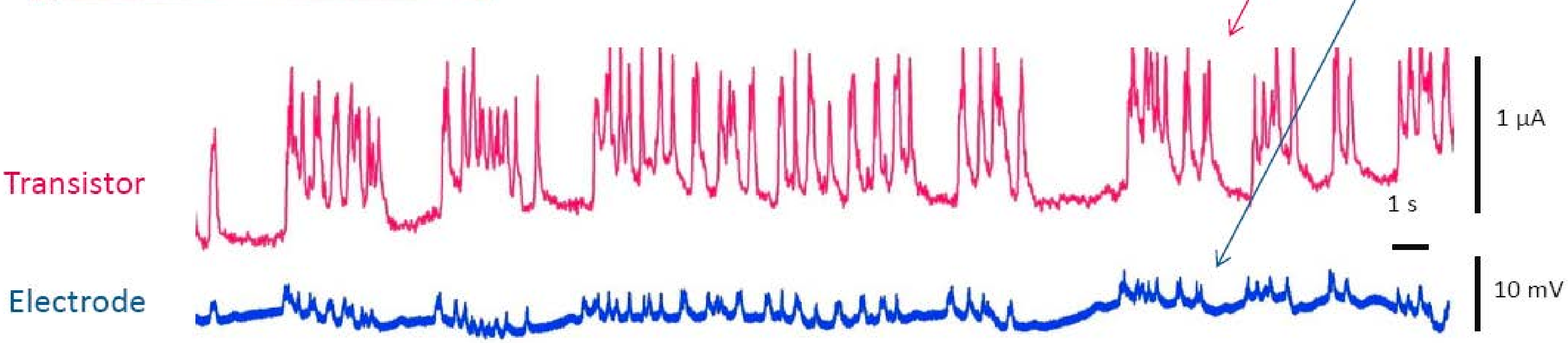

D. Khodagholy, T. Doublet, P. Quilichini, M. Gurfinkel, P. Leleux, A. Ghestem, E. Ismailova, T. Herve, S. Sanaur, C. Bernard, and G.G. Malliaras , *Nature Comm. 4, 1575 (2013).*

Transistors enable less invasive recordings

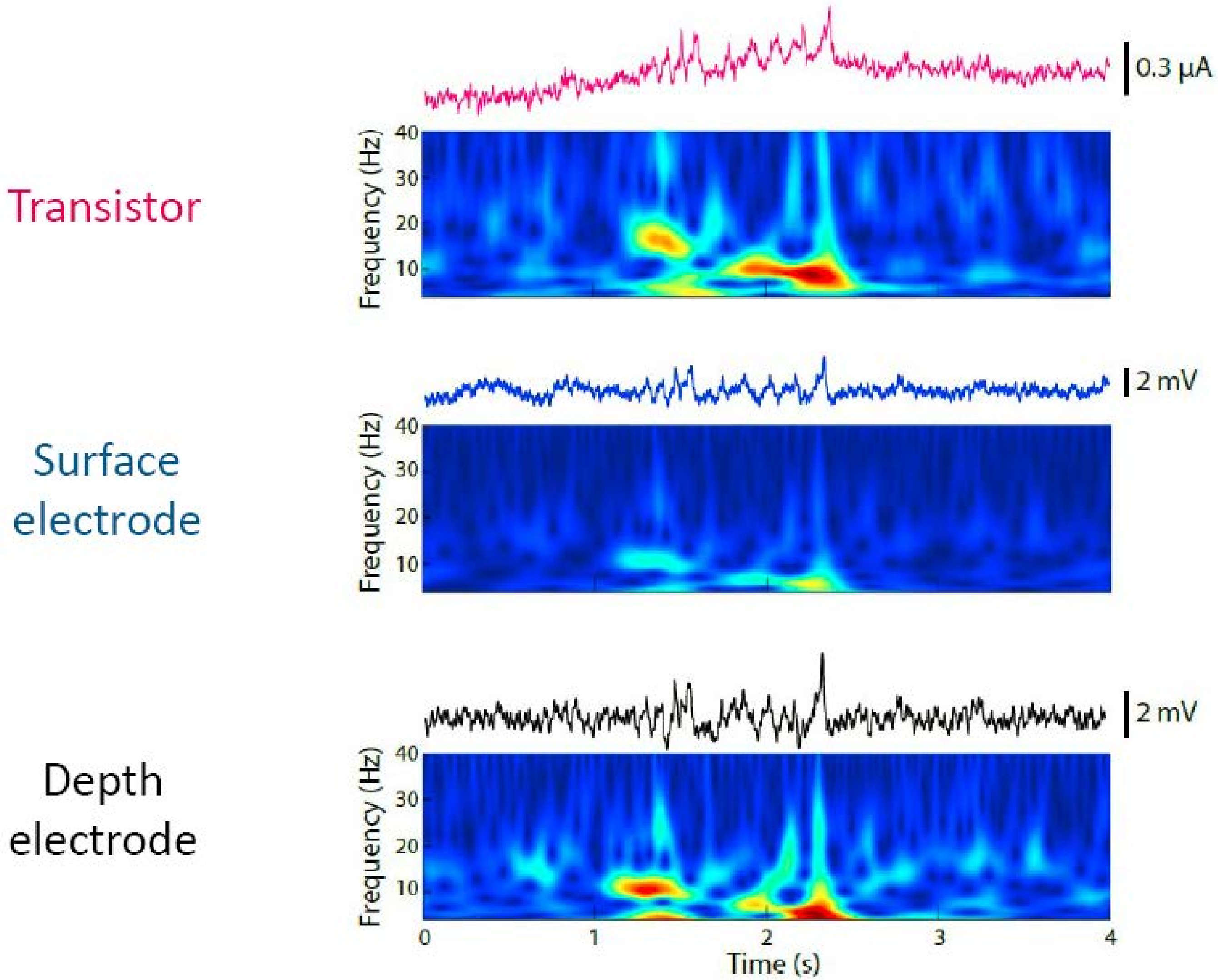

D. Khodagholy, T. Doublet, P. Quilichini, M. Gurfinkel, P. Leleux, A. Ghestem, E. Ismailova, T. Herve, S. Sanaur, C. Bernard, and G.G. Malliaras , *Nature Comm. 4, 1575 (2013).*

Model for OECT operation

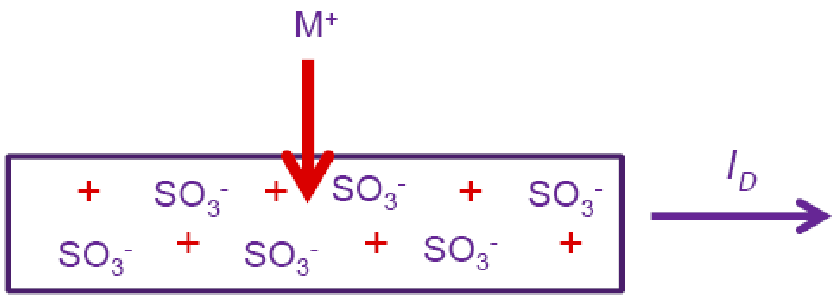

$$I_D = W \cdot d \cdot e \cdot \mu \cdot p(x) \cdot [dV(x)/dx]$$

$$p(x) = SO_3^- - M^+(x)$$

$$M^+(x) = (C^*/e) \cdot [V_G - V(x)]$$

Integrating I_d over the length of the channel:

$$I_D = (W \cdot d/L) \cdot \mu \cdot C^* \cdot [V_T - V_G + V_D/2] \cdot V_D$$

$$V_T = e \cdot SO_3^-/C^*$$

$$I_D^{SAT} = [W/(2 \cdot L)] \cdot d \cdot \mu \cdot C^* \cdot [V_T - V_G]^2$$

Scaling with geometry

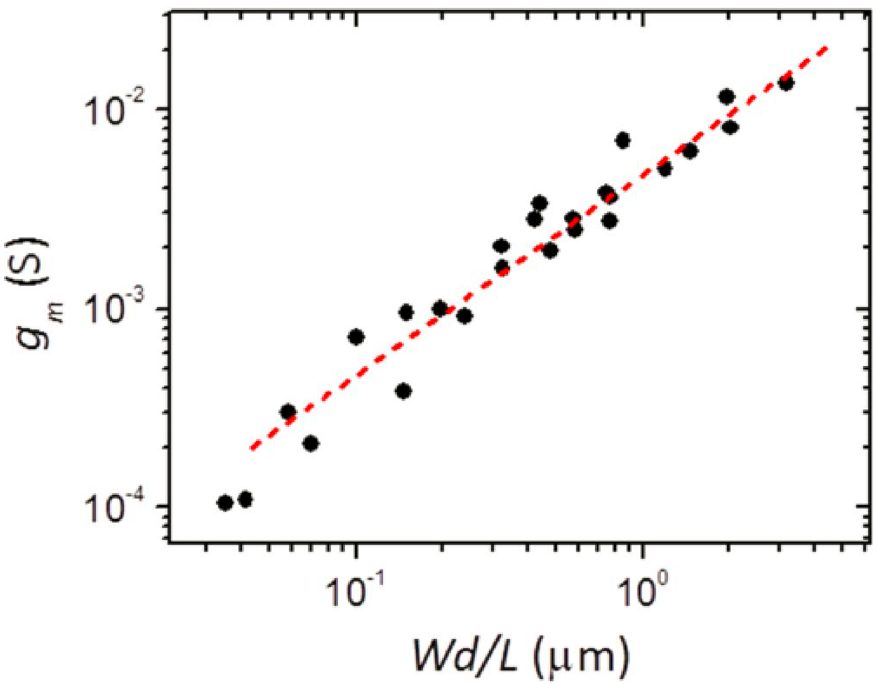

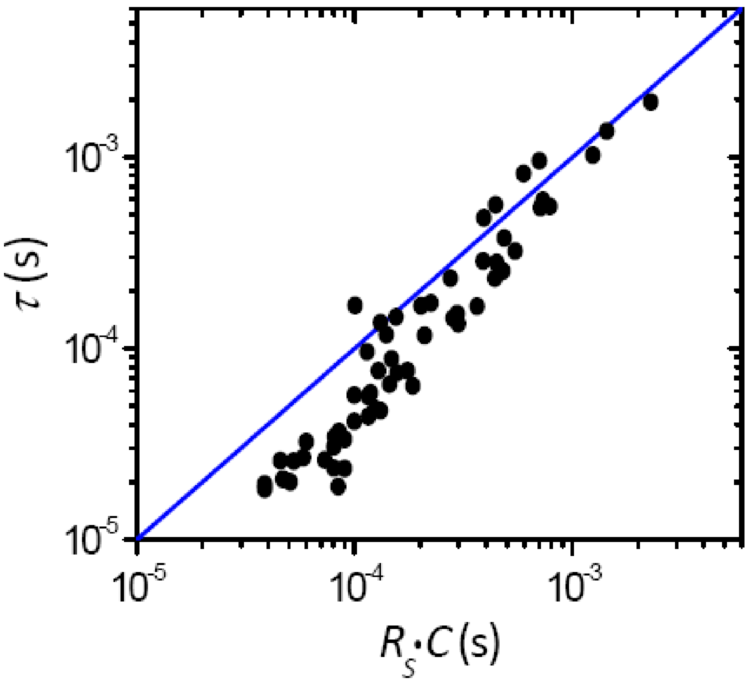

$$g_m = \left(\frac{W \cdot d}{L}\right) \cdot \mu \cdot C^* \cdot (V_T - V_G)$$

J. Rivnay, P. Leleux, M. Ferro, M. Sessolo, A. Williamson, D.A. Koutsouras, D. Khodagholy, M. Ramuz, X. Strakosas, R.M. Owens, C. Benar, J.-M. Badier, C. Bernard, and G.G. Malliaras, SCIENCE Advances1, e1400251 (2015).

Geometry Design of OECTs for improving device sensitivity

Bottom-contact (BC)

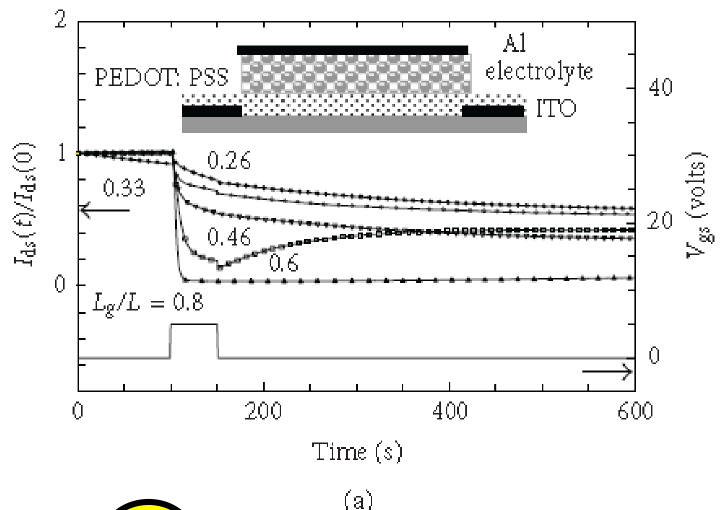

Top-contact (TC)

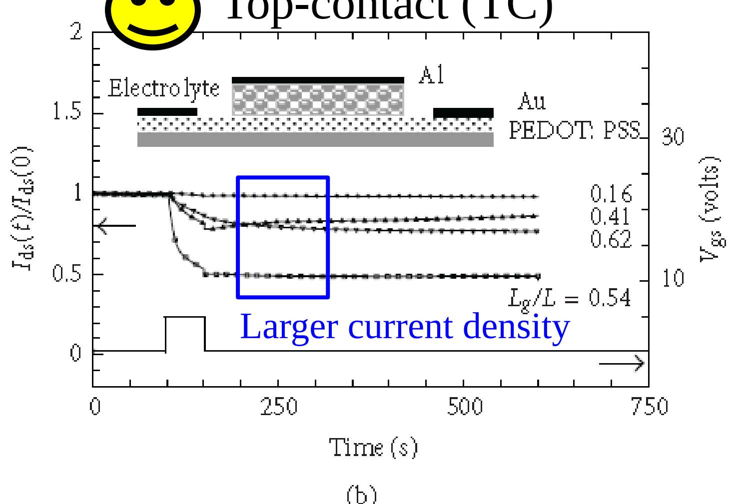

Solid-electrolyte: PVA

S (sensitivity)= $\beta/(L_g/L)$

$\beta = \Delta I_{ds}/I_{ds}$

Channel length (L) = 12 mm; Width (W)= 3 mm

Gate length (L_g)

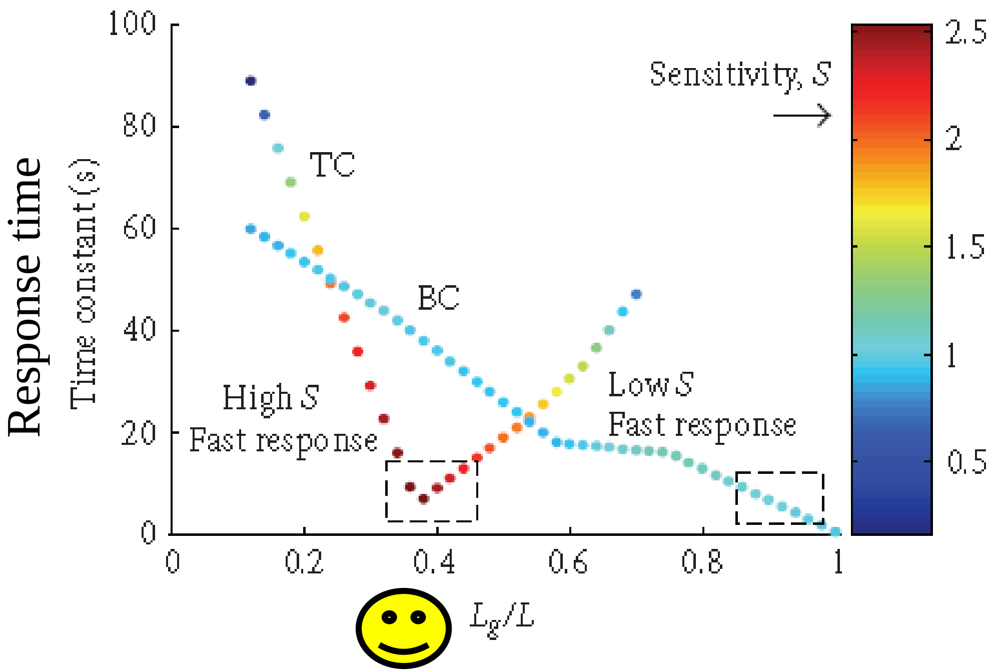

Journal of Sensors, Volume 2008, Article ID 702161.

High transconductance means high SNR

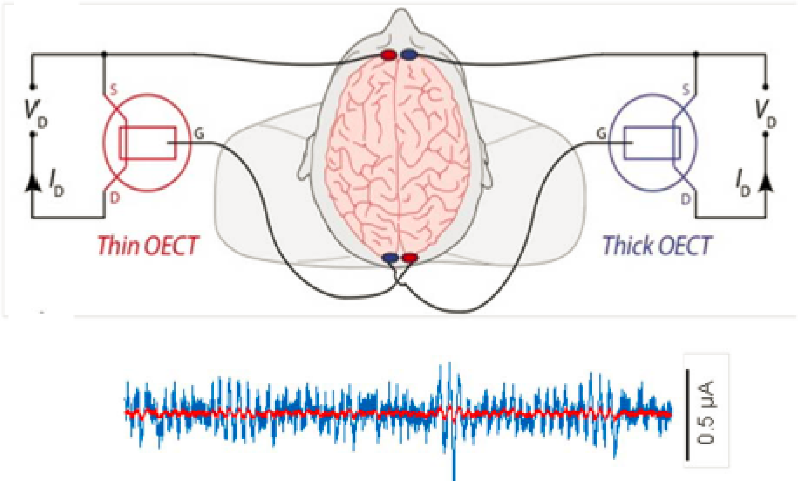

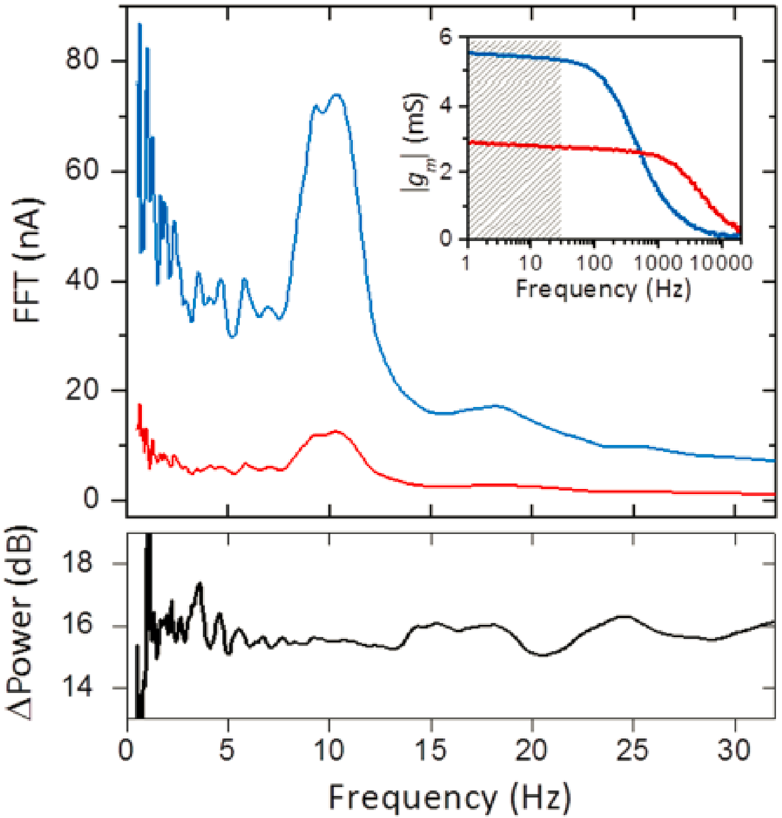

J. Rivnay, P. Leleux, M. Ferro, M. Sessolo, A. Williamson, D.A. Koutsouras, D. Khodagholy, M. Ramuz, X. Strakosas, R.M. Owens, C. Benar, J.-M. Badier, C. Bernard, and G.G. Malliaras, SCIENCE Advances 1, e1400251 (2015).

Organic electronic ion pumps control epileptiform activity

The organic electronic ion pump

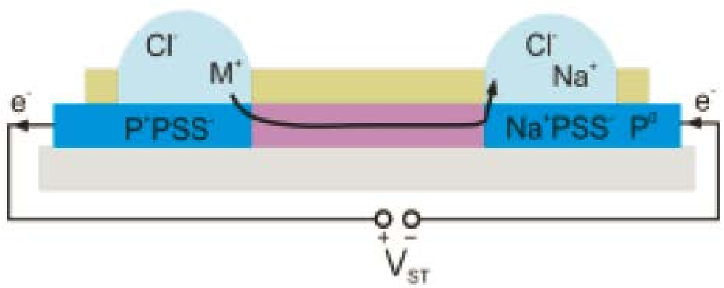

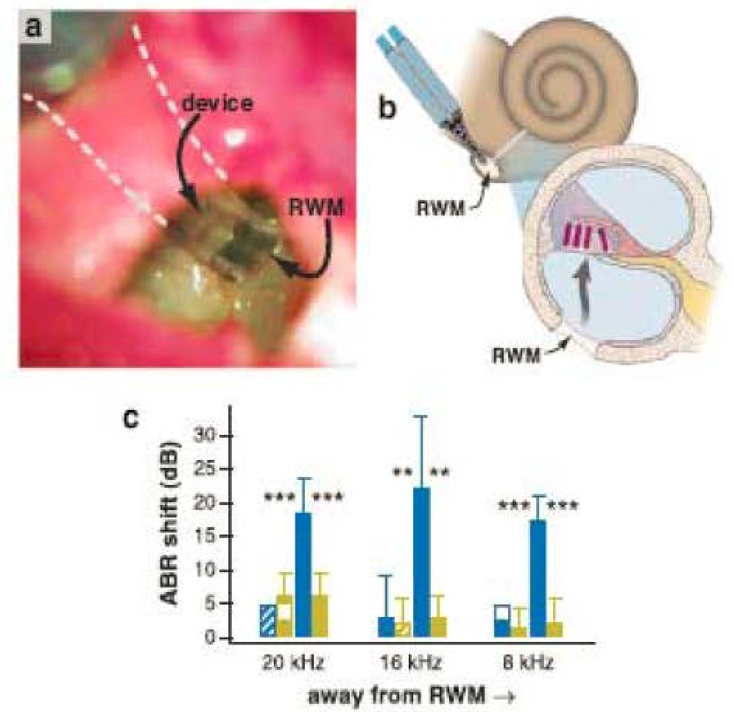

D. T. Simon, S. Kurup, K. C. Larsson, R. Hori, K. Tybrandt, M. Goiny, E. H. Jager, M. Berggren, B. Canlon, and A. Richter-Dahlfors, *Nature Materials 8, 742 (2009).*

Ion Pump Operation

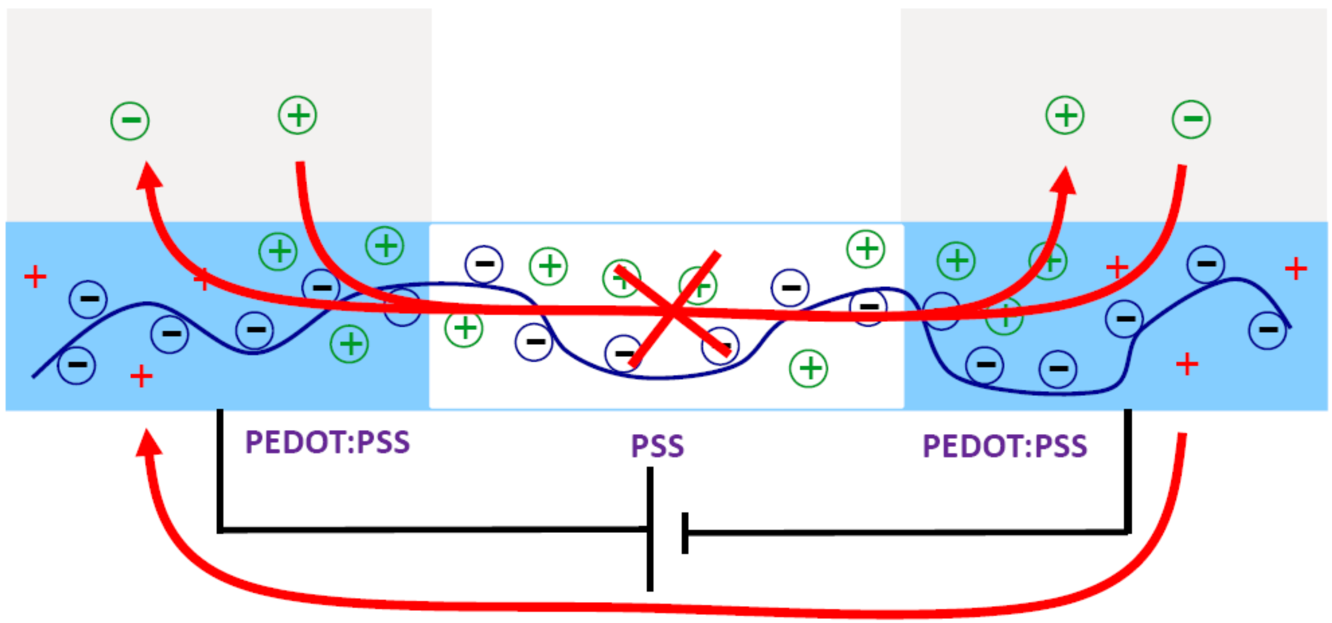

Ion pump for local delivery in neural networks

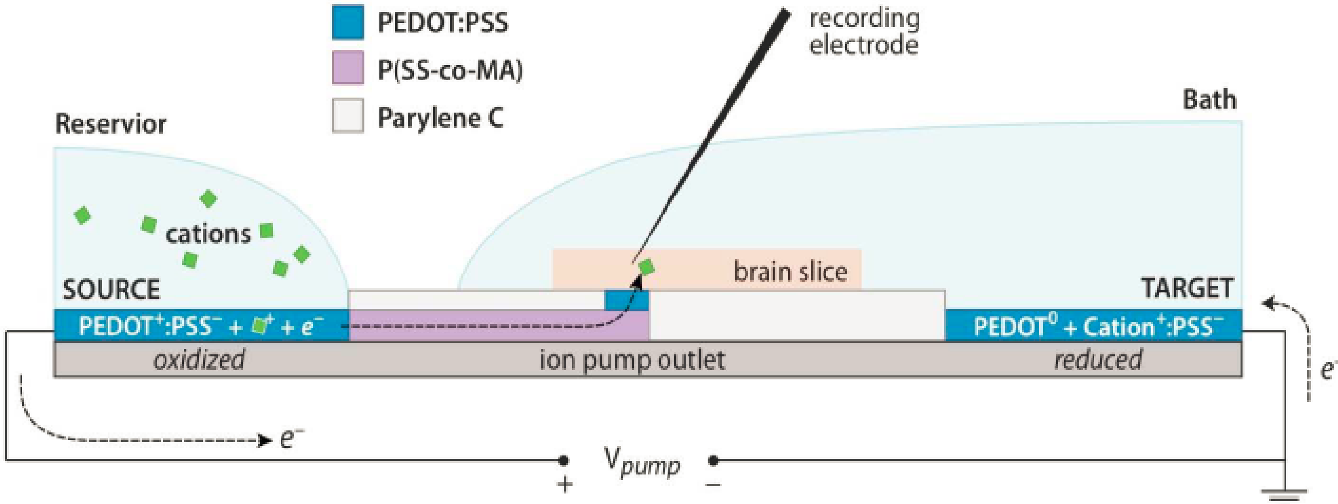

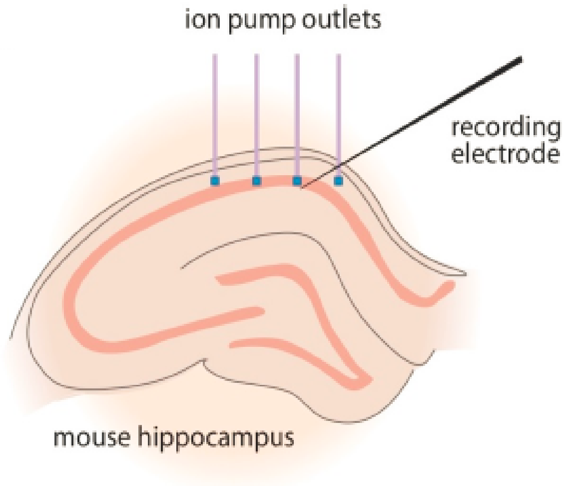

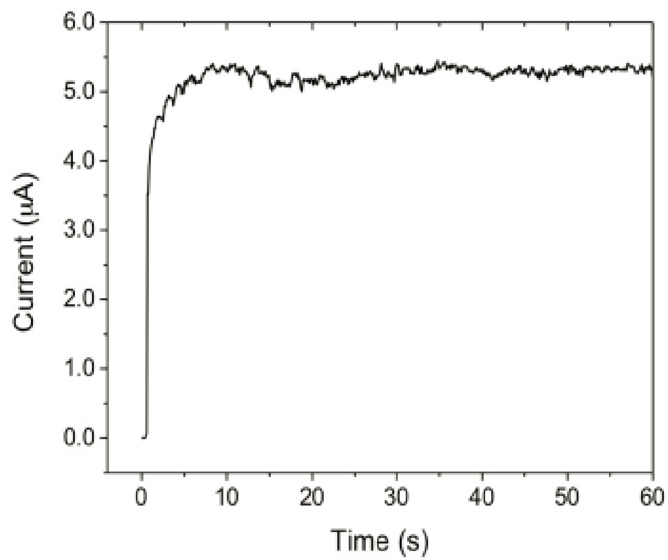

Christophe Bernard (INSERM), Magnus Berggren (Linköping)

Local delivery of GABA suppress seizure activity

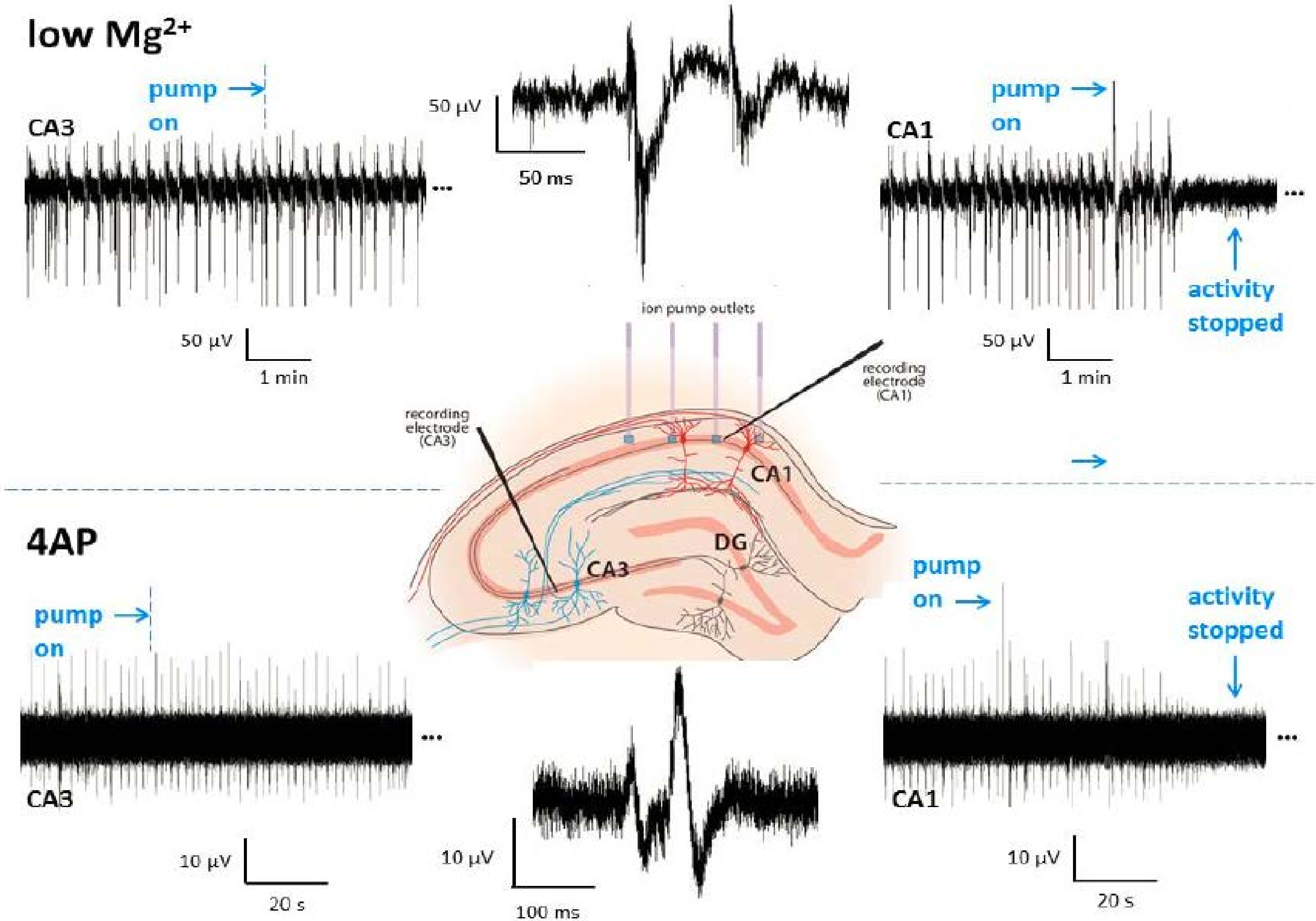

Christophe Bernard (INSERM), Magnus Berggren (Linköping)

μC* as the materials figure of merit

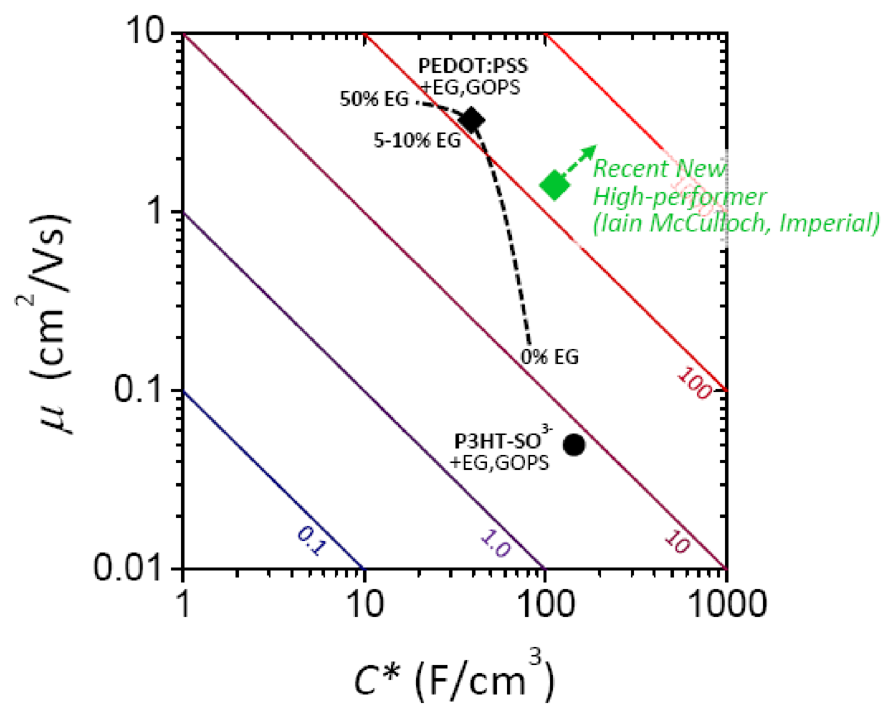

Such maps provide a way to compare materials as potential candidates in OECTs

PEDOT:PSS
(+EG, +GOPS)

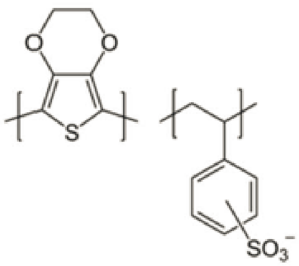

μC^* = 128 F/cmVs

μ = 3.3 cm²/Vs

C^* = 39 F/cm³

$P3HT\text{-}SO_3^-$
(+EG +GOPS)

w/ M. Thelakkat, U. Bayreuth

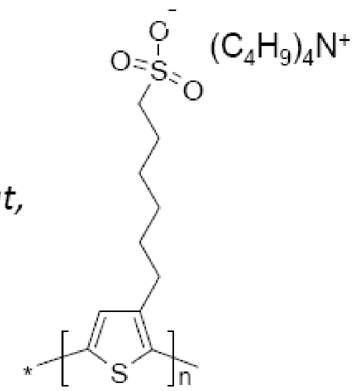

μC^* = 7.2 F/cmVs

μ = 0.05 cm²/Vs

C^* = 144 F/cm³

S. Inal, J. Rivnay, P. Leleux, M. Ferro, M. Ramuz, J.C. Brendel, M. Schmidt, M. Thelakkat, and G.G. Malliaras, Adv. Mater. 26, 7450 (2014).

PEDOT:PSS as a champion material

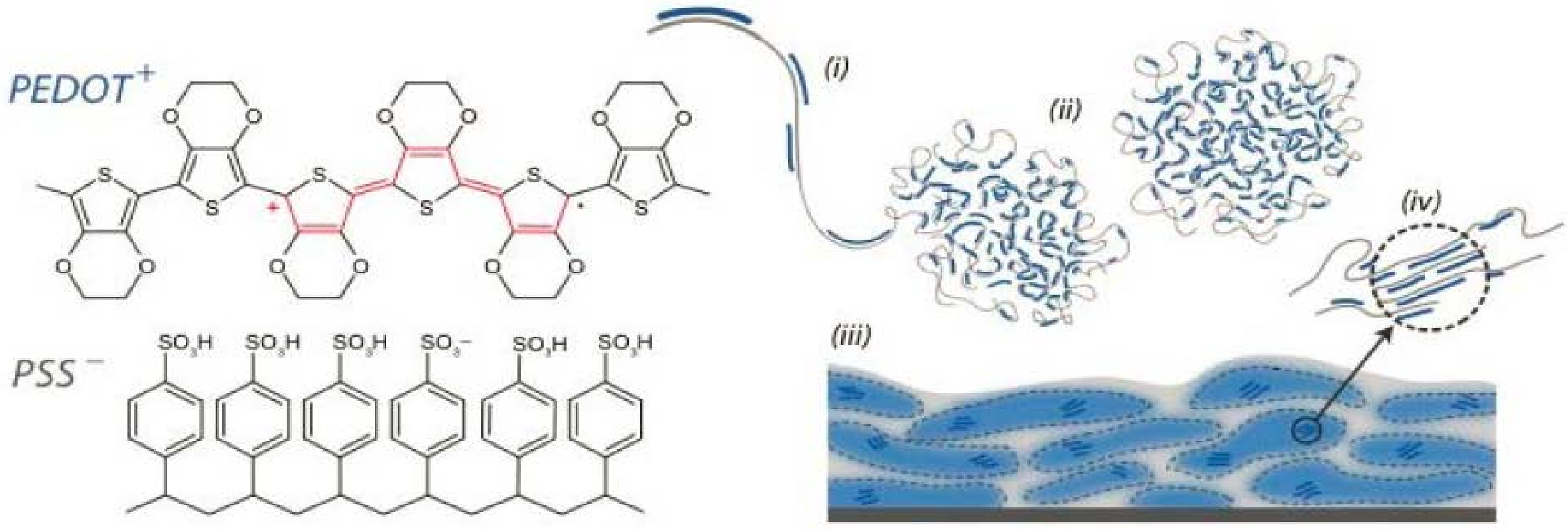

- Phase separated morphology
- Hole transport in PEDOT-rich domains, ion transport in PSS matrix

"Moving front" measurements

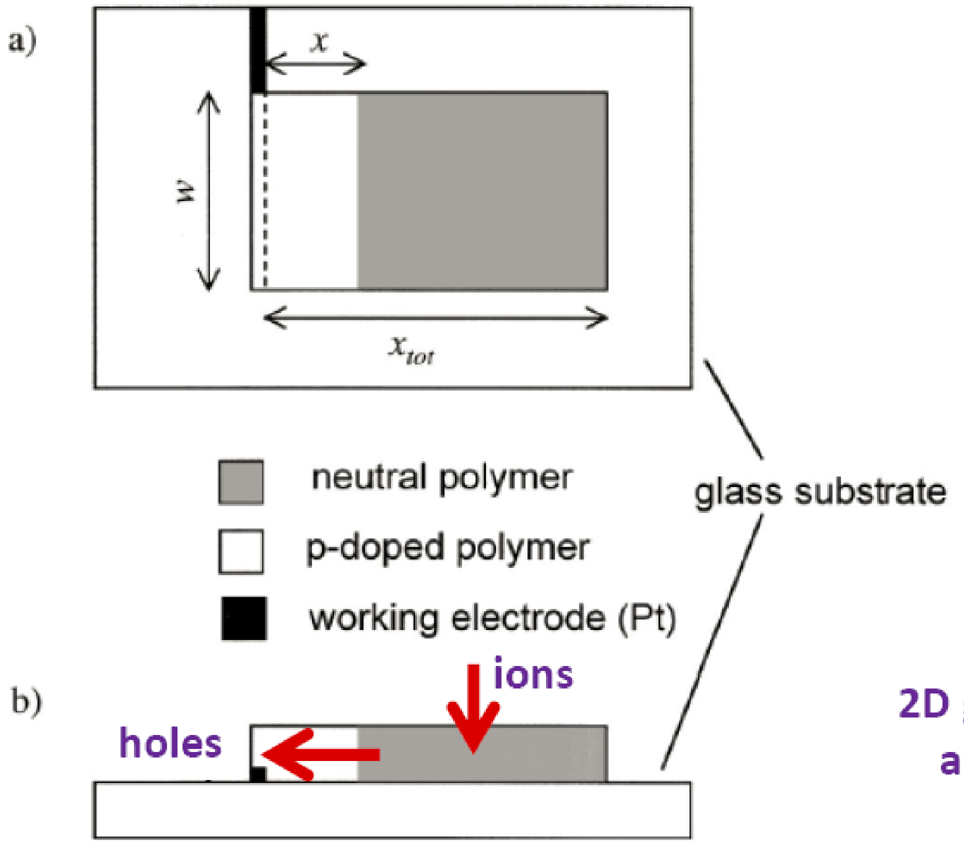

2D geometry makes analysis difficult

K. Aoki, T. Aramoto and Y. Hoshino, Journal of Electroanalytical Chemistry 340, 127 (1992).
T. Johansson, N. K. Persson and O. Inganas, Journal of the Electrochemical Society 151, E119 (2004).
X. Wang and E. Smela, The Journal of Physical Chemistry C 113, 369 (2008).

A simple way to measure ion transport

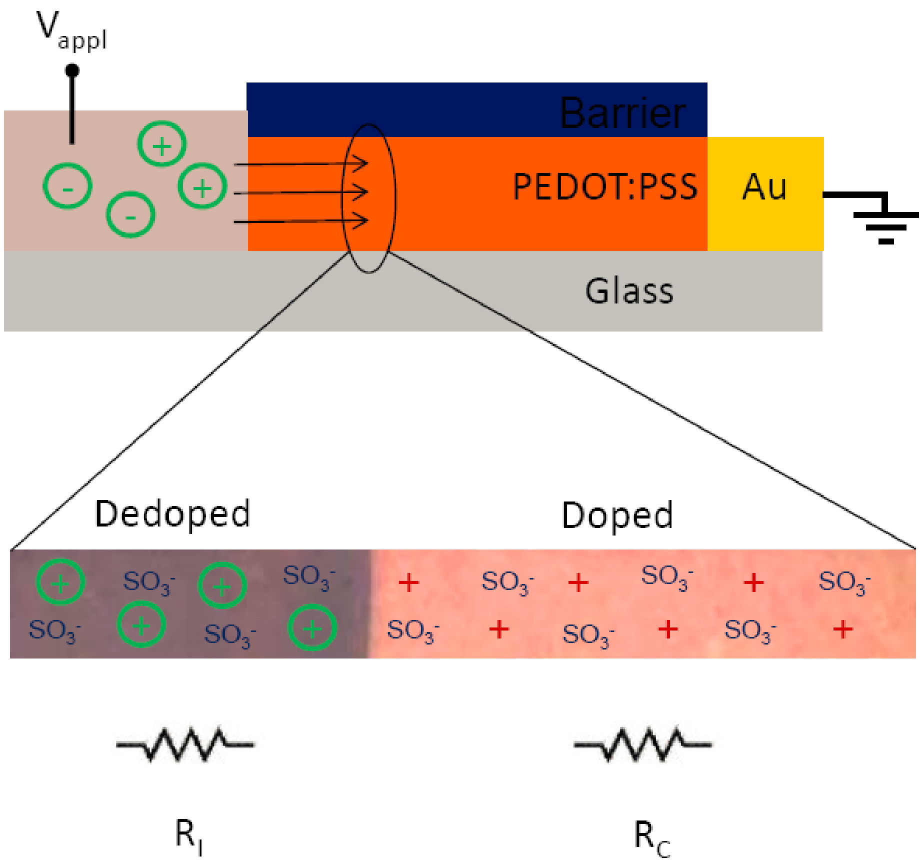

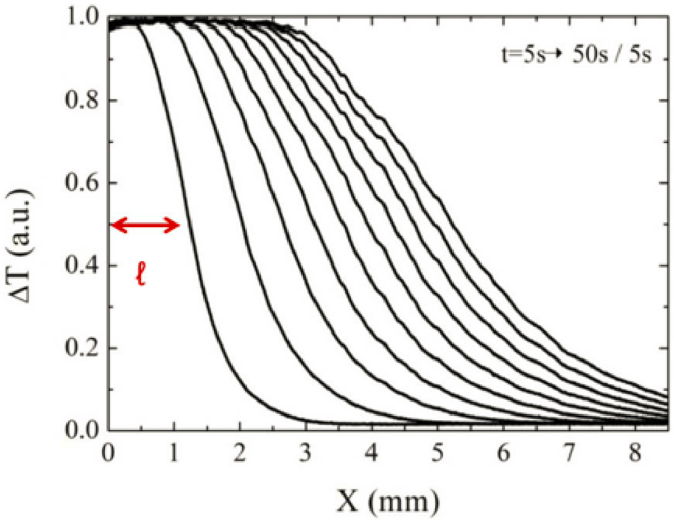

$$\ell^2 = \mu \cdot V_{appl} \cdot t$$

$$j = \frac{e \cdot P\sqrt{2 \cdot \mu \cdot V_{appl}}}{2\sqrt{t}}$$

E. Stavrinidou, P. Leleux, H. Rajaona, D. Khodagholy, J. Rivnay, M. Lindau, S. Sanaur, and G.G. Malliaras, Adv. Mater. 25, 4488 (2013).

Ions are highly mobile in PEDOT:PSS

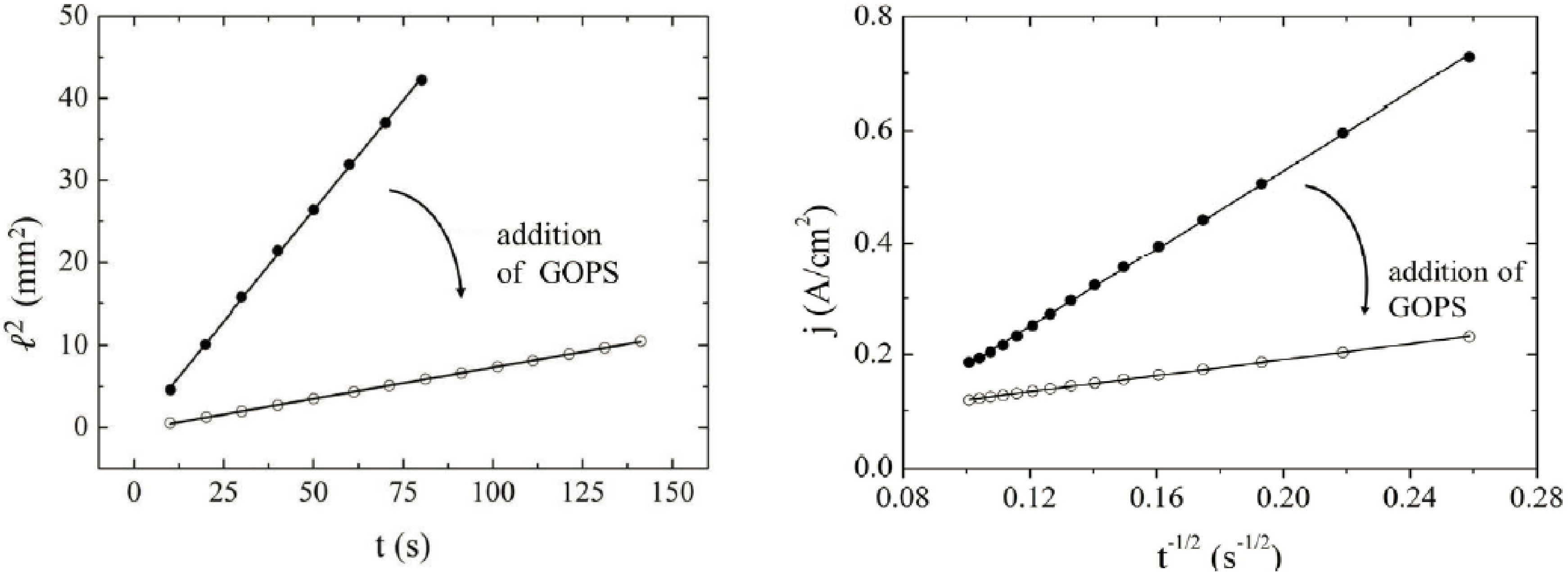

	K^+ mobility in film ($cm^2V^{-1}s^{-1}$)	K^+ density in film (cm^{-3})
PEDOT:PSS	$1.4 \cdot 10^{-3}$	$5.9 \cdot 10^{20}$
PEDOT:PSS :GOPS	$1.9 \cdot 10^{-4}$	$3.2 \cdot 10^{20}$

E. Stavrinidou, P. Leleux, H. Rajaona, D. Khodagholy, J. Rivnay, M. Lindau, S. Sanaur, and G.G. Malliaras, Adv. Mater. 25, 4488 (2013).